Identification and functional characterization of secreted effector proteins of the hemibiotrophic fungus *Colletotrichum higginsianum*

Inaugural-Dissertation

zur
Erlangung des Doktorgrades
der Mathematisch-Naturwissenschaftlichen Fakultät
der Universität zu Köln

vorgelegt von
Jochen Kleemann
aus Köln

Köln, September 2010

Die vorliegende Arbeit wurde am Max-Planck-Institut für Pflanzenzüchtungsforschung in Köln in der Abteilung für Molekulare Phytopathologie (Direktor: Prof. Dr. P. Schulze-Lefert) angefertigt.

Berichterstatter:

Prof. Dr. Paul Schulze-Lefert

Prof. Dr. Martin Hülskamp

Prof. Dr. Martijn Rep

Prüfungsvorsitzender: Prof. Dr. Ulf-Ingo Flügge

Tag der Disputation: 20. Oktober 2010

Table of contents

Abstract

The hemibiotrophic ascomycete fungus *Colletotrichum higginsianum* causes anthracnose on cruciferous crops and the model plant *Arabidopsis thaliana*. Successful infection of wild-type plants requires sequential development of specialized infection structures, including melanized appressoria for initial penetration, and bulbous biotrophic hyphae formed inside living epidermal cells. It was hypothesized that appressoria and biotrophic hyphae secrete effector proteins that permit the fungus to evade or disarm host defence responses and to reprogram host cells. This study aimed to define the repertoire of fungal effectors expressed during plant infection and to characterise their biological activity. Discovery of *C*olletotrichum *h*iggins*i*anum Effector Candidates (ChECs) was accomplished by computational mining collections of infection stage-specific expressed sequence tags (ESTs) for genes encoding solubly secreted proteins with either no homology to known proteins or resembling presumed effectors from other pathogens. Fungal cell types and infection stages sampled for cDNA generation and pyrosequencing included developing and mature *in vitro* appressoria, early invasive growth *in planta*, biotrophy and late necrotrophy. After assembling contiguous sequences, analysis of their EST composition allowed the identification of putative plant-induced genes and the definition of a set of 69 *ChEC* genes that are preferentially expressed at biotrophy-relevant stages. In relation to other infection stages, the early host invasion transcriptome was enriched for genes encoding *higginsianum*-specific proteins and plant-induced secreted proteins, including ChECs. This suggests that the initial establishment of biotrophy requires the highest proportion of stage-specific effectors and diversified genes. One further ChEC was identified using a complementary proteomic analysis of secreted proteins produced by conidial germlings developing *in vitro*. Expression analysis showed that transcription of most of the *ChECs* chosen for further study were highly stage-specific, with *ChEC3*, *ChEC3a*, *ChEC4* and *ChEC6* all being plant-induced. Targeted gene replacement showed that neither ChEC1 nor ChEC2 contribute measurably to fungal virulence. Upon transient expression in tobacco, ChEC3, ChEC3a or ChEC5 all suppressed plant cell death evoked by a *C. higginsianum* homologue of *Necrosis and Ethylene-inducing Peptide1-like proteins*, but not by the *Phytophthora infestans* elicitin INF1, suggesting that there is functional redundancy between *C. higginsianum* effectors. ChEC4 was found to contain a functional nuclear localization signal and signal peptide, and was

shown to be secreted by the fungus during plant infection using fluorescent protein-tagging. This raises the possibility that ChEC4 is translocated into the host nucleus for transcriptional re-programming.

Zusammenfassung

Der hemibiotrophe Ascomycet *Colletotrichum higginsianum* gilt als Erreger der Anthraknose bei Kulturpflanzen aus der Familie der *Brassicaceae* und kann die Modellpflanze *Arabidopsis thaliana* befallen. Eine erfolgreiche Infektion der Pflanze erfordert die sequenzielle Ausbildung von spezialisierten Infektionsstrukturen: Melanisierte Appressorien ermöglichen die Penetration des Wirts und verdickte Primärhyphen treten in eine biotrophe Interaktion mit der penetrierten, lebenden Zelle. Es wird vermutet, dass Appressorien und biotrophe Primärhyphen Effektorproteine sekretieren, die es dem Pilz ermöglichen, die pflanzliche Wirtszelle umzuprogrammieren und ihre Immunabwehr auszuschalten oder zu unterwandern. Zielsetzung dieser Arbeit war die Bestimmung des Repertoirs an *in planta* exprimierten *C. higginsianum* Effektorprotein-Kandidaten (ChECs) und die Charakterisierung ihrer biologischen Aktivität. Identifizierung von ChECs erfolgte durch bioinformatisches Screening von infektionsstadiums-spezifischen *expressed sequence tags* (ESTs). Gesucht wurde dabei nach pilzlichen Genen die für löslich sekretierte Proteine kodieren und die entweder keine Homologie zu bekannten Proteinen aufweisen oder Ähnlichkeit mit vermuteten Effektorproteinen anderer Pathogene haben. cDNA Präparation und Pyrosequenzierung erfolgte von folgenden Zelltypen und Infektionsstadien: Sich entwickelnde und ausgereifte *in vitro* Appressorien, frühe Wirtspenetration sowie biotrophes und spätes nekrotrophes Stadium. Die Analyse der EST Zusammensetzung der *contigs* nach Assemblierung erlaubte die Identifizierung pflanzeninduzierter Gene und von 69 *ChEC* Genen mit vorwiegender Expression in biotrophie-relevanten Stadien. Im Vergleich zu anderen Infektionsstadien zeigte das wirtspenetrations-spezifische Transkriptom den höchsten Anteil an *higginsianum*-spezifischen Genen sowie an Genen, die für sekretierte Proteine im Allgemeinen und ChECs im Besonderen kodieren. Dies lässt vermuten, dass für die Etablierung der biotrophen Interaktion der höchste Anteil an infektionsstadiums-spezifischen Effektoren und diversifizierten Genen notwendig ist. Proteine die während der *in vitro* Appressorien-Morphogenese sekretiert wurden, konnten mit Hilfe einer Proteomanalyse direkt identifiziert werden. Dieser ergänzende Ansatz erlaubte außerdem die Identifizierung eines weiteren ChECs. Expressionsanalyse zeigte, dass die Expression der meisten der zur weiteren Untersuchung ausgewählten ChECs sehr infektionsstadiums-spezifisch war. *ChEC3*,

ChEC3a, *ChEC4* und *ChEC6* konnten als pflanzeninduziert identifiziert werden. *Knockout* Mutanten, denen *ChEC1* und *ChEC2* fehlte, zeigten keine messbare Reduzierung der Virulenz. Mit Hilfe transienter Expression in Tabak konnte gezeigt werden, dass der durch ein *C. higginsianum* Homolog eines *Necrosis and Ethylene-inducing Peptide1-like protein* hervorgerufene Zelltod durch Co-Expression von ChEC3, ChEC3a oder ChEC5 supprimiert werden kann, was funktionale Redundanz zwischen *C. higginsianum* Effektoren vermuten lässt. Dahingegen war der Zelltod, der durch das Elizitin INF1 von *Phytophthora infestans* hervorgerufen wurde, nicht supprimierbar. Für ChEC4 konnte sowohl eine funktionale Kern-Lokalisationssequenz als auch ein funktionales Signalpeptid experimentell bestätigt werden. Durch Fusion mit einem fluoreszierenden Protein konnte die Sekretion von ChEC4 während der Infektion der Pflanze gezeigt werden. Dies zeigt, dass ChEC4 das Potenzial hat, in den Zellkern der Wirtszelle transloziert zu werden, um dort möglicherweise die Transkription zu beeinflussen.

1. Introduction

1.1 *Colletotrichum higginsianum*, the causal agent of crucifer anthracnose

The large Ascomycete genus *Colletotrichum* (teleomorph: *Glomerella*) occurs worldwide and comprises many important plant pathogens. The genus attacks a wide range of agricultural crops such as cereals and grasses, legumes, vegetables, ornamental plants and fruits, especially in tropical and sub-tropical regions. The capability to cause anthracnose (dark necrotic spots) or blight on all aerial parts of plants and at all stages of development, even post-harvest on maturing fruits, underlines the economic importance of *Colletotrichum* (Bailey and Jeger, 1992; Latunde-Dada, 2001). Besides causing devastating yield losses in agriculture, *Colletotrichum* has become a valuable model system of increasing interest in research because of its fascinating pathogenic lifestyle and amenability to genetic manipulation.

1.1.1 Hemibiotrophy – a hallmark of many *Colletotrichum* species

Fungal phytopathogens have evolved different strategies to obtain water and nutrients from their host plants. Based on these strategies, phytopathogenic fungi can be classified as biotrophs, necrotrophs or hemibiotrophs (Mendgen and Hahn, 2002). Obligate necrotrophs (e. g. the grey mould fungus *Botrytis cinerea*) begin to decompose plant tissues immediately after penetration, converting it into fungal biomass and thereby killing plant cells during colonization (Van Kan, 2006). By contrast, biotrophic fungi like the powdery mildews and rusts (e. g. *Blumeria* and *Uromyces* spp.) develop a stable and complex interaction with living host cells, which become reprogrammed by the parasite to support its biotrophic lifestyle. Despite the extraordinary economic importance of fungal biotrophs, the molecular mechanisms underlying the establishment and maintenance of biotrophic interactions are still poorly understood and are the subject of intense research. Obligate biotrophs are entirely reliant on a living host cell to fulfill their lifecycle and thus cannot be cultured and propagated *in vitro* (O'Connell and Panstruga, 2006). This presents difficulties for the application of molecular genetic approaches: despite intensive efforts, there is still no stable transformation system available for any obligate biotroph (Chaure *et al*., 2000; Wirsel *et al*., 2004; Voegele *et al*., 2006). However, stable transformation for several generations of the flax rust fungus (*Melampsora lini*) was recently achieved by

using an elegant avirulence gene-based *in planta* selection system (Lawrence *et al*., 2010).

With the exception of few purely necrotrophic species (Bailey and Jeger, 1992; Peres *et al*., 2005), most *Colletotrichum* spp. have a hemibiotrophic lifestyle, combining aspects of both biotrophy and necrotrophy at different infection stages. After an initial biotrophic phase associated with intracellular primary hyphae which invaginate the intact host plasma membrane, the pathogen switches to necrotrophic proliferation (Perfect *et al*., 1999). Due to this capacity for necrotrophic growth, *Colletotrichum* spp. can be cultured axenically as saprotrophs and are able to complete at least their asexual life-cycle *in vitro*. This property renders these fungi accessible to genetic transformation by a variety of different methods, including restriction enzyme-mediated, polyethylene glycol- or agrobacterium-mediated transformation (Redman and Rodriguez, 1994; Epstein *et al*., 1998; Redman *et al*., 1999; Robinson and Sharon, 1999; Chen *et al*., 2003; Tsuji *et al*., 2003a; O'Connell *et al*., 2004, Huser *et al*., 2009). As a further advantage, these fungi are haploid organisms and have uninucleate conidia, which facilitates mutational analysis (O'Connell *et al*., 2004; Huser *et al*., 2009, this study). Thus, studying hemibiotrophic interactions involving *Colletotrichum* circumvents the practical difficulties encountered with obligate biotrophs and may reveal whether obligate biotrophic and hemibiotrophic parasites have mechanisms of pathogenesis in common.

1.1.2 *Colletotrichum* appressoria: structures enabling forceful host intrusion

Colletotrichum conidia, which are dispersed by rain splash, adhere to the cuticle of the host plant by passive hydrophobic interactions, presumably mediated by glycoproteins in the outer coat of the conidium (Hughes *et al*., 1999). The hydrophobic plant cuticle with its surface waxes provides a host-specific inductive cue for the germination of the spore as well as for appressorium formation (Podila *et al*., 1993). Furthermore, hard surfaces can also contribute to the induction of germination and appressorium formation (Liu and Kolattukudy, 1998; Kim *et al*., 2000). On such inductive surfaces, germination begins with mitosis followed by deposition of a septum and emergence of a germ-tube from one of the daughter cells. The germ-tube tip becomes delimited by a septum and swells to form appressorial initials. Mature appressoria are asymmetric, polarized cells exhibiting a domed shape with a flattened base facing the plant

epidermis. Maturation of the appressorium involves the release of adhesive extracellular matrix material, the formation of a basal penetration pore, the deposition of extra cell wall layers and incorporation of the phenolic polymer melanin into the cell wall (Perfect *et al*., 1999). For *Magnaporthe grisea*, with which *Colletotrichum* spp. share a remarkably similar infection strategy, appressorium morphogenesis was strongly dependent on the concomitant autophagic cell death of the germinating conidium, mediated by the autophagy-related gene *ATG8* (Veneault-Fourrey *et al*., 2006). Similarly, the *C. orbiculare* homologue *CoAtg8* was recently demonstrated to be required for normal appressorium development (Asakura *et al*., 2009). Furthermore, appressorial maturation, melanization and penetration ability require functional peroxisomes, providing β-oxidation of fatty acids derived from storage lipid bodies (Kimura *et al*., 2001; Asakura *et al*., 2006; Wang *et al*., 2007; Fujihara *et al*., 2010). However, peroxisome degradation via pexophagy is also required for appressorium-mediated penetration of *C. orbiculare* (Asakura *et al*., 2009).

The reinforcement of the appressorial cell wall by means of melanin deposition and polymerization renders it impermeable to solutes and is thought to be a prerequisite for the generation of turgor pressure (Deising *et al*., 2000). The non-melanized penetration pore is the only site that allows an evaginating penetration peg to grow downwards through the host cell wall (Latunde-Dada, 2001). The turgor pressure that is exerted by the appressorial cell on the penetration peg generates an invasive force estimated to reach 17 µN in *C. graminicola* (Bechinger *et al*., 1999), which is analogous to the force exerted by an eight ton school bus on the palm of a human hand (Money, 1999), and allows *Colletotrichum* species to penetrate plastic membranes without the aid of enzymes (O'Connell, 1991).

1.1.3 *Colletotrichum higginsianum* is part of a species complex

In the present study the epithet '*higginsianum*' is used, whereas in the reference publication describing the *C. higginsianum* - *Arabidopsis* pathosystem '*destructivum*' was preferred, since phylogenetic analysis of different *C. higginsianum* isolates revealed a close relationship to *C. destructivum* (O'Connell *et al*., 2004). Furthermore, cytological and molecular taxonomic analyses suggested that *C. higginsianum* is part of a species aggregate of very closely related species including *C. linicola* (attacking flax), *C. truncatum* (attacking legumes) and *C. destructivum* (attacking legumes,

tobacco and cruciferous plants) (Latunde-Dada and Lucas, 2007; Moriwaki *et al*., 2002). A key taxonomic character of this group is their so-called 'localized biotrophy', with biotrophic primary hyphae restricted to the initially penetrated epidermal cell. For *C. higginsianum* the biotrophic phase lasts only for approximately 30 hours at 25 °C incubation temperature. From the large multilobed and bulbous primary hyphae, narrow secondary necrotrophic hyphae spread subsequently into the surrounding tissue, producing water-soaked lesions and tissue maceration. From these, monosetate acervuli (fruiting bodies) emerge onto the surface of the dead tissue, carrying conidia for asexual reproduction. The localized biotrophy is in sharp contrast with the 'sequential biotrophy' displayed by hemibiotrophs from graminaceous hosts (*C. sublineolum, C. graminicola*) and *C. lindemuthianum*, for example, where the biotrophic hyphae colonize many host cells (O'Connell *et al*., 1985; Perfect *et al*., 1999).

1.1.4 The *Colletotrichum higginsianum – Arabidopsis* interaction

The *C. higginsianum* strain described by O'Connell and co-workers, which became the genome-sequenced reference strains at the MPIPZ, was initially collected in 1991 in Trinidad and Tobago from *Brassica rapa*. This strain caused anthracnose leasons on many (but not all) cruciferous plant species tested (O'Connell *et al*., 2004 and references herein). Interestingly, the host range is not confined to *Brassicaceae*. *C. higginsianum* is also able to complete its asexual life cycle on some *Fabaceae*, including cowpea (*Vigna unguiculata*) and lentil (*Lens culinaris*) (O'Connell *et al*., 2004). Conversly, *C. destuctivum* isolates from cowpea were able to infect *Arabidopsis* (Sun and Zhang, 2009). This versatile host range implies that effectors (see below) employed by *C. higginsianum* evade and/or manipulate the immune system of plant species from highly diverged plant families and that their molecular targets are sufficiently conserved.

Several resistance genes conferring crucifer anthracnose resistance were recently discovered in *Arabidopsis*. *RCH1* is a locus providing dominant resistance in *A. thaliana* accession Eil-0 (Narusaka *et al*., 2004). Furthermore, both *RRS1* and *RPS4* were recently found to provide resistance to *C. higginsianum* in accessions Ws-0, Kondara, Gifu-2 and Can-0 (Birker *et al*., 2009; Narusaka *et al*., 2009). Both resistance genes also appear to cooperate in conferring resistance to two bacterial pathogens,

Ralstonia solanacearum and *Pseudomonas syringae* pv. tomato strain DC3000 (Narusaka *et al*., 2009). Remarkably, *RPS4/RRS1*-mediated resistance correlated with an early arrest of fungal invasion at the level of appressorial penetration of the cuticle and cell wall, preventing establishment of biotrophic hyphae at most infection sites (Birker *et al*., 2009). Despite the dependency on *EDS1*, a typical component of post-invasive defenses against biotrophic and hemibiotrophic pathogens (Wiermer *et al*., 2005), *RPS4/RRS*-mediated resistance to *C. higginsianum* was not associated with the prototypical hypersensitive response (HR) involving accumulation of reactive oxygen species (ROS). Also deposition of callose papillae was not observed underneath appressoria, suggesting that atypical plant defence responses are employed against *C. higginsianum* (Birker *et al*., 2009). Since both, *RPS4*- and *RRS1*-mediated resistance appear to require nucleocytoplasmic relocalization (Deslandes *et al*., 2003; Wirthmueller *et al*., 2007), it is conceivable that *C. higginsianum* effectors are translocated into the host cell followed by direct or indirect ('guard hypothesis', see below) recognition by these resistance proteins.

1.2 The arms race between plants and pathogens

1.2.1 The plant immune system

In a plethora of plant parasites, including viruses, bacteria, fungi, oomycetes, nematodes and insects the struggle for life results in a constant arms-race with their corresponding plant hosts. The theatre of war in this battle is the plant cell, with pre-formed structural and chemical barriers and an inducible innate immune system designed to frustrate pathogen efforts to conquer a niche for growth and reproduction. The plant immune system shows striking similarities as well as significant differences with the vertebrate innate immune system. In contrast to vertebrates, which employ an innate immune system for early defence and an adaptive immune system for late-phase defence and immunological memory, plants rely entirely upon an innate immune system (Nürnberger *et al*., 2004; Akira *et al*., 2006). As a conceptual breakthrough, Jones and Dangl (2006) introduced the 'zigzag' model of the co-evolutionary arms race between plants and pathogens and proposed that the inducible plant immune system can be divided into two main branches: pathogen-associated molecular pattern (PAMP)-triggered immunity (PTI) and effector-triggered immunity (ETI).

1.2.2 The first layer: microbial pattern recognition and non-host resistance

PAMPs are highly conserved molecules with a wide phylogenetic distribution among microbial species. In fact, they are not confined to pathogenic microbes and, thus, the term 'microbe-associated molecular patterns' (MAMPS) is considered to be more accurate. They are essential components of microbes but are absent from the potential host (Medzhitov and Janeway, 2002; Nürnberger *et al*., 2004; Bittel and Robatzek, 2007). The archetypical example for a PAMP is the main structural protein of the bacterial flagellum, flagellin (Gomez-Gomez and Boller, 2002). For those pathogens that can overcome preformed barriers and enter plants either by direct penetration or through wounds or natural openings like stomata and hydathodes, specific pattern recognition receptors (PRRs) can then detect PAMPs as foreign molecules. These plasma membrane-spanning PRRs can be grouped into 2 classes: the receptor-like kinases (RLKs) that carry a serine/threonine kinase domain and the receptor-like proteins (RLPs) that have a short cytoplasmic tail at the extracellular side (Göhre and Robatzek, 2008). Fungi contain several PAMPs, like chitin, ergosterol and β-1,3-glucan. However, so far only two receptor proteins recognizing chitin were identified in rice and *Arabidopsis*, respectively. CEBiP, a rice transmembrane protein binds extracellular chitin, and requires the co-receptor OsCERK1 for signalling (Kaku *et al*., 2006; Shimizu *et al*., 2010). *Chitin Elicitor Receptor Kinase* (*CERK1*) was initially identified in *A. thaliana* and shown to be involved in chitin perception and signaling via its intracellular serine/threonine kinase activity (Miya *et al*., 2007; Wan *et al*., 2008). CERK1 of *A. thaliana* was recently shown to bind chitin directly (Petutschnig *et al*., 2010; Iizasa *et al*. 2010). Interestingly, CERK1 appears to be the major chitin-binding protein of *A. thaliana* and also binds de-acetylated chitin, chitosan (Petutschnig *et al*., 2010).

Typical PTI responses comprise pre-invasive defence such as stomatal closure, as well as e. g. activation of mitogen-activated protein kinase (MAPK) relays, transcriptional activation of pathogen-responsive (PR) genes, production of reactive oxygen species (ROS), deposition of callose to reinforce the cell wall at sites of infection, and ethylene production (Asai *et al*., 2002; Gomez-Gomez and Boller, 2002). In most cases, PTI is sufficient to arrest microbial growth, with host cells usually staying alive (Nürnberger *et al*., 2004). Treatment with elicitor-active peptides of the bacterial elongation factor and flagellin, has been shown to induce expression of nearly

identical gene sets (Zipfel *et al.*, 2006). This indicates that PAMP recognition converges on a limited number of signalling pathways (Jones and Dangl, 2006).

The processes activated by PTI are thought to contribute to non-host resistance of plants (Jones and Dangl, 2006; Ellis, 2006). Pathogen-induced cell wall reinforcements (papillae) arise from the localized synthesis and deposition of callose, a β-1,3-glucan, often associated with the accumulation of phenolic compounds and reactive oxygen species (Nicholson and Hammerschmidt, 1992; Matern *et al*., 1995; Thordal-Christensen *et al*., 1997). Papillae have long been proposed to function as physical and chemical barriers against microbial attack (Bushnell and Bergquist, 1975). However, the role of callose depositions in plant defence is open to question (Schulze-Lefert, 2004; O'Connell and Panstruga, 2006) as the Arabidopsis callose synthase isoform PMR4/GSL5 was recently shown to act as a susceptibility factor between *Arabidopsis* and powdery mildew fungi and oomycetes (Jacobs *et al*., 2003; Nishimura *et al*., 2003).

Actin-based polarization of the penetrated plant cell is thought to be a prerequisite for focal callose deposition and targeted delivery of antimicrobial compounds or proteins to the penetration site via vesicle-mediated exocytosis (Kobayashi and Hakuno, 2003; Shimada *et al*., 2006; Kwon *et al*., 2008). Recently, *Arabidopsis* PEN1 was characterized as a component of non-host penetration resistance against the non-adapted barley powdery mildew, *Blumeria graminis* f. sp. *hordei* and shown to be a plasma membrane-resident syntaxin (Collins *et al*., 2003). *Arabidopsis* PEN1, as well as the homologous barley ROR2 syntaxin, focally accumulate in plasma membrane microdomains beneath powdery mildew appressoria (Assaad *et al*., 2004; Bhat *et al*., 2005), indicating a link between cell polarization events and vesicle-associated resistance responses at the cell periphery. Actin-based cell polarization was recently described in both host and non-host interactions with *Colletotrichum* spp. (Shan and Goodwin, 2004; Shan and Goodwin, 2005; Shimada *et al*., 2006). Shan and coworkers could show that initial actin rearrangement towards the penetration site occurred in interactions with adapted as well as non-adapted *Colletotrichum* spp. on *Nicotiana benthamiana*. A functional actin cytoskeleton focused to the penetration site was found to be involved in penetration resistance and papilla formation in non-host interactions of non-adapted *Colletotrichum* spp. with *Arabidopsis* (Shimada *et al*., 2006). Interestingly, the latter study revealed that PEN1 does not focally accumulate underneath appressoria of either adapted or non-adapted

Colletotrichum species, indicating that the accumulation of this protein is not a generalized, stereotypical response to wounding or pathogen ingress. Thus, depending on the pathogen, plants might be able to deploy specific subsets of defense-related proteins, or the pathogen itself might be able to suppress their accumulation (O'Connell and Panstruga, 2006).

1.2.3 Pathogen effectors evolved to suppress PTI

According to Kamoun (2006), pathogen effectors are defined as "*molecules that manipulate host cell structure and function, thereby facilitating infection (virulence factors or toxins) and/or triggering defence responses (avirulence factors or elicitors)*." The dual and conflicting activities of effectors probably reflect the co-evolutionary arms-race occurring between plant and pathogen (see below). Since PAMPs fulfill important functions in pathogens and cannot be modified or jettisoned without fitness cost, any (hemi)biotrophic pathogen that succeeded in host colonization must have evaded or suppressed host PTI by secretion of effectors. Conceptionally, this was recognized as effector-triggered susceptibility (Jones and Dangl, 2006). Although most pathogen effectors known to date are 'small' secreted proteins with mostly limited homology to known proteins (see below), it is important to note that effectors are not *necessarily* proteins. Examples of secondary metabolites or nonribosomal peptides include *Mycosphaerella pinodes* supprescins, Brefeldin A-derivatives produced by several pathogenic fungi and a currently unknown secondary metabolite of the *ACE1* gene product of *Magnaporthe grisea* (Shiraishi *et al*., 1992; Driouich *et al*., 1997; Böhnert *et al*., 2004).

Direct evidence for suppression of PAMP-triggered transcriptional responses by effector proteins comes from studies of plant pathogenic bacteria that are deficient in their type III secretion system, the molecular syringe that is required for effector injection into host cells (Thilmony *et al*., 2006). To control host cell functions, such as defense gene expression and vesicle trafficking, bacteria deploy effectors with various biochemical activities, including protein modification, transcriptional regulation, and hormone mimicry (da Cunha *et al*., 2007). A remarkable example is HopM1 from *Pseudomonas syringae*: this effector targets the host protein AtMIN7 for proteasomal degradation (Nomura *et al*., 2006). AtMIN7 is a GTPase exchange factor (GEF) of the adenosine diphosphate ribosylation factor (ARF) subfamily, which are important for

vesicle formation and intracellular trafficking. Furthermore, *Arabidopsis* mutants lacking AtMIN7 were reduced in polarized callose deposition in response to non-pathogenic bacteria (Nomura *et al*., 2006). This suggests that bacterial pathogens modulate host vesicle trafficking to interfere with localized host responses. Similarly, XopJ from *Xanthomonas campestris* pv. *vesicatoria* was recently shown to suppress callose deposition and to affect protein secretion (Bartetzko *et al*., 2009), suggesting that interference with the host secretory pathway is a common strategy of plant pathogens.

Several recent reports provide evidence for extensive transcriptional reprogramming of host cells by adapted fungal pathogens, including *Cladosporium*, *Magnaporthe* and *Ustilago*, with defense-related genes only being induced at low levels or with a delay (Doehlemann *et al*., 2008; van Esse *et al*., 2009; Mosquera *et al*., 2009). Conversingly, host genes that are highly expressed during invasion by adapted pathogens may be involved in effector-triggered susceptibility. Although expected, direct experimental evidence for interference of filamentous pathogens effectors with PAMP-triggered immune responses is sparse. For example, ATR13 from the downy mildew *Hyaloperonospora parasitica* can suppress PAMP-induced callose deposition and ROS accumulation (Sohn *et al*., 2007). Recently, Ecp6 a LysM-domain containing protein of *Cladosporium fulvum* was demonstrated to sequester chitin oligosaccharides, thereby preventing archetypical PTI-associated responses (de Jonge *et al*., 2010).

1.2.4 Plant resistance proteins lying in wait for pathogen effectors

The evolution of secreted effector proteins by pathogens led plants to acquire proteins that specifically recognise these effectors, thereby providing effector-triggered immunity (ETI) (Chisholm *et al*., 2006; Jones and Dangl, 2006). This specific recognition of pathogen effectors by cognate plant resistance (R) gene products has been characterized genetically as race-specific gene-for-gene resistance (Flor, 1971). Effector proteins that are recognized are called avirulence proteins (AVR), and the corresponding pathogen race is not virulent (‘avirulent’) on this particular plant cultivar. AVR protein recognition initiates a cascade of downstream events, such as an increase in cytosolic calcium, depolarisation of the plasma membrane, a localised ROS burst, nitric oxide (NO) production and MAPK cascade activation (Dangl and Jones, 2001). ETI responses therefore show a significant overlap with PTI responses and have

been considered as an amplified PTI response, resulting in a hypersensitive cell death response (HR) at the infection site, which efficiently terminates pathogenesis of (hemi)biotrophic fungi (Nürnberger *et al*., 2004; Jones and Dangl, 2006; Göhre and Robatzek, 2008).

To date, numerous R genes have been cloned from a wide range of plant species and most of them can be classified into two main classes according to their domain organisation: the nucleotide binding leucine-rich repeat (NB-LRR) genes and the extracellular LRR genes (Jones and Dangl, 2006). The NB-LRR genes represent the largest class of R genes and can be further subdivided into coiled-coil (CC)-NB-LRR and Toll-interleukin-1 receptor (TIR)-NB-LRR genes according to their N-terminal domain. More than 150 proteins with NB-LRR domain structure have been predicted in *Arabidopsis* (Chisholm *et al*., 2006).

To date, direct interaction between R and AVR has been observed only infrequently. For example, AVR-Pita from *M. grisea* and Pi-ta from rice was the first AVR/R protein pair that was shown to interact directly *in vitro* (Jia *et al*., 2000). Interestingly, *RRS1* which is also involved in resistance of *A. thaliana* to *C. higginsianum* (see above) was also shown to physically interact with its corresponding effector PopP2 from *Ralstonia solanacearum.*

Several NB-LRR proteins have been shown to recognize effectors indirectly by detecting the products of their action on host targets, consistent with the 'guard hypothesis' formulated by Dangl and Jones (2001). The most extensively studied guarded host protein is *Arabidopsis* RIN4 (RPM1 interacting protein 4), which is a negative regulator of PTI (Kim *et al*., 2005). Three unrelated *Pseudomonas syringae* effector proteins (AvrRpm1, AvrB and AvrRpt2) modify RIN4, which leads to activation of the CC-NB-LRR immune receptors RPM1 and RPS2. AvrRpt2 is a cysteine protease and cleaves RIN4, thereby activating RPS2 (Axtell and Staskawicz, 2003; Mackey *et al*., 2003), whereas the presence of AvrB and AvrRpm1 mediates hyper-phosphorylation which is predicted to activate RPM1 (Kim *et al*., 2005).

1.2.5 The latest 'zag' of the zigzag: co-evolved effectors overcoming resistance

The complex interaction between RPM1, RPS2, AvrRpt2 and AvrRpm1 is considered to be the outcome of a molecular arms-race between plant and pathogen, in which both opponents try to overtrump each others innovations, leaving only temporary winners.

Suppression of ETI by bacterial effectors has been described several times (Abramovitch *et al*., Guo *et al*., 2009; Macho *et al*., 2010). In fact, suppression of ETI was also recently reported for eukaryotic filamentous pathogens: Halterman and co-workers (2010) reported that *Phytophthora infestans* IPI-O4, a variant of the diverse multigene effector family *IpiO*, was found to suppress IPI-O1-induced HR mediated by the corresponding R gene *RB* of the wild potato species *Solanum bulbocastanum*. The presence of IPI-O4 was highly correlated with increased aggressiveness of a surveyed set of *P. infestans* isolates.

The first Ascomycete effector shown to defeat ETI was identified in *Fusarium oxysporum* f.sp. *lycopersici*: secretion of Avr1 by this xylem-colonizing fungus triggered resistance in tomato plants carrying the corresponding *I* resistance gene, but suppressed resistance in tomato plants carrying *I-2* or *I-3* (Houterman *et al*., 2008). These findings allowed the molecular reconstruction of the 'agricultural' arms-race that occurred over the past decades since *I*, *I-2* and *I-3* have been introgressed into commercial tomato cultivars and permitted the prognosis of resistance gene combinations providing durable resistance (Houterman *et al*., 2008; Takken and Rep, 2010).

1.2.6 Fungal effectors carry the marks of ongoing co-evolution with host plants

Performing sequence similarity-based database searches with pathogen effectors usually is a tedious and fruitless undertaking. A hallmark of many (although not all) effectors is that they appear to be precedents without any similarity to known proteins or domains and with a limited, though occasionally patchy phylogenetic occurence. This may be explained by (i) their rapid evolution that precludes the detection of orthologues with increasing phylogenetic distance, (ii) gene losses, that may be selected for, especially for avirulence genes, and (iii) horizontal gene transfers, a mechanism that allows the acquisition of new molecular weapons (van der Does and Rep, 2007; Aguileta *et al*., 2009). The high rate of molecular evolution observed in effectors is a result of mutations, driven by extensive sequence diversification, gene expansion and genetic rearrangements (Stergiopoulos and Wit, 2009).

As a consequence of the arms race with hosts, avirulence genes show accelerated mutation rates compared to genes in the core genome which are not involved in the interaction with the host. The ratio of non-synonymous to synonymous

nucleotide substitution rates is a valuable parameter to detect genes that are under positive selection (Aguileta *et al*., 2009). Positive selection, by definition, favours non-synonymous nucleotide substitutions to change or to optimize the function of the protein, resulting in divergent phenotypes (diversifying selection). Resulting effector alleles that increase the reproductive success of the pathogen will be immediately favored by natural selection and positively selected. (Aguileta *et al*., 2009; Hogenhout *et al*., 2009). Signs of positive selection were found, for example, in the effector genes *Avr4* from *Cladosporium fulvum* (Stergiopoulos *et al*., 2007), *Avr-Pita* from *M. grisea* (Orbach *et al*., 2000) and the effector locus *AvrL567* from the flax rust *Melampsora lini* (Catanzariti *et al*., 2006; Dodds *et al*., 2006). In these examples, the avirulence gene was shown to be directly recognized by the corresponding resistance protein. It appears that direct Avr/R interaction correlates with point mutation-driven allelic variation of *Avr* genes, which abolishes recognition without affecting the virulence function of the protein (Stergiopoulos and Wit, 2009).

In contrast, the jettisoning of avirulence effectors appears to be the method of choice for pathogens in cases of indirect recognition by R proteins, which imposes selection against effector function rather than structure (Stergiopoulos and Wit, 2009). In the face of strong selection pressure imposed by a resistant plant cultivar, the beneficial effect of gene loss is higher than the associated fitness penalty. Alternatively, a repertoire of functionally redundant effectors could compensate for the gene loss and thus minimize the fitness penalty involved. Prominent examples for effector gene deletions being the main mechanism for loss of avirulence include *Avr9* of *C. fulvum* (Stergiopoulos *et al*., 2007), *AvrLm1* (Gout *et al*., 2007) of *Leptosphaeria maculans*, and *Avr-Pita* of *M. grisea* (Zhou *et al*., 2007).

Conspiciously, many effector loci are surrounded by transposable elements (Stergiopoulos and Wit, 2009). The most extreme example for this to date is the above-mentioned gene *AvrLm1* from *L. maculans*, the causal agent of black leg disease on *Brassica* crops. AvrLm1 was the only predicted gene within 270 kb of a heterochromatin-like genomic region which is essentially composed of nested long tandem repeat (LTR) retrotransposons (Gout *et al*., 2006). Repetitive elements can trigger frequent genomic rearrangements (Daboussi and Capy, 2003), thus enabling higher genetic flexibility to rapidly overcome R-mediated resistance. Subtelomeric regions of chromosomes also constitute highly dynamic chromatin and appear to be a playground for *M. oryzae* effectors (Farman, 2007).

However, there are some exceptions from the above-mentioned observation that fungal secreted effectors do not have homologues or recognizable protein domains. For example, AvrP123 from *M. lini* and EPI1 from *P. infestans* contain a motif typical for the Kazal family of serine protease inhibitors (Tian *et al*., 2004; Catanzariti *et al*., 2006). Avr-Pita from *M. grisea* has similarity to metalloproteases *via* its metalloprotease domain (Orbach *et al*., 2000). AvrP4 from *M. lini* shows homology to cystine-knotted proteins, as does Avr9 of *C. fulvum* (Catanzariti *et al*., 2006; van den Hooven *et al*., 2001). *C. fulvum* Ecp6 contains LysM chitin-binding domains and is remarkably conserved in several fungal species, including *Colletotrichum* spp. (Bolton *et al*., 2008; de Jonge *et al*., 2010; Perfect *et al*., 1998).

1.2.7 Destination of pathogen effectors in the host tissues

Effectors of filamentous pathogens can be divided into apoplastic and cytoplasmic effectors. Effectors from exclusively extracellular pathogens such as *C. fulvum* often contain a large and even number of cysteine residues. These cysteines might be involved in disulfide bridge formation, which provides protein stability in the protease-rich host apoplast (Stergiopoulos and Wit, 2009). Well-studied examples are Avr4 and Avr9 of *C. fulvum*, for which disulfide bonds between cysteine residues were required for stability and activity (van den Burg *et al*., 2003; van den Hooven *et al*., 2001). The virulence function of many extracellular effectors includes protection against hydrolytic host enzymes, e. g. plant pathogenesis-related proteins like secreted chitinases, proteases and glucanases. As an active counter-defence mechanism, inhibitiors of host hydrolases have evolved, which in turn have been defeated by plants employing cognate resistance genes (Rooney, 2005; van der Hoorn and Kamoun, 2008)

In contrast, the majority of effectors described from filamentous pathogens are considered to act in the host cytoplasm. In most cases, experimental evidence for effector uptake is lacking and their intracellular localization is infered from the cytoplasmic location of their corresponding host R proteins (Stergiopoulos and Wit, 2009). However, in a few cases the translocation of fungal effectors into host cells could be shown experimentally. For example, RTP1, a protein of the bean rust fungus *Uromyces fabae*, was found to be secreted into the extrahaustorial matrix, from which it appeared to enter the plant cytoplasm and nucleus at late stages of infection (Kemen

et al., 2005). Similarly, AvrM from *M. lini* was shown recently by immunofluorescence to be translocated into flax cells at late stages of infection (Rafiqi *et al*., 2010). However, the uptake mechanism remains to be elucidated. Several studies point to an as yet unknown host-encoded translocation machinery, since it was shown that oomycete and rust effector protein-reporter fusions can enter the host cell in the absence of the pathogen (Dou *et al*., 2008; Rafiqi *et al*., 2010). In contrast, uptake of ToxA, a host-selective toxin from *Pyrenophora tritici-repentis*, which is internalized into sensitive wheat cultivars, is dependent on a solvent-exposed Arg-Gly-Asp-containing loop which appears to interact with the host plasma membrane (Manning *et al*., 2008). These authors proposed that uptake occurs *via* receptor-mediated endocytosis, which must require the subsequent escape of internalized proteins from endosomes in order for them to exert cytoplasmic activity. For *Magnaporthe* effectors, uptake into host cells was recently correlated with accumulation of the proteins within biotrophic interfacial complexes, which are structures into which fluorescently labelled effectors appear to be focally secreted (Mosquera *et al*., 2009; Khang *et al*., 2010). The latter study provided a very elegant strategy to improve visualization of effector translocation into the infected and neighboring uninfected host cells by adding nuclear localization signals to fusion proteins between effectors and fluorescent proteins so that fluorescence becomes concentrated into a small compartment.

Interesting clues to effector internalization come from oomycete research, where a conserved RXLR motif was initially discovered in the sequence of cloned oomycete avirulence proteins that are recognized in the plant cytoplasm. This motif is located within 60 amino acids downstream of the N-terminal signal peptide for secretion and is followed by a stretch of acidic amino acids. Both motifs were required *in vivo* to drive effector-ß-glucuronidase fusions into host cells (Whisson *et al*., 2007). The position and sequence of the RXLR motif are similar to, and interchangeable with, an amino acid motif from effectors of the malaria pathogen *Plasmodium falciparum*, which is required for targeting effectors into red blood cells (Bhattacharjee *et al*., 2006; Grouffaud *et al*., 2008). The RXLR motif has allowed the bioinformatic identification of a highly expanded effector gene family that proliferated within oomycete genomes (Jiang *et al*., 2008; Haas *et al*. 2009). Although experimental evidence is lacking, conserved amino acid motifs have recently been proposed to

function for host translocation of effectors of true fungi, like rusts and mildews (Rafiqi *et al*., 2010; Godfrey *et al*., 2010).

1.3 Thesis aims

The mechanisms by which hemibiotrophic *Colletotrichum* species establish and maintain a biotrophic interaction with their hosts is completely unknown. Extrapolation from other pathosystems strongly suggests that the secretion of proteinaceous effectors plays a key role in host manipulation. One aim of the present study was therefore to determine the repertoire of effector proteins deployed by *C. higginsianum* during plant infection. *C*olletotrichum *h*igginsianum Effector Candidates (ChECs) are defined herein as proteins that are predicted to be solubly secreted and which show no homology to known proteins or are similar to presumed effectors of other plant pathogens. Given the highly transient and localized biotrophic phase of *C. higginsianum*, it was hypothesized that appressoria, and the penetration pegs that emerge from them, must be a key source of secreted ChECs for the establishment of biotrophy. Therefore, the other major goal of this study was to functionally characterize selected ChECs that are preferentially expressed before or during host penetration. It should be noted that, when this project was initiated, ChEC selection was constrained by the limited availability of EST data and genomic resources, which increased substantially in years two and three of the study.

Specific objectives were as follows:

- To produce EST libraries specific to appressoria formed *in vitro* and *in planta*.
- To use computational prediction tools to identify ChECs from EST collections representing different stages of *in planta* pathogenesis and to define the ChEC repertoire preferentially expressed during biotrophy-relevant stages.
- To directly identify proteins secreted by infection structures *in vitro* using a proteomics approach.
- To establish procedures for targeted gene replacement in *C. higginsianum* and to use this approach to test the role of selected *ChEC*s in fungal virulence.
- To determine the ability of selected ChECs to suppress plant cell death using transient expression assays.
- To localize selected ChECs during host infection.

2 Materials and methods

Basic molecular biological techniques (e. g. agarose gel electrophoresis, SDS-PAGE, preparation of transformation-competent cells, nucleic acid handling etc.) as well as standard buffers, stock solutions and growth media were based on recipes and protocols from Sambrook *et al.* (1989).

2.1 Plant and fungal material and growth conditions

Arabidopsis thaliana Landsberg *erecta* (Ler-0) and Columbia (Col-0) as well as *Brassica rapa* subsp. *chinensis* (Horticulture Research International (HRI) accession number 007570), *Brassica napus* subsp. *napobrassica* (HRI accession number 003470) and *Brassica carinata* (HRI accession number 013160) were used for plant infection assays.

Plants were grown in a peat-based compost. *Arabidopsis* seeds were stratified for two days at 4 °C in darkness to allow for synchronous germination. Germination was induced by transfer of the plants to controlled environment chambers under a regime of a 10-h light period at 150 to 200 mE $m^{-2}s^{-1}$, 65% relative humidity, with 22 °C during the day and 20°C during the night. *Nicotiana benthamina* was grown under long day conditions in a greenhouse with an ambient temperature of 22-25°C and high light intensity. Agroinfiltration experiments were conducted with 4-6-week-old plants.

C. higginsianum isolate IMI 349063A was used for EST generation, as background strain for targeted gene replacements and for genome-sequencing. In addition, the Δ*KU70* mutant impaired in non-homologous end-joining was also used as background strain for targeted gene replacements and was maintained on Czapek-Dox medium (Difco) supplemented with bialaphos (10 mg/mL). This mutant was prepared in the IMI 349063A background and was a gift from Dr. Gento Tsuji (Kyoto Prefectural University, Japan). Fungal cultures were obtained from the following culture collections: LARS, Long Ashton Research Station, MAFF, Japanese ministry of agriculture fisheries and food and IMI, International mycological institute of the UK. Fungal culture were grown grown and brought to sporulation as described by O'Connell *et al*. (2004). Conidial suspensions were obtained by irrigation of 8- to 12-day-old cultures and the spore concentration was adjusted using a haemocytometer. Fungal transformants were grown on potato dextrose broth or potato dextrose agar

(both Difco), supplemented with hygromycin (100 µg/mL) and Cefotaxime and Spectinomycin (both 50 µg/mL) (all Sigma-Aldrich).

2.2 Plant infection

To obtain fungal material for RNA preparation during *in planta* pathogenesis, the abaxial surface of detached leaves was densely inoculated and incubated as described previously (Takahara *et al*., 2009).

For plant infection assays of ChEC mutants, four-week-old *Arabidopsis* (Col-0) plants were spray-inoculated with spore suspension (1×10^{-5} spores/mL) using an atomizer with a defined number of puffs. For experimental replicates, care was taken to inoculate plants at the same time of the day (0.5-3 h before dusk). Inoculated plants were placed in sealed propagator boxes to maintain 100 % humidity and incubated in a controlled environment chamber at 25 °C, 20 °C or 14 °C (16-h light period, 20-60 µmol). For droplet inoculation of leaves, 1.5 µL droplets of spore suspension (5×10^{4} spores/mL) were placed on leaves of intact plants and were incubated as above (at 25 °C). After symptom development (6 dpi), leaves were detached and photographed on a light screen. To determine appressorial penetration efficiency, cotyledons of synchronously germinated Col-0 seedlings were spray-inoculated and incubated as above (at 25 °C). Seedlings were harvested after 42 hpi and 54 hpi and cleared in 3:1 ethanol:chloroform before microscopy.

2.3 Preparation of epidermal peels from infected leaves.

Epidermal peels from infected detached leaves were prepared by adhering the adaxial surface with double-sided tape and quickly stripping off the epidermis using two tweezers with fine, curved tips. Pieces of remaining mesophyll were quickly cut off with a razor blade and the epidermal peels (usually 15 mm^2 per leaf) were flash-frozen in liquid nitrogen and stored at -80 °C until RNA isolation. The following infection time points were sampled: 5 hpi (germling stage for RT-PCR), 20 hpi (appressorial stage for EST library), 22 hpi (appressorial stage for RT-PCR and EST library), 42 hpi (biotrophic stage for RT-PCR) and from mock-inoculated leaves (for EST library).

2.4 Production of *in vitro* infection structures

Harvested spores were washed twice by centrifugation (1000 g, 5 min) and resuspended in sterile distilled water. To produce a monolayer of appressoria, 45 ml of conidial suspension (2×10^6 spores ml^{-1}) was placed into a 15 cm-diameter polystyrene Petri dish, and after allowing the spores to settle and attach to the polystyrene for 40 min, a disc of sterilized nylon mesh (50 µm pore-size) was applied to the liquid surface. The liquid was then decanted, leaving the nylon mesh on the base of the dish to provide a continuous thin film of water by capillary action. The dishes were incubated in a humid box at 25 °C for 5-6 h (germ tubes with appressorial initials) or 18–22 h (mature, fully-melanized appressoria). All manipulations were performed aseptically. The developmental stage and average number of appressoria per dish were determined microscopically.

2.5 Staining of protein haloes around conidial germlings with colloidal gold

Well-spaced conidial germlings formed on the surface of a polystyrene Petri dish (see above) were fixed with 4 % p-formaldehyde for 30 min, washed three times for 5 min with phosphate-buffered saline (PBS) and stored at 4 °C in PBS until all samples from the time-course experiment had been prepared in this manner. The Petri dishes with the attached fungal structures were incubated for 15 min at 37 °C with PBS containing 0.3 % (v/v) Tween-20, followed by three washes with the same buffer at room temperature. The colloidal gold solution (Protogold, Brititsh BioCell International, Cardiff, UK) was added to the Petri dishes until the dish base was completely covered with solution, and incubated for 30 min with continous agitation. After thorough washing with distilled water, the dishes were dried and an approx. 2 x 2 cm area was delimited using a hydrophobic liquid barrier marker. Silver enhancer solution (Brititsh BioCell International, Cardiff, UK) was prepared according to the manufacturer's instructions and added to the marked area. Staining development was monitored continuously by microscopic inspection under low-light conditions and the reaction was stopped for all samples after 100 sec by thorough washing with distilled water. Samples were stored at 4 °C under a film of water until microscopic analysis.

2.6 Microscopic analysis

Fungal infection structures formed on polystyrene and stained protein haloes were directly inspected with a 63x long working distance water-immersion lens (Zeiss). Infected leaf tissue was cleared in ethanol-chloroform (3:1) mixture overnight followed by overnight incubation in lactophenol. The cleared samples were then mounted in glycerol prior to microscopy with Nomarski differential interference contrast. Images were recorded with a Zeiss Axioplan 20 microscope (Carl Zeiss, Oberkochen, Germany) connected to a Nikon DS-L1 imaging system. Confocal images were obtained with a Leica TCS-SP2 confocal laser scanning microscope (http://www.leica.com). For imaging GFP fluorescence, excitation was provided by the 488 nm emission line of an argon/krypton laser, and the resulting fluorescence was collected between 503 and 602 nm. For imaging mCherry fluorescence, excitation was provided by the 563 nm emission line of a helium/neon laser. The fluorescence emission spectrum of transformant culture supernatant was measured with a Zeiss LSM confocal laser scanning microscope, after excitation at 435 nm. To assess the presence and ultrastructure of penetration pores, appressoria were disrupted by scraping (see below), and cell wall fragments remaining attached to the polystyrene were air-dried, sputter-coated with platinum and examined at 10 kV using a Zeiss SUPRA 40VP field-emission scanning electron microscope.

2.7 Fungal RNA extraction

RNA from spores, mycelium and *in vitro* germlings and appressoria was prepared using TRIzol (Invitrogen), followed by a clean-up with theRNeasy Mini Kit (Qiagen). RNA from epidermal peels and leaves from later stages of infection (biotrophy-necrotrophy switch, late necrotrophy) was extracted directly using the RNeasy Mini Kit (Qiagen). All RNAs were on column-treated with RNase-free DNAse (Qiagen).

To extract RNA from *in vitro* infection structures, sterile water (approx. 20 mL) was added to each polystyrene dish to gently separate the nylon mesh from the cells without damaging them, followed by quick decanting of the water and removing residual liquid by vigorous shaking. The RNA of conidial germlings was extracted by scraping them with a plastic cell scraper (Costar, Corning Incorporated) from the polystyrene surface into liquid nitrogen prior to grinding with mortar and pestle and treatment with TRIzol. The RNA of mature appressoria was extracted by scraping

them directly into TRIzol with a plastic cell scraper, which was found to result in effective disruption of the appressorial cells (Fig. 3 C).

To prepare RNA from fungal saprophytic mycelium, the liquid culture was filtered through miracloth (Calbiochem) and the mycelium was quickly blotted on Whatman paper to remove excess of medium. The mycelium was flash-frozen in liquid nitrogen and then ground with a mortar and pestle.

2.8 Expression analysis with RT-PCR

Total RNA (2.5 µg) was mixed with 50 ng Oligo-dT-primer, heated to 80 °C for 3 min to remove any secondary structures and than quickly chilled on ice. The following components were added (the final concentration in a 20 µL-reaction is indicated): 1x First strand buffer (Invitrogen), 0.5 mM dNTPs (Roth), 10 mM dithiothreitol (Invitrogen), 0.5 U/µL RNase Inhibitor (Roche) and 10 U/µL SuperScript II (Invitrogen). Reverse transcription was carried out for 5 min at 23 °C, 1 h at 42 °C and 10 min at 50 °C, followed by heat inactivation at 80 °C for 3 min. The resulting cDNAs were diluted 1:50 to 1:100 with TE and represented the cDNA stock that was used for RT-PCR experiments. PCR was carried out using Taq DNA polymerase (Amplicon) according to the manufacturer's instructions. The *C. higginsianum* β-tubulin gene was used to adjust cycle numbers and loading of individual PCR reactions to allow for variation in fungal biomass. Each RT-PCR was performed at least three times with similar results. Sequences of the employed primers are listed in Table 1.

2.9 Fungal transformation and screen of fungal transformants

Fungal transformation was carried out as described by Huser and co-workers (2009). For targeted gene replacement experiments, fungal transformants were screened by Mulitplex-PCR with primers specific for double-cross-over events (Tab. 1). For this, template DNA from transformant mycelium was extracted with Chelex-100 resin (Talhinhas *et al*., 2008). Usually, approximately 1 mm^3 mycelium was used. For bulk DNA extraction, the colonies from several Petri dishes were pooled. To identify transformants expressing consititutively the ChEC4-mCherry fusion protein, saprophytic mycelium of hygromycin-resistant colonies was screened by RT-PCR to detect full-length ChEC4-mCherry transcripts.

Table 1: Primer sequences used in this study.

Primer	Usage remark	Sequence (5'→3')
For cloning of protein coding sequences		
ChEC3 ORF fw		CACCATGTACTTTACAAACATCTTCG
ChEC3 ORF –SP fw	without signal peptide	CACCATGCTCCCTGCCAATAAGCATATAGG
ChEC3 ORF rev	with stop codon	TCAACATTTAAACTTTCCACAG
ChEC3a ORF fw		CACCATGTACGCCACCAAGATCATCT
ChEC3a ORF –SP fw	without signal peptide	CACCATGCTCCCTGCTGAAGTGCATAAGG
ChEC3a ORF rev	with stop codon	TTAACACTTGACCTTCCCACAA
ChEC5 ORF fw		CACCATGCAGCTCTCCGGCCTCGTC
ChEC5 ORF –SP fw	without signal peptide	CACCATGGTCTCCGTCTCCTACGACACCG
ChEC5 ORF rev	with stop codon	CTACAGGCCGCAGGCGTTAAGG
ChEC4 ORF fw		CACCATGAAGCTCCTTCTACCTGTAACCATTCTCG
ChEC4 ORF –SP fw	without signal peptide	CACCATGGCTCCCACGGGCGATAACATAAGCACTTCCATTGC
ChEC4 ORF rev	without stop codon	CTGGCCAACCTTGCCACCG
ChNLP1 ORF fw		CACCATGGCCCCCTCGCTCTTCCGTC
ChNLP1 ORF rev		TTACAACGCGGCCTTGCCG
ChNLP1 ORF rev oS	without stop codon	CAACGCGGCCTTGCCG
Chitinase ORF fw		CACCATGTCCTTCGCTAAGTTGTCGCTCGCGGCCTTGC
Chitinase ORF rev		GTATCCCGCAAAATACGTCGAG
mCherry fw		CACCATGGTGAGCAAGGGCGAGGAGGATAACATGG
mCherry rev		TTACTTGTACAGCTCGTCCATGC
upChEC4-fw	To amplify the ChEC4 promoter	GCCAACTCGAAACCAGTATCAAC
mCherry-trpCterm	For fusion overlap PCR of mCherry and the trpC terminator of *A. nidulans*	CGGCATGGACGAGCTGTACAAGTAATTTAATAGCTCCATGTCAACAAG
ChEC4-3'-mCherry-f	For fusion overlap PCR of ChEC4 and mCherry	CCGCCGGTGGCAAGGTTGGCCAGGCGATGGTGAGCAAGGGCGAGGAGGATA
For Cloning of targeted gene replacement construct and multiplex PCR screen		
HPH fw	Amplifies the hygromycin resistance cassette	CTTGGCTGGAGCTAGTGGAT
HPH rev	Amplifies the hygromycin resistance cassette	GGTCGGCATCTACTCTATTCCTT
XbaI-Lfl-ChEC1-fw	Amplifies the upstream flanking sequence with the following primer	AAAAAATCTAGACCCAGAATCACTTGCAGTAGGTC
Lfl-ChEC1-HPH-ref	Overlaps with hygromycin resistance cassette	TCCACTAGCTCCAGCCAAGACCGGATACTGCACAGACTTCC
Rfl-ChEC1-HPH-fw	Amplifies the downstream flanking sequence with the following primer. Overlaps with hygromycin resistance cassette	AATAGAGTAGATGCCGACCATGTCAAACATGGCATCAAAGG
BamHI-Rfl-ChEC1-R		AAAAAAGGATCC GATGTACGGGATGTGAATCTCAG
upLfl-ChEC1-fw	Together with Lfl-ChEC1-HPH-rev in Multiplex PCR	GCCCAACAAGAGCTGATTACG
upRfl-ChEC1-rev	Together with Rfl-ChEC1-HPH-fw in Multiplex PCR	TTCGCTGCATTCAGGAGTA
XbaI-Lfl-ChEC2-fw	Amplifies the upstream flanking sequence with the following primer	AAAAAATCTAGACGGAACTTCTTCGCTGATTCTC
Lfl-ChEC2-HPH-rev	Overlaps with hygromycin resistance cassette	CACTAGCTCCAGCCAAGGGATTGCTTGCTTGTTTGTCTG
Rfl-ChEC2-HPH-fw	Amplifies the downstream flanking sequence with the following primer. Overlaps with hygromycin resistance cassette	AATAGAGTAGATGCCGACCGGGTTGTACTGGGCTGTGTA
BamHI-Rfl-ChEC2-rev		AAAAAAGGATCCGTGGTTGTGATTGTCCTCAACC
upLfl-ChEC2-fw	Together with Lfl-ChEC2-HPH-rev in Multiplex PCR	CCTCTTGCTCCTCGTGAACTTG
upRfl-ChEC2-rev	Together with Rfl-ChEC2-HPH-fw in Multiplex PCR	CTGATGTGCGAATGTCTCGTCT
EcoRI-Lfl-ChEC3-fw	Amplifies the upstream flanking sequence with the following primer	AAAAAAGAATTCGCGGAGTTTGTTGTATTACCTTG
Lfl-ChEC3-HPH-rev	Overlaps with hygromycin resistance cassette	TCCACTAGCTCCAGCCAAGGGATTTGCGTATAGGAGACAGTCA
Rfl-ChEC3-HPH-fw	Amplifies the downstream flanking sequence with the following primer. Overlaps with hygromycin resistance cassette	AAAAAAGAATTCAATAGAGTAGATGCCGACCGAGGGGCCAAGACTAGTGACC

Primer	Usage remark	Sequence (5'→3')
EcoRI-Rfl-ChEC3-rev		AAAAAAGAATTCATAGACGAGCTACGACTACG
upLfl-ChEC3-fw	Together with Lfl-ChEC3-HPH-rev in Multiplex PCR	TCCCGGCTCCTTTAATACACTC
upRfl-ChEC3-rev	Together with Rfl-ChEC3-HPH-fw in Multiplex PCR	TCTTTTATACTGGCGCTTTAGCC
EcoRI-Lfl-ChEC3-fw-2	For the shorter construct B	AAAAAAGAATTCTTCTTACACTACCTTAGAGACTCTAGTAAAGC
EcoRI-Rfl-ChEC3-r2	For the shorter construct B	AAAAAAGAATTCGTGACTAGCTACGAT
cDNA generation and RT-PCR		
OligodT primer		CGGCCGCGAATTCACTAGTGTTTTTTTTTTTTTTTT
ChEC1 fw		CAAACACAATCGCCAAAAATGAAGTCC
ChEC1 rev		CTCGCGCCCTGCAACAATACCTG
ChEC2 fw		ACTGTGGACGCGGGGTAAATGAG
ChEC2 rev		CCTTGCAGTTGGGGTAGTGGTTGTC
ChEC3 fw		TACTTTACAAACATCTTCG
ChEC3 rev		TCAACATTTAAACTTTCCACAG
ChEC3a fw		TCCTCCTTCTCACTGTTCCCTTTG
ChEC3a rev		ACCTTCCCACAATGTGCTAGGTTC
ChEC4 fw		CATCATTAGGACGATTTTCCAAGC
ChEC4 rev		TAGGACAGCGAGAATGGTTACAGG
ChEC5 fw		GTCTCCGTCTCCTACGACACCG
ChEC5 rev		CTACAGGCCGCAGGCGTTAAGG
ChEC6 fw		TACAGAAAACATGAAGTCCGCCATT
ChEC6 rev		GTCTCTCGTAAAGCACGAGGGATCT
ChNLP1 fw		ATGGCCCCCTCGCTCTTCCGTC
ChNLP1 rev		TTACAACGCGGCCTTGCCG
ChNLP2 fw		AGGTTCAACCCACTTCTCCATGTC
ChNLP2 rev		TCGTTTAGAGCACTCTGCATCGTC
ChNLP3 fw		TACTGGCAGTCTAGGTGGTGGTTTG
ChNLP3 rev		GCACTTGGCTCGCATAATAATTGG
ChNLP4 fw		ATACCCTCCTGAGGCGTAAAGCTC
ChNLP4 rev		AAAACCACTTCCCAAGGTGATATCTC
ChNLP5 fw		GGCACTACTACCTGACTGTCGTCGT
ChNLP5 rev		GTTCGTATTGGATGCCGTTGAACT
ChNLP6 fw		TGAGGCCACTCTCAAGTTCATTACC
ChNLP6 rev		CGGTTGTCCAACAAAAATGAGACAC
Tubulin fw		GCCCTATTCTCGCTCGTCTTCC
Tubulin rev		GGGCTCCAAATCGCAGTAAATG
Southern probes		
ChEC1 fw		GATCAAACACAATCGCCAAAAATGAAGTC
ChEC1 rev		TGTTCCTTTGATGCCATGTTTG
ChEC2 fw		ATGCTCTACTCCAAAATCCTCATCGCCGCC
ChEC2 rev		ATCATCTAAGCCTGGTTGACG
ChEC3 fw		GATACGCAAATCCTTAGTATTAAAGAAGC
ChEC3 rev		ATCTTTGCATCACTTGTATTGC
Hygromycin fw		CGTTGCAAGACCTGCCTGAA
Hygromycin rev		GGATGCCTCCGCTCGAAGTA

2.10 Southern blot analysis

Extraction of fungal genomic DNA was carried out as described by Huser and co-workers (2009). For Southern blot hybridization, 10 µg of genomic DNA was digested to completion with 10 U of restriction enzyme EcoRV (New England Biolabs, Frankfurt, Germany). After gel-electrophoresis, the DNA was transferred onto Amersham Hybond N++ membrane (GE Healthcare) by alkaline transfer. The membrane was hybridized with a full-length cDNA probe, labelled with digoxigenin (DIG)-dUTP, using the PCR DIG probe synthesis kit (Roche, Mannheim, Germany) according to the manufacturer's instructions.

For characterization of transformants, the membrane was hybridized and washed under high stringency conditions (prehybridization and hybridization at 50 °C, high-stringency wash at 68 °C with 0.1x SSC containing 0.1 % SDS). For detection of homologous sequences in different *Colletotrichum* species and isolates, the membrane was hybridized and washed under low stringency conditions (prehybridization and hybridization at 35 °C, high-stringency wash at 60 °C with 0.5x SSC containing 0.1 % SDS). Assuming 1.1 M Na+ and 50 % formamide, these conditions were calculated to allow 25 % mismatches between probe and target DNA. Probe hybridization was detected using the DIG luminescence detection kit according to the manufacturer's instructions (Roche). Membranes were stripped afterwards for further hybridizations using alkaline treatment, as recommended by the manufacturer.

2.11 Cloning of fungal sequences

All preparative PCRs for cloning of fungal sequences were carried out with the proof-reading polymerase *Pfx50* (Invitrogen), following the manufacturer's instructions. Final concentrations of dNTP, primer and enzyme in 50 µL reactions were 0.3 mM, 0.3 µM and 0.1 U/µL, respectively. The thermal cycling conditions were 94 °C for 2 min, and 30 cycles of 94 ° for 15 sec, X °C for 20 sec, 68°C for 1 min/kb and final extension at 68 °C for 5 minutes with X being 5 °C lower than the melting temperature of the primer, which was predicted with the primer3 program (http://biotools.umassmed.edu/bioapps/primer3_www.cgi) using default parameters. Preparative PCR reactions were purified with NucleoSpin extract II Kit (Macherery&Nagel) using columns in the case of discrete amplicons, or after separation by gel-electrophoresis in the case of multiple amplicons. Chemically-

competent *Escherichia coli* DH5α cells (Top10 (Invitrogen) or in-house made) were used for propagation of plasmids containing cloned inserts. Bacterial clones were checked by colony PCR with insert and vector-specific primers before plasmid isolation (NucleoSpin Plasmid Kit, Macherery&Nagel). Insert sequences were verified by sequencing in-house (ADIS/Max Planck Genome Centre Cologne). For fungal transformation, verified constructs were introduced into transformation-competent cells of *Agrobacterium tumefaciens* strain C58C1, carrying a genomic rifampicin resistance (50 µg/mL).

2.11.1 Cloning of targeted gene replacement constructs

The upstream and downstream sequences flanking the target genes were obtained by primer walk sequencing of the corresponding clone of a cosmid library of *C. higginsianum* genomic DNA (Huser *et al*., 2009). Later, when a draft assembly of the *C. higginsianum* genome was available, flanking sequences were obtained by identification of the corresponding genomic contig by BLAST searches. Flanking sequences were amplified individually using genomic DNA of *C. higginsianum* isolate IMI 349063A and fused to a hygromycin resistance gene cassette by overlap fusion PCR (Szewczyk *et al*. 2006). The hygromycin resistance gene cassette was amplified from pBIG2RHPH2 (Tsuji *et al*., 2003b). The 5' and 3' end of the final amplicon contained restriction sites provided by the primers (Tab. 1) which after digestion allowed ligation into the binary vector pBIG4MRBrev (Tanaka *et al*., 2007), digested with the corresponding restriction enzymes.

2.11.2 Cloning of a ChEC4-mCherry fusion

The full-length protein coding sequence (without stop codon) of ChEC4 was PCR-amplified using cDNA derived from epidermal peels infested with penetrating appressoria (see above) as template and fused in-frame to the mCherry coding sequence (Clontech) by overlap fusion PCR (Szewczyk *et al*. 2006). The resulting amplicon was blunt-ligated between the *Aspergillus nidulans trpC* promoter and *trpC* terminator sequence of the SmaI-digested binary vector pBIG4MRH-OV1, a derivative of pBIG4MRHrev (Tanaka *et al*., 2007) constructed by Dr. Hiroyuki Takahara at MPIPZ, Cologne.

2.11.3 Cloning of fungal coding sequences for transient expression assays

The protein coding sequences from ChEC4 (without stop codon) and ChEC3, ChEC3a, ChEC5 and a *C. higginsianum* predicted secreted chitinase (with stop codon) were amplified from cDNAs prepared from epidermal peels infested with penetrating appressoria or biotrophic hyphae (see above), respectively. The primers used to amplify full-length coding sequences or constructs lacking signal peptides or stop codons are shown in Table 1. A cDNA pool from infected leaves showing first appearance of pin-point water-soaked lesions was used to amplify ChNLP1 with and without its stop codon. All 5' primers were designed to carry the sequence 5'-CACC-3' at the 5'end, which allowed TOPO cloning using pENTR D-TOPO (Invitrogen). For ChEC constructs lacking their signal peptide for secretion, the codons following the predicted signal peptide cleavage site were fused to an artificial start codon. Cloned coding sequences were shuttled into the binary plant expression destination vector pB7WG2 (VIB Gent, Gent university) using Gateway recombination (Invitrogen), providing tag-less over-expression driven by the CaMV 35S promoter. *A. tumefaciens* strain C58C1 pGV2260 were used as the recipient strain. For a C-terminal translational fusion of ChEC4 to GFP, pXCSG GFP (Feys *et al*., 2005) was used as a destination vector. To express hemagglutinin (HA)-tagged ChNLP1, the cDNA lacking the stop codon was shuttled into the destination vector pXCSG3xHA (Feys *et al*., 2005), providing a C-terminal triple HA-tag.

A. tumefaciens strain GV3101 pMP90RK carrying the construct for INF1 expression (in pAMPAT) as well as the strains C58C1 pGV2260 carrying contructs for $Avr3a^{KI}$ and YFP expression (both in the destination vector pB7WG2) were provided by Dr. Ruslan Yatusevich (MPIPZ, Cologne).

2.12 Transient expression in *N. benthamiana*

Recombinant *A. tumefaciens* strains were grown in LB supplemented with appropriate antibiotics: rifampicin, carbenicillin, spectinomycin and streptomycin (all at 50 µg/mL) for constructs in pB7WG2 and bacterial strain C58C1 pGV2260; rifampicin (100 µg/mL), carbenicillin (50 µg/mL), kanamycin (25 µg/mL) and gentamycin (15 µg/mL) for constructs in pAMPAT and pXCSG3xHA; rifampicin and kanamycin (both at 50 µg/mL) for an *A. tumefaciens* strain carrying a construct for expression of p19, a viral suppressor of gene silencing (Voinnet *et al*., 2003). All bacterial cultures

were grown to stationary phase to maximize transformation efficiency (Marion *et al*., 2008). Bacterial cells were pelleted and resuspended in infiltration buffer (10 mM $MgCl_2$, 5 mM MES (pH 5.6) supplemented with 200 µM acetosyringone) before infiltration into the abaxial side of *N. benthamiana* leaves using a needle-less syringe.

Infiltration mixtures containing bacterial strains harbouring constructs for co-expression of cell death inducers (INF1 and ChNLP1) together with ChECs or YFP as control were mixed according to Table 2. Infiltration mixures were kept at room temperature for 2-4 h before infiltration into fully-expanded leaves of *N. benthamiana* plants. To allow pairwise comparisons, infiltration mixtures containing ChEC/cell death inducer constructs and YFP/cell death inducer constructs were infiltrated side-by-side into the same leaf. Plants were incubated in a controlled environment chamber (19 °C/21 °C day/night temperature cycles and 16-h-light/8-h-dark cycles) to which they were adapted at least 24 h before infiltration. Six to eight days after infiltration, infiltration site pairs were inspected in a blinded manner to determine whether the site co-expressing ChECs with cell death inducer showed reduced necrosis compared to the corresponding control site on the same leaf expressing YFP with cell death inducer.

Table 2. Final OD_{600} of recombinant *A. tumefaciens* strains used in infiltration mixtures.

	Final OD_{600} of respective *A. tumefaciens* strains expressing the indicated proteins				
Infiltration mixture	1. ChEC	2. ChEC	YFP	Cell death inducer	p19
For single ChEC expression	1.0	-	-	0.1	0.5
Corresponding YFP control	-	-	1.0	0.1	0.5
For co-expression of two ChECs	1.0	1.0	-	0.1	0.5
Corresponding YFP control	-	-	2.0	0.1	0.5

2.13 SDS-PAGE and Western blot analysis

Protein samples boiled for 5 min in 2x SDS sample buffer were subjected to SDS-PAGE on a gel containing 12 % polyacrylamide, followed by electroblotting on a Hybond ECL nitrocellulose membrane (Amersham, GE Healthcare). To monitor protein transfer and loading, the membrane was stained with 0.1 % Ponceau S (Sigma-Aldrich) in 5 % acetic acid, followed by extensive washes in PBS and photographic documentation. For HA and mCherry detection commercial antibodies were used (Roche and Clontech, respectively). The polyclonal anti-ChEC4 antibody was raised

against the synthetic peptide “YIFTDDPAAGGKVGQ” of ChEC4 by Eurogentec S.A., (Liège, Belgium) using proprietary procedures. Chemiluminescence was detected using ECL™ Western Blotting Detection Reagents (Amersham, GE Healthcare) according to the manufacturer’s instructions.

Preparation of fungal samples

Culture supernatant (4 mL) and mycelium of fungal liquid cultures were harvested by filtration. Mycelium was blotted on Whatman filter paper to remove access medium and flash-frozen in liquid nitrogen. After grinding with mortar and pestle, samples were thawed in 1 mL protein extraction buffer (50 mM Tris pH 8, 50 mM NaCl, 5 mM EDTA acid, 0.01 % Triton, 5 mM DTT) including 1x complete protease inhibitor (Roche)). Cell debris was removed by centrifugation, leaving the mycelial extract as supernatant. The culture supernatant was centrifuged (2000 g, 4 °C) to remove mycelium remnants. The sample was concentrated using Ultracel-10k centrifugal filter units (Millipore, 10 kDa cut-off) according to the manufacturer’s instructions. This resulted in 15x-concentrated samples which were frozen at -20 °C until further use. A Bradford assay (Quick start Bradford protein assay kit, BioRad) allowed determination of the protein concentration in the mycelial extracts and concentrated culture supernatants. Based on this, four times more mycelial proteins than supernatant proteins were loaded onto the gel to corroborate that the obtained signals were specific to the culture supernatant samples.

Preparation of *N. benthamiana* samples

Leaf discs (6 mm diameter) of agroinfiltrated areas of *N. benthamiana* leaves were harvested at 3 dpi, before the onset of visible necrotic symptoms. Eight leaf discs from sites expressing ChEC/cell death inducer were pooled, likewise eight sites expressing YFP/cell death inducer. After grinding in liquid nitrogen, ground tissue was thawed in 1 mL extraction buffer (see above).

2.14 Proteomic analysis of the secretome of germlings forming appressoria *in vitro*

The thin film of water surrounding mature appressoria formed on polystyrene Petri dishes (see above) was decanted and stored at -20 °C until further processing. The samples from several preparations were pooled, representing the liquid film

surrounding a monolayer of 2.9 x 10^9 appressoria in total. This sample was ultrafiltrated with Centricon concentrator units YM-3 (3 kDa cutoff, Amicon/Millipore) according to the manufacturer's instructions, resulting in 40x concentration. The proteins were precipitated with one volume of 10 % trichloroacetic acid in acetone overnight at –20 °C. After centrifugation at 10 000 g for 15 min at 4 °C, the supernatant was discarded and the pellet was washed with chilled 90 % acetone. Residual liquid was removed and, after drying on ice, the crude extract was stored at –80 °C until electrophoretic analysis.

Isoelectric focusing using a ZOOM strip (7.7 cm, pI 3-10), second dimension PAGE, tryptic in-gel digestion as well as mass spectrometry was carried out at the MPIPZ mass spectrometry facility as described by Noir and co-workers (2009). The peptide mass fingerprint (MS) and peptide fragment fingerprint (MS/MS) data were used to screen a six-frame translation of the *C. higginsianum* genome (version March 2009) and to identify the corresponding proteins using the ProteinScape 1.3 database system (Protagen AG, Bruker Daltonics, Bremen, Germany), which allowed Mascot (Matrix Science Ltd., London, UK) searches. Matching peptide sequences from protein spots, which gave rise to MS and/or MS/MS match scores exceeding the Mascot 95 % probability threshold, were used to identify the full-length ORF predicted with FGENESH (Softberry) using a *Fusarium* matrix within the corresponding genomic contig. The theoretical molecular weight of the predicted proteins was determined using EditSeq (Lasergene). Predictions of conserved domains and signal peptide predictions were conducted as described for the EST analysis (see below)

2.15 cDNA preparation for EST sequencing

Methods for preparation of the cloned cDNA library from mature appressoria formed *in vitro*, their Sanger-sequencing and EST assembly were described previously (Kleemann *et al*., 2008). cDNAs for 454 sequencing were prepared from three different stages of plant infection by Vertis Biotechnologie AG (Freising, Germany) using proprietary procedures, as described below.

For cDNAs representing the biotrophic stage, biotrophic hyphae were purified from infected leaves at 40 h after inoculation using fluorescence activated cell sorting and total RNA was extracted as described by Takahara *et al*. (2009). cDNA was synthesized using an oligo(dT) linker primer for first strand synthesis, and then amplified with 21 cycles of PCR using a high fidelity DNA polymerase. Normalization

was carried out by one cycle of denaturation and reassociation, and the double-stranded (ds) cDNA was separated from remaining single-stranded (ss) cDNA (normalized cDNA) by passing the mixture over a hydroxylapatite column. The resulting ss cDNAs were amplified with eight PCR cycles.

For cDNAs representing the necrotrophic infection stage, heavily infected, macerated leaf tissue (72 hai) was ground in liquid nitrogen using a mortar and pestle and 100 µg total RNA was isolated using TRIzol reagent (Invitrogen) following the manufacturer's instructions. Full length cDNA was synthesized from polyadenylated RNA after incubation with calf intestine phosphatase and tobacco acid pyrophosphatase, followed by ligation of an RNA adapter to the 5' phosphate of decapped mRNAs. First strand cDNA synthesis was performed with an oligo(dT)-adapter primer and M-MLV RNase H reverse transcriptase. Resulting cDNA was amplified with 17 cycles of PCR and after one cycle of normalization as described above, the ss cDNAs were amplified with 10 PCR cycles.

To enrich for transcripts expressed in fungal appressoria during early stages of host penetration, a subtracted library was prepared using cDNA from epidermal peels of infected leaf epidermis as 'tester' and cDNA from epidermal peels of mock-inoculated leaves as 'driver'. Total RNA was extracted from epidermal strips at 20 hai (no visible penetration) and 22 hai (first infection vesicles formed) as described above and mixed in equal amounts. Full-length cDNA was synthesized from polyA-purified tester RNA and driver RNA (16 µg each) as described for the necrotrophic stage library. The two resulting cDNA pools were then amplified with 22 cycles of PCR. For subtractive hybridization, an excess of ss antisense driver cDNA was hybridized with ss sense tester cDNA. Reassociated tester/driver ds cDNAs were separated from the remaining ss cDNAs (subtracted cDNA) on hydroxylapatite and the latter were specifically amplified with 14 PCR cycles.

To prepare cDNAs representing *in vitro* infection structures, total RNA from conidial germlings producing appressorial initials and total RNA from mature appressoria (see above) were pooled in equal amounts. After isolation of polyadenylated RNA, full-length cDNAs were prepared as described for cDNAs from the necrotrophic stage. The resulting cDNAs were amplified with 14 PCR cycles using a high fidelity polymerase. Normalization was carried out as described for the preparation of cDNAs from the biotrophic stage. Resulting ss cDNAs were PCR-amplified with 13 cycles.

2.16 EST sequencing, quality control and assembly

cDNAs from FACS-isolated biotrophic hyphae, *in planta* appressoria and the necrotrophic stage (3 µg) were sequenced with 454 GS-X technology, whereas cDNAs from in vitro infection structures were sequenced with 454 Titanium technology according to the manufacturer's instructions (Roche, Basel, Switzerland) at the Max-Planck-Institute for Molecular Genetics (Berlin, Germany). After removal of low-quality and short reads (<80 bp), terminal PolyN stretches and adaptors for barcoding, 454-sequencing and cDNA library preparation were removed using in-house perl scripts. Contaminating plant sequences were filtered by screening against the *A. thaliana* genome sequence (TAIR v.8) for ESTs with 96 % identity over 100 bp (pre-screen) and ESTs matching with an expect value $<1e^{-12}$ (final screen).

The resulting grand total of 500,265 reads of high-quality fungal ESTs from *in planta* infection stages were co-assembled using SeqMan pro v.8 (Lasergene) with default parameters for Roche 454 data, resulting in 35,500 contigs, leaving 75,681 singletons. Similarly, 454 ESTs from *in vitro* infection stages were assembled separately into 22,549 contigs. EST contigs clustering together on the fungal genome with at least one base-pair overlap were defined as transcriptional units.

2.17 Bioinformatic analyses of ESTs

EST contigs or their corresponding ORFs were queried using BLAST (Altschul *et al*., 1990; Altschul *et al*., 1997) against several databases:

(1) GenBank's non-redundant protein database using BLASTX
(2) GenBank's non-redundant nucleotide sequence database using BLASTN
(3) GenBank's non-mouse and non-human EST database using TBLASTX
(4) The *C. graminicola* genome accessible via the Fungal Genome Initiative of the Broad Institute (http://www.broadinstitute.org/annotation/fungi/) using TBLASTX
(5) a draft assembly of the in-house sequenced *C. higginsianum* genome using BLASTN

Independent of the algorithm and database, matches with an expect value $<1e^{-5}$ were considered significant. EST contigs giving no matches in searches (1) – (3) were

considered as orphan sequences. Of those, the sequences likely to be *higginsianum*-specific were determined with search (4). Contigs that were exclusively composed of ESTs from the necrotrophic phase that failed search (5) were considered as being contaminating sequences from extraneous saprotrophic organisms and were excluded from further analysis.

A publicly available draft assembly of the *C. higginsianum* genome was interrogated via BLAST and a GBrowse genome browser (Stein *et al*., 2002) at http://www.mpiz-koeln.mpg.de/english/research/pmi-dpt/Fungal_genomes. Similarly, the contigs and their constituent ESTs can be visualized and downloaded via their identifier at http://gbrowse.mpiz-koeln.mpg.de/cgi-bin/gbrowse/colletotrichum_ higginsianum. However, this requires authorization by the principal investigator Dr. Richard J. O'Connell (Max-Planck-Institute for Plant Breeding Research, oconnel@mpipz.mpg.de).

ORFs were predicted with BESTORF (Molquest package, Softberry) employing a *Fusarium graminearum* matrix. To identify soluble secreted proteins, the programs SignalP and TMHMM were used, following recently published guidelines (Emanuellson *et al*., 2007). Orphan EST contigs with ORFs predicted to be solubly secreted proteins were defined as ChECs (*Colletotrichum higginsianum* Effector Candidates), supplemented with those proteins found during manual curation to have similarity to presumed effectors of plant pathogens. For each EST contig, all bioinformatic parameters, including EST composition, were collated in an Excel spreadsheet, which allowed data filtering for subsets of contigs with specific characteristics.

For selected subsets of identified ChECs, protein motifs and domains were sought by querying the predicted protein sequences against the NCBI conserved domain database (http://www.ncbi.nlm.nih.gov/Structure/cdd/wrpsb.cgi), InterProScan (http://www.ebi.ac.uk/ InterProScan), PlanTAPDB (Richardt *et al*., 2007) and PlantTFDB (http://planttfdb.cbi.pku. edu.cn/). Potential glycosyl-phosphatidylinositol (GPI)-anchored proteins were identified using the Fungal Big-PI Predictor (Eisenhaber *et al.*, 2004). Censor (Kohany *et al*., 2006) was used to search RebBase, a database of repetitive elements (http://www.girinst.org/repbase/index.html). Sequence alignments and secondary structure predictions were made using ClustalW (http://www.ebi.ac.uk/Tools/clustalw2/index.html) and the PSIPRED software (http://bioinf.cs.ucl.ac.uk/psipred/), respectively.

3 Results

3.1 Characterization of the secretome of *in vitro*-formed germlings and appressoria of *Colletotrichum higginsianum*

Insights about components of the extracellular matrices surrounding conidia, germ tubes, appressoria and intracellular hyphae of *Colletotrichum* and their developmental regulation during infection structure morphogenesis have been obtained from intensive studies with monoclonal antibodies and other cytochemical probes (Green *et al*., 1995; Perfect *et al*., 1999; O'Connell *et al*, 1996), mostly exploiting the *C. lindemuthianum* – bean interaction. However, the cloning and identification of the epitope-containing proteins was technically challenging and laborious. Apart from bioinformatics predictions made from EST data (Kleemann *et al*., 2008, Takahara *et al*., 2009; this study), neither soluble secreted proteins nor extracellular matrix proteins of *C. higginsianum* infection structures have been identified to date. It was aimed to exploit the genomic and transcriptomic resources now available for this fungus to directly identify constituents of the secretome of infection structures by using a proteomics approach involving mass spectrometry (MS). As a starting point towards direct discovery of infection-related secreted proteins, a proteomic analysis of *in vitro*-formed appressoria was initiated.

3.1.1 Cytochemical detection of secreted proteins

Conidia that germinated *in vitro* on a polystyrene surface elaborated heavily melanized appressoria that were indistinguishable from appressoria formed on the plant epidermis (Kleemann *et al*., 2008). To trace protein secretion during germination and appressorium morphogenesis, a highly sensitive protein stain was used, based on silver-enhancement of colloidal gold particles. (Jones *et al*., 1995). As early as two hours after settling onto an inductive surface, spores had secreted proteinaceous material, giving rise to intensely labelled concentric circular or ovoid haloes with an average outer diameter of 23 µm (Fig. 1). Once formed, these haloes did not increase in size even after 22 h of incubation. However, germ tubes emerging from conidia at 4 h, and appressorial initials developing at germ-tube apices, secreted distinct protein haloes which were fully-expanded after 8.5 h. As with the protein haloes emerging from spores, haloes released from germ tubes and appressoria did not increase further in size at later time points. In addition to being temporally and spatially distinct, the

protein haloes were clearly distinguishable by their colour, indicating a different density of gold and silver deposits, which may reflect differing protein compositions. After melanization of the appressorial cell wall was initialized, the extracellular matrix immediately adjacent to the appressorial cell wall failed to label, suggesting that these proteins were either not accessible, or not able to bind, the colloidal gold probe (Fig. 1 D). Remarkably, when appressoria were completely detached from the polystyrene surface by ultrasonication, gold labelling revealed protein spots at the site of former appressorial penetration pores (Fig. 1 F), indicative of the highly localized release of proteins at the point of contact between the substratum and the non-melanized pore, through which penetration pegs would emerge *in planta*.

3.1.2 Proteomic analysis of the *in vitro* secretome

To investigate the possibility of identifying halo proteins and outer cell wall proteins by liquid chromatography coupled with mass spectrometry, germlings including their protein haloes were subjected to protease digestion, employing trypsin, V8 and pronase E. Trypsin and V8 failed to digest protein haloes, suggesting that these proteins were not enriched with the basic and acid residues targeted by these enzymes, or were not accessible to these proteases. In contrast, when pronase E was used at 1 µg/µL, spore and appressorial protein haloes completely disappeared (Fig. 1 G), suggesting that they are composed of proteins rich in consecutive hydrophobic residues. However, the low specificity of pronase E and the relatively high concentration that was required to release halo proteins was considered unsuitable for liquid chromatography-coupled mass spectrometry analyses.

In an alternative approach, the extracellular proteins that were solubly secreted and accumulated in the thin film of water within which appressoria developed (Kleemann *et al*., 2008), were collected and analyzed. In brief, the liquid film surrounding 2.9×10^9 appressoria on a total surface of 0.8 m^2 of polystyrene was concentrated by ultrafiltration, allowing the enrichment of proteins larger than 3 kDa, and subjected to mass spectrometry following two-dimensional (2D-) gel electrophoresis.

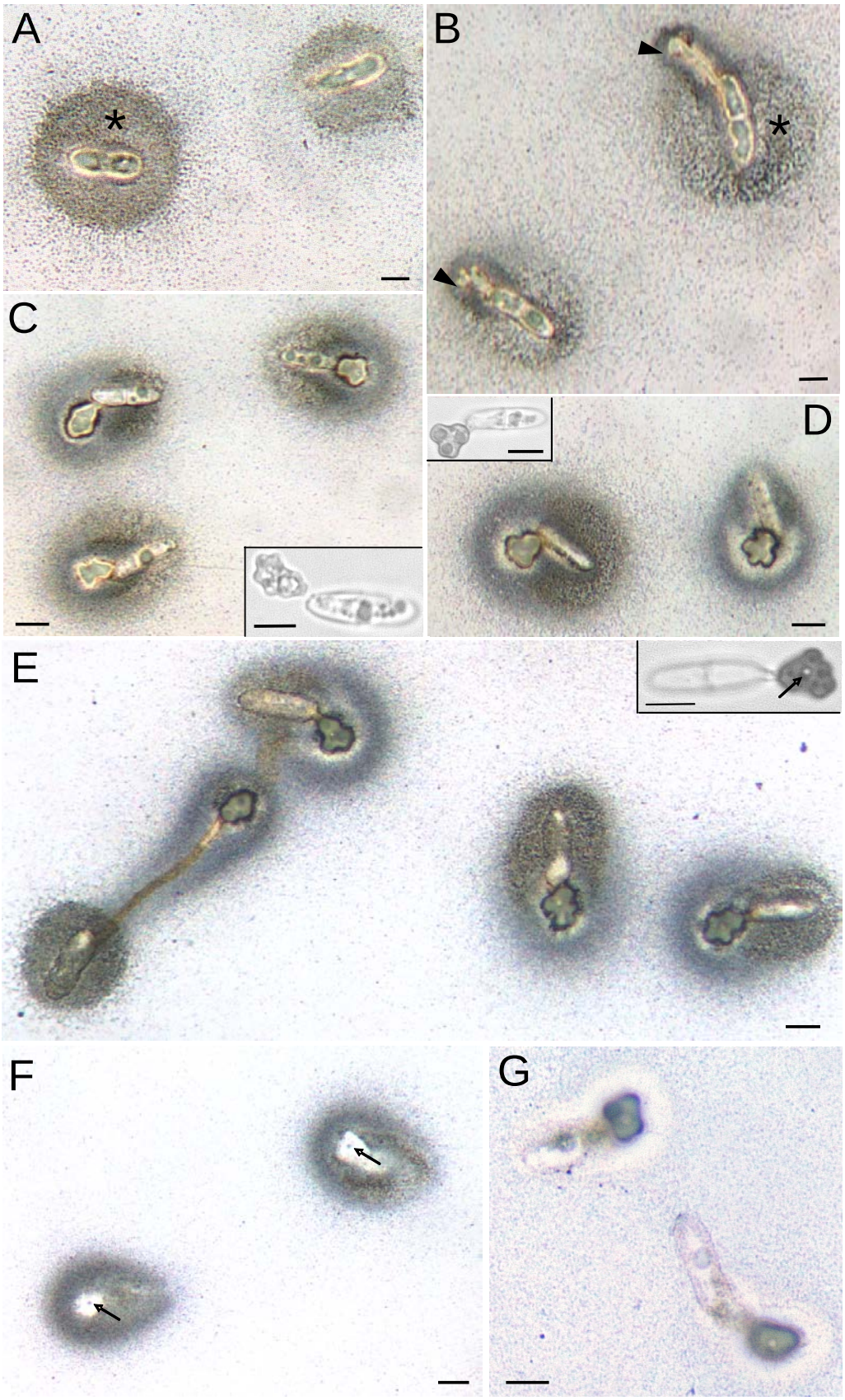
A
B
C
D
E
F
G

Figure 1. Protein secretion of germinating spores and appressoria of *Colletotrichum higginsianum* onto polystyrene substratum.

Silver-enhanced staining with colloidal gold was used to visualize secreted proteins of the extracellular matrix.

Spores were incubated for 2h (A), 4 h (B), 6 h (C), 8.5 h (D) and 22 h (E) on a polystyrene surface before staining. Insets in C, D and E demonstrate the degree of appressorial melanization at the given time points. Fully-melanized appressoria have elaborated a penetration pore (Inset E, arrow) during maturation. Note that germ tubes and appressorium initials (B, arrowheads) secrete proteins which give rise to protein haloes distinct in appearance from those released from spores (A and B, asterisks).

F, Staining after removal of fungal infection structures by ultrasonication reveals locally secreted proteins underneath former penetration pores (arrows).

G, Pronase E digestion prior to staining abolishes protein haloes. Scale bars: 5 µm.

Most of the Coomassie-stained proteins spots appearing on the 2D-gel had a high apparent molecular mass and low pI (Fig. 2). From two replicate gels, 96 spots were excised. Following tryptic in-gel digestion, MS and tandem MS analysis resulted in peptide mass fingerprints and peptide fragment fingerprints for 61 of the selected protein spots. After Mascot searches against a draft assembly of the *C. higginsianum* genome and extensive manual curation, 29 spots (30 % of excised spots) could be unambigously assigned to a unique genomic contig. All *de novo* gene predictions from these genomic contigs resulted in ORFs which were matched by the MS and tandem MS data. These proteins yielded significant (e value $e<10^{-5}$) matches in GenBank's non-redundant protein database, summarized in Table 3. Twenty-three spots matched to functionally characterized proteins, or their orthologues automatically annotated from fungal genome sequencing projects. Searches against a conserved domain database revealed 24 proteins containing recognizable protein domains, of which five appeared to be multi-domain proteins. Four proteins matched to hypothetical proteins without a predicted domain.

Remarkably, a high proportion of identified proteins (41 %) were potentially involved in modification of fungal or plant cell wall polymers. These included a laccase and a feruloyl esterase, as well as a plethora of carbohydrate-modifying enzymes. The latter comprised a putative cellulase, a 1,4-mannosidase, β–1,3- and β–1,6-glucanases, glucanosyltransferases and two paralogous chitin deacetylases, sharing 40 % amino acid identity. In contrast, only two putative proteases were found.

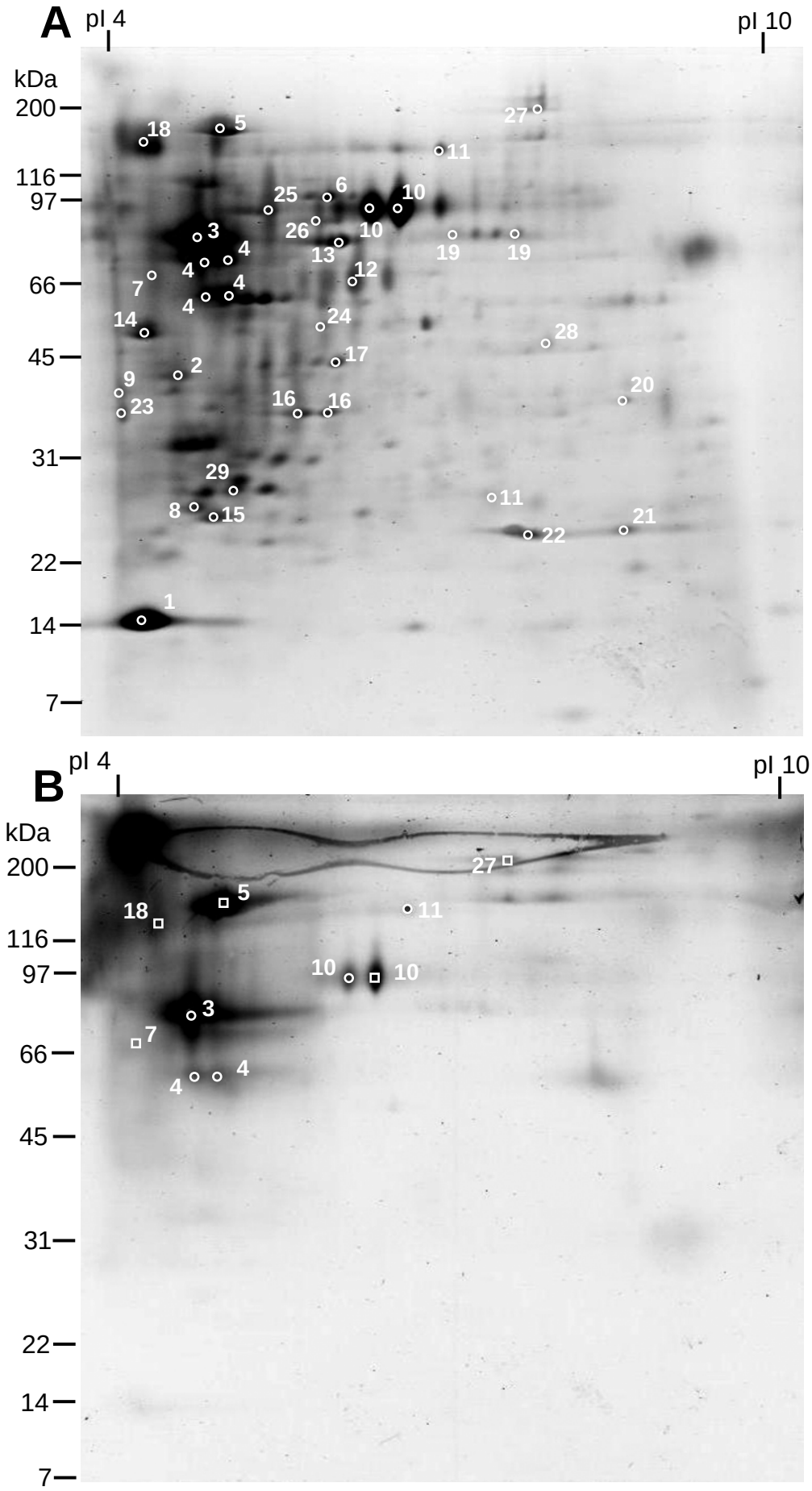
A
pI 4
pI 10
kDa
200
116
97
66
45
31
22
14
7
18
5
27
11
25
6
10
26
10
3
19
19
4
13
12
4
7
4
4
14
24
28
17
2
9
20
23
16
16
29
11
8
15
21
22
1
B
pI 4
pI 10
kDa
200
116
97
66
45
31
22
14
7
27
5
18
11
10
10
3
7
4
4

Figure 2. Cumulative secretome of *Colletotrichum higginsianum* sporelings developing appressoria *in vitro*.

Proteins that were solubly secreted into the liquid film surrounding mature appressoria were subjected to two-dimensional gel electrophoresis and stained with (A) Coomassie blue (for total proteins) or (B) Pro-Q Emerald (for glycosylated proteins) before spot excision and MS analysis. Spot numbers refer to the entries in Table 3. The identity of spots labelled with □ in (B) was inferred from their position. Note that gel B was loaded with approx. ten times less sample.

Proteins homologous to a phytase (Fig. 2 A, spot 4), 1,4-mannosidase (spot 10), cellulase (spot 11) and isoamyl alcohol oxidase (spot 19) were found on more than one position in the gel, as revealed by distinct protein spots, probably as a result of differential posttranslational modifications altering pI or apparent molecular weight. A replicate gel run with approximately ten times less total protein compared to the gel shown in Figure 2 revealed that the phytase localizes in four distinct protein spots.

Table 3. Identified *C. higginsianum* proteins secreted during spore germination and appressorium maturation *in vitro*.

Spot ID	Genomic contig matched by MS data[1)]	Open reading frame prediction of the matched genomic region using FGENESH					
		Nearest informative homologue given by BLASTP			Identified protein domains[3)]	SP?[4)]	$Mr_{obs} > Mr_{pred}$[6)]
		Description	Accession number	Species			
Effector-like							
1	contig07894_373 [8139–7423]	Eliciting plant response-like protein 1	CAL80754	*Trichoderma atroviride*	Cerato-platanin family domain (pf07249)	Y	
Enzymes capable of modifying fungal and/or plant cell wall polymers							
13[2)]	contig07091_321 [1783–677]	Laccase Lcc5	ABS19941	*Fusarium oxysporum*	Multicopper oxidase (pf07732) Laccase (TIGR03389)	Y	
8	contig06223_116 [6553–5597]	Chitin deacetylase	AAT68493	*Glomerella lindemuthiana*	Polysaccharide deacetylase domain (pf01522)	Y	
27[2)]	contig00133_19 [1050–2558]	Chitin binding protein	BAB79692	*Magnaporthe grisea*	Polysaccharide deacetylase (pf01522) Chitin recognition protein (pf00187)	Y	**Y**
10[2)]	contig05880_108 [10756–11157]	endo-1,4-β-mannosidase	EEY17826	*Verticillium albo-atrum*	Fungal cellulose binding domain (pfam00734) endo-β-mannanase domain (COG3934)	weak	**Y**
11[2)]	contig07273_171 [17043–18641]	Cellulase Cel61A	O14405	*Trichoderma reesei*	Fungal cellulose binding domain (pfam00734) Glycosyl hydrolase family 61 (pf03443)	weak	**Y**
17	contig07259_415 [20008–19514]	endo-β-1,6-Glucanase	ABF50867	*Emericella nidulans*	Endoglucanase (COG2730)	Y	
7	contig00220_141 [7459–6773]	GPI-anchored β-1,3-Glucanosyltransferase GEL1	AAC35942	*Aspergillus fumigatus*	GPI-anchored surface protein (pf03198) Cellulase domain (pf00150)	Y	**Y**
18	contig02698_34 [2373–4001	Feruloyl esterase B	Q8WZI8	*Aspergillus nidulans*	Tannase and feruloyl esterase (pf07519)	Y	**Y**

Spot ID	Genomic contig matched by MS data[1)]	Open reading frame prediction of the matched genomic region using FGENESH					
		Nearest informative homologue given by BLASTP			Identified protein domains[3)]	SP?[4)]	$Mr_{obs} > Mr_{pred}$[6)]
		Description	Accession number	Species			
5[2)]	contig01574_290 [15220–12368]	Copper radical oxidase	ABD61576	*Phanerochaete chrysosporium*	Putative carbohydrate binding domain of WSC proteins, polycystins and fungal exoglucanases (sm00321) Glyoxal oxidase N-terminus domain (pf07250) Galactose oxidase C-terminus domain (cd02851)	N	**Y**
3	contig01513_786 [9136–8036]	Secreted protein	CAQ16258	*Glomerella graminicola*	O-Glycosyl hydrolase domain (cd00413) GPI-anchored glucanosyltransferase (cd02183)	Y	**Y**
9	contig02652_25 [1056–7]	rAsp f 9	CAA11266	*Aspergillus fumigatus*	Same as spot 3: O-Glycosyl hydrolase domain (cd00413) GPI-anchored glucanosyltransferase (cd02183)	Y	
6	contig06672_169 [7682–6069]	β-1,3-Glucanase	AAW47927	*Acremonium blochii*	None	Y	
Proteolytic enzymes							
14[5)]	contig06245_424 [41128–39515]	Secreted aspartic proteinase	ABK64120	*Hypocrea lixii*	Aspartic proteinases secreted from fungal pathogens to degrade host proteins (cd05474)	nd	Nd
28	contig00368_110 [11635–12993]	Peptidase M14	XP_001931884	*Pyrenophora tritici-repentis*	M14 family of metallocarboxypeptidases (cd06228)	Y	
Modification of extracellular environment and nutrient aquisition							
4	contig07163_34 [2637–3980]	3-Phytase A	O00107	*Thielavia heterothallica*	Histidine phosphatase domain of histidine acid phosphatases and phytases (cd07061)	Y	**Y**
24	contig05550_398 [16950–16258]	Carbonic anhydrase	EEY23154	*Verticillium albo-atrum*	Prokaryotic-like carbonic anhydrase subfamily (cd03124)	Y	Y
Protein folding							

Spot ID	Genomic contig matched by MS data[1)]	Open reading frame prediction of the matched genomic region using FGENESH					
		Nearest informative homologue given by BLASTP			Identified protein domains[3)]	SP?[4)]	$Mr_{obs} > Mr_{pred}$[6)]
		Description	Accession number	Species			
21	contig00435_273 [12265–11969]	Cyclophilin BCP1	AAQ16572	*Botrytis cinerea*	Cyclophilin-type peptidylprolyl cis- trans isomerase domain (cd01926)	N	
Other putative enzymes							
16	contig05674_182 [1547–1104]	Transaldolase	XP_366548	*Magnaporthe grisea*	Transaldolases (cd00957)	N	
19	contig06095_216 [24315–25136]	Isoamyl alcohol oxidase	ABB90284	*Gibberella zeae*	FAD binding domain (pf01565)	Y	
20	contig02324_393 [25894–24965]	Malate dehydrogenase	EEY22479	*Verticillium albo-atrum*	Glyoxysomal and mitochondrial malate dehydrogenases (cd01337)	N	
25	contig01894_86 [974–123]	6-Phosphogluconolactonase	EEY21694	*Verticillium albo-atrum*	3-Carboxymuconate cyclase (COG2706)	Y	Y
26	contig01595_220 [2412–1885]	Esterase EstA precursor	AAS13488	*Aspergillus niger*	Carboxylesterase (pf00135)	N	
Matches to hypothetical proteins predicted from microbial genomes							
2	contig00714_110 [3601–2912]	Hypothetical protein	XP_363071	*Magnaporthe oryzae*	None	Y	Y
12	contig01072_28 [2024–3556]	Hypothetical protein	YP_972959	*Azidovorax avenae*	None	Y	Y
15	contig07511_172 [1270–908]	Hypothetical protein	XP_002146702	*Penicillium marneffei*	None	Y	
22	contig01546_88 [8043–8681]	Hypothetical protein	EEU37621	*Nectria haematococca*	None	Y	
23	contig05531_189 [8719–7937]	Conserved hypothetical protein	EEY15211	*Verticillium albo-atrum*	Ferritin-like superfamily of diiron-containing proteins (cd00657)	Y	
29	contig04195_10 [674–1114]	Hypothetical protein	XP_001221624	*Chaetomium globosum*	Ricin-type lectin domain (cl00126)	Y	

[1)] Referring to *C. higginsianum* genome assembly from March 2009. The identifier after the underscore specifies an artificial open reading frame derived from a six-frame translation covering the base pairs given in square brackets.

[2)] Multi-domain protein with the indicated domains present in different regions of the polypeptide chain.

[3)] Identifier of the Conserved Domain Database (CDD) at NCBI in parentheses.

[4)] SignalP (Emanuellson *et al*., 2007) was used to predict a signal peptide (SP) for secretion from the open reading frame. A weak signal peptide prediction was obtained if one score of the SignalP-NN algorithm was below its treshold ("no").

[5)] The genomic contig lacked the N-terminus. Signal peptide prediction was not possible.

[6)] “Y” means that the observed molecular mass was more than 20 kDa bigger, as inferred from the protein marker. Bold face indicates that these proteins were found on a gel stained for glycosylated proteins.

To test whether the identified proteins carried canonical signal peptides, all N-terminally complete ORFs (28 out of 29) resulting from the *de novo* gene prediction were subjected to analysis with SignalP (Emanuelsson *et al*., 2007). Surprisingly, five (18 %) proteins were found to lack a signal peptide. These included mainly enzymes involved in basic house-keeping cellular processes, e. g. transaldolase, malate dehydrogenase, esterase and cyclophilin. Additionally, a 190 kDa protein homologous to fungal copper radical oxidases also failed signal peptide prediction. Furthermore, the proteins having homology to cellulose and 1,4-mannosidase, respectively, also gave weak signal peptide predictions, with the score for the cleavage site probability of the SignalP-NN algorithm below its threshold of significance.

C-terminal glycosylphosphatidylinositol(GPI)-modification sites are involved in the covalent linkage of secreted proteins to the extracellular face of the plasma membrane or to β-1,6-glucans in the fungal cell wall (Klis *et al*., 2010) and thus not expected to be solubly secreted proteins. However, three secreted proteins (spot 3, 7 and 9) were found to be homologous to known GPI-anchored glucanosyltransferases, of which two (spot 3 and spot 9) were paralogues displaying 51 % amino acid identity. Despite that, only the protein found in spot 3, which appeared to be a major constituent of the appressorial secretome, did not contain a predicted GPI-modification site. Taken together, the direct proteomic analyis of the extracellular fluid allowed the unambiguous identification of a diverse set of genuine secreted proteins which, in addition to proteins with predicted signal peptides, also comprised proteins lacking signal peptides or containing GPI-anchors, which would have evaded any bioinformatic discovery pipeline.

Twelve proteins were found to have much higher (>20 kDa) apparent molecular weight than inferred from the amino acid sequence. To test whether glycosylation could account for these size discrepancies and to evaluate the proportion of glycosylated proteins, a replicate gel loaded with less total protein was stained with Pro-Q Emerald before spot excision (Fig. 2 B). Remarkably, only a small fraction of proteins appeared to be strongly labelled, indicative of extensive glycosylation. 15 spots were excised and subjected to in-gel de-glycosylation before mass spectrometry. Only five spots provided high quality mass spectrometry data, with most of the spots failing to give any detectable peptide ions, probably as a result of low protein amount. However, five further spots could be identified based on comparisons to Coomassie-stained gel replicates. Eight of the twelve protein spots migrating with a higher

apparent molecular weight than expected from their amino acid sequence were indeed found to be glycosylated (Tab. 3).

The degree of overlap between the secretomes defined by this direct proteomic approach and the computational prediction approach based on stage-specific ESTs (Kleemann *et al*., 2008) was determined by BLAST. Strikingly, only the laccase was found with both approaches. Although the cyclophilin and malate dehydrogenase were also represented among the appressorial ESTs, they were not predicted to be secreted since they lack a canonical signal peptide. Nevertheless, the direct proteomic investigation allowed identification of cyclophilin and malate dehydrogenase as protein components of the extracellular liquid surrounding mature appressoria (Fig. 2 A, spot 20 and 21), although their relatively weak spot intensities suggest that they are not major constituents.

In terms of identification of *Colletotrichum higginsianum* effector candidates (ChECs), small (<25 kDa) proteins are of particular interest. Relatively few (~15) protein spots are visible in this size range, most of which did not provide sufficient protein after excision or only produced poor mass spectrometry data. All 29 proteins identified in this study yielded significant BLAST matches to proteins in public databases, and were therefore not novel, *Colletotrichum*-specific proteins. However, this approach allowed the identification of a small (14 kDa) secreted protein containing a cerato-platanin domain, typical for some effector proteins from plant pathogenic fungi and beneficial biocontrol fungi. Given its small size, resulting in low Coomassie-binding capacity, this protein appeared to be a major constituent of the secretome (Fig. 2 A, spot 1). Because of its similarity to effectors from plant-interacting fungi, this protein was characterized further and is named ChEC5 hereafter.

3.2 Analysis of expressed sequence tags from different fungal cell types and stages of pathogenesis

In addition to their critical role in host penetration, it was hypothesized that *Colletotrichum higginsianum* appressoria, and the penetration pegs that emerge from them, secrete soluble effector proteins that permit the fungus to overcome host defence responses and to reprogram host cells for biotrophy. Similarly, *C. higginsianum* biotrophic hyphae have been suggested to secrete effectors for host manipulation (Takahara *et al*., 2009). As a first step towards discovery of secreted effecors in *C. higginsianum* we have generated expressed sequence tags (ESTs) from several fungal cell types and stages of *in planta* pathogenesis (Tab. 4, Fig. 3). These included biotrophic hyphae isolated by fluorescence-activated cell sorting (Takahara *et al*., 2009, termed FACS BH hereafter), developing and mature appressoria formed *in vitro* (termed IV APP hereafter) and plant-penetrating appressoria (termed PEN APP hereafter). In addition, ESTs from the late necrotrophic phase of infection (NECRO hereafter) allowed the identification of contigs lacking or depleted in ESTs from the necrotrophic stage.

Given the relatively short (approx. 30 h) and transient biotrophic phase of *C. higginsianum*, analyses were focused on ESTs from appressoria formed *in vitro* and from plant-penetrating appressoria, since they are likely to represent the most critical stage of fungal development for preparing the host cell for biotrophic invasion.

Table 4: Overview of the fungal cell types and infection stages used for generating expressed sequence tags (EST).

Biological material	Abbreviation used hereafter	Sequencing method	cDNA treatment	Remark
Mature appressoria formed *in vitro* (20 h)	-	Sanger	-	First insight into a *Colletotrichum* appressorial transcriptome and first reported attempt to systematically identify expressed *C. higginsianum* genes encoding secreted proteins (Kleemann *et al*., 2008).
Appressoria penetrating the host cell (20/22 hpi)	PEN APP	454 GS-FLX	Subtracted with cDNA from mock-inoculated material	Epidermal peels of densly inoculated *A. thaliana* leaves were used to enrich for fungal transcripts expressed early in host penetration.
Mature appressoria (20 h) and germ tubes with appressoria initials (5 h) formed *in vitro*	IV APP	454 Titanium	Normalized	Two stage-specific cDNAs were mixed prior to sequencing to maximize gene discovery. Allows the *in silico* discrimination of plant-induced genes.
Biotrophic hyphae isolated by FACS (45 h)	FACS BH	Sanger / 454 GS-FLX	Normalized	Fluorescence-activated cell sorting (FACS) was used to specifically isolate viable biotrophic hyphae from infected *A. thaliana* leaves (Takahara *et al*., 2009).
Macerated leaves heavily colonized with necrotrophic hyphae (72 hpi)	NECRO	454 GS-FLX	Normalized	Allows the *in silico* identification of biotrophy-relevant contigs depleted in necrotrophy-related ESTs.

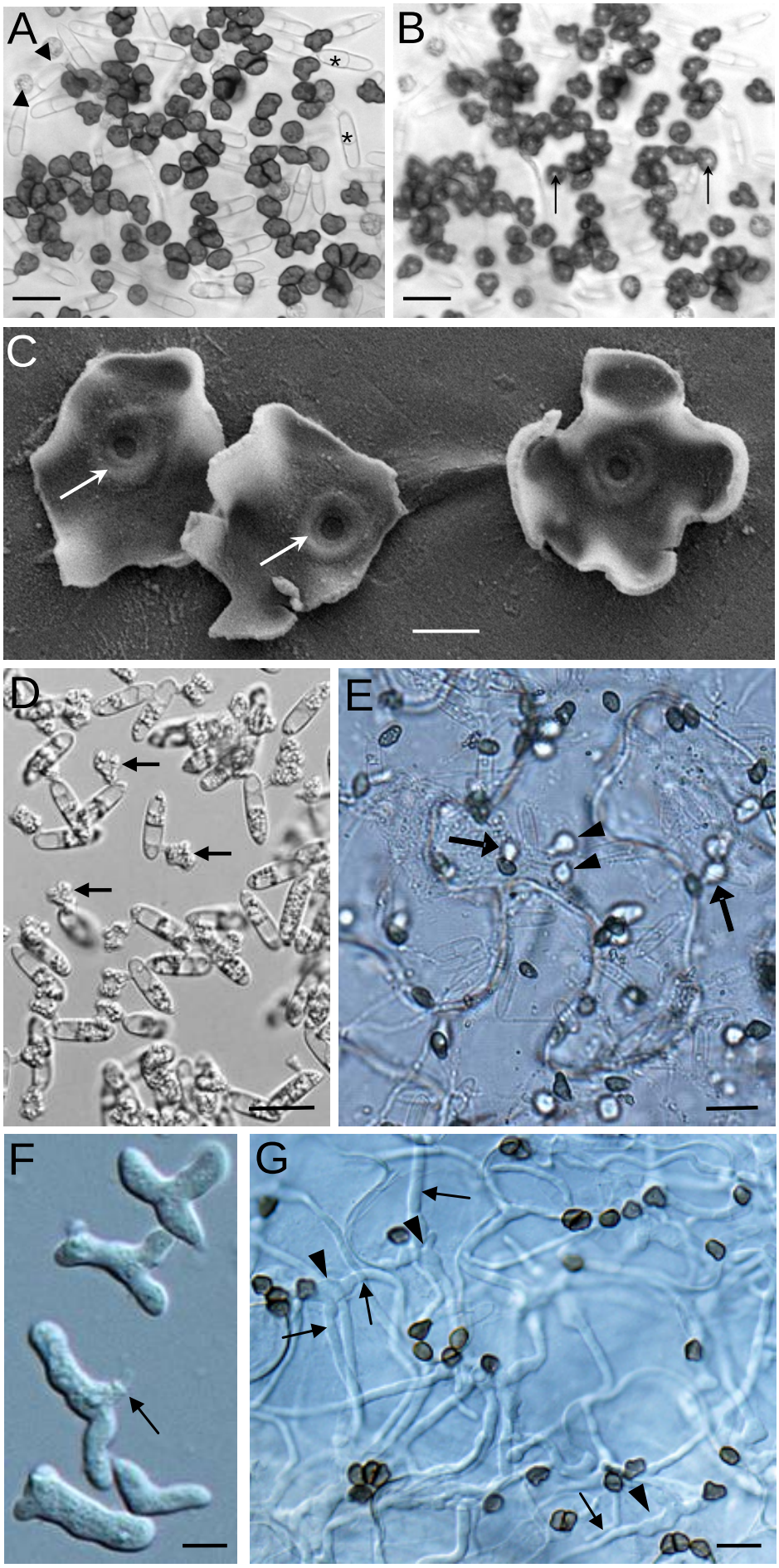
A
B
C
D
E
F
G

Figure 3. Representative micrographs demonstrating the biological material used for generation of *Colletotrichum higginsianum* expressed sequence tags.

A to D, Mature appressoria (A to C) and germ tubes with appressorial initials (D) formed *in vitro* on a polystyrene Petri dish. A and B, light micrographs showing a monolayer of darkly melanized appressoria formed after incubation for 18 h. Scale bars, 10 µm.

A, focal plane near the middle of the appressorial cells. Germinated conidia appear empty and are clearly septate (asterisks). Immature (non-melanized) appressoria are very infrequent (arrowheads).

B, Focal plane at the base of appressoria. Note the non-melanized penetration pores in the appressorial cell wall (arrows).

C, Scanning electron micrograph showing fragments of mature appressoria remaining attached to the polystyrene surface after mechanical disruption by scraping. The upper, domed part of the cell has been removed, revealing the presence of a penetration pore in the basal cell wall attached to the substratum. The pore is surrounded by an annular wall thickening (arrows). Within the pore, the surface of the polystyrene has not been indented by the fungal penetration peg. Scale bar, 2 µm.

D, Light micrograph showing germlings with non-melanized appressorial initials (arrows). Note that conidial cells are vacuolated but still contain cytoplasm.

E, Light micrograph of an epidermal peel of a densely inoculated *A. thaliana* leaf at 22 hpi.. The light micrograph shows a region of an epidermal peel in which small intracellular infection vesicles had already been formed underneath appressoria, appearing as objects with high optical refraction (arrows). Occasionally, appressoria became detached during the stripping process (arrowheads). The RNA used for cDNA generation was mixed from peels with unpenetrated and penetrated appressoria.

F, Biotrophic hyphae physically isolated from infected leaves at 45 hpi by fluorescence-activated cell sorting (Takahara *et al.*, 2009). Note that the cytoplasm is retained within hyphal cells by the presence of a septum in the neck region (arrow). Viewed with Nomarski interference contrast, scale bar 5 µm.

G, Light micrograph of cleared leaf tissue heavily infested with necrotrophic hyphae (70 hpi). At this stage, most parts of the leaf are completely macerated and liquified. The morphological difference between the thick biotrophic hyphae (arrow heads) and thinner necrotrophic hyphae (arrows) is still obvious. Viewed with Nomarski interference contrast microscopy, scale bar 10 µm.

3.2.1 Expressed sequence tags from *in vitro* infection structures

The timing and morphology of appressorial development by *C. higginsianum* on polystyrene were indistinguishable from that previously observed on *A. thaliana* leaf tissue (Narusaka *et al.*, 2004; O'Connell *et al.*, 2004, Huser *et al*., 2009). The generation of sufficient numbers of appressoria on polystyrene required the use of a nylon mesh to maintain a uniformly thin film of water over the highly hydrophobic plastic substratum. Under these conditions, fungal development was well-synchronized, so that after 18 h approximately 97 % of conidia had germinated to form appressoria. These were considered fully mature because they had darkly melanized cell walls containing a basal penetration pore (Fig. 3 B, C), the developmental stage that immediately precedes host penetration *in planta*. Inspection of mechanically disrupted appressoria at this time point by scanning electron microscopy (SEM) confirmed the presence of penetration pores, but the surface of the polystyrene within the pores was not indented, suggesting that fungal penetration pegs had not yet developed or were unable to penetrate this plastic substratum (Fig. 3 C). Importantly for generation of appressorium-specific ESTs, both germinated spores and germ tubes appeared to be empty of cytoplasm at 18 h (Fig. 3 A), so the contribution of transcripts from earlier developmental stages to the total mRNA pool was likely to be small. The appressoria developed as a dense, uniform monolayer of cells, allowing approximately 8×10^7 mature appressoria to be harvested from each Petri dish.

RNA harvested from this material was used to construct a randomly-primed cDNA library (Kleemann *et al*., 2008). A relatively small set of cDNA clones (980) were subjected to bidirectional Sanger sequencing, and the resulting ESTs could be assembled into 518 unique sequences. Forty-nine (9.5 %) showed significant (E<1e-5) similarity to entries in the Pathogen-Host Interaction (PHI-) database of experimentally-verified pathogenicity, virulence and effector genes from fungal and oomycete pathogens of plants, animals and fungi (Baldwin *et al*., 2006) (see Supplementary Table 1). As expected, many of these homologues are involved in appressorium morphogenesis and function, including transcription factors (e. g. STE12 (Caracuel-Rios and Talbot, 2007)), signalling pathway components (e. g. G-protein β-subunit CGB1 (Ganem *et al*., 2004)), enzymes required for melanin biosynthesis (e. g. trihydroxynaphthalene reductase THR1 (Perpetua *et al*., 1996)) and genes of unknown function (e. g. GAS1 (Xue *et al*., 2002)). BLAST searches against public

EST and protein databases revealed that 27 % of the unique sequences had no matches at the stringent cut-off of E<1e-4 and are therefore likely to be *Colletotrichum*-specific sequences.

Potential ORFs from six-frame-translations were subjected to signal peptide prediction, which resulted in 72 potential ORFs harbouring N-terminal signal peptides. BLASTX matches, ORF predictions with the BESTORF program, and predictions of transmembrane domains and glycosylphosphatidylinositol (GPI)-modification sites allowed genuine start methionines to be discriminated from internal methionines associated with signal peptide-mimicking transmembrane domains, and thus to distinguish soluble secreted proteins from integral membrane proteins and GPI-anchored proteins. 3' RACE was used to assign directionality to those contigs without any BLASTX match and to obtain independent support for their predicted ORFs. This finally resulted in the identification of 26 soluble secreted proteins. Significant BLASTP matches could be used to infer probable subcellular localizations for 11 of these proteins. These included proteins secreted to the lumena of endomembrane compartments (e. g. a vacuolar carboxypeptidase) or to the extracellular space (e. g. pectin methyl esterase and laccases). A further 10 proteins resembled fungal hypothetical proteins predicted from automated whole-genome sequencing and annotation projects but lacking functionally-characterized homologues. Furthermore, two soluble secreted proteins appeared to be *Colletotrichum*-specific and were considered as being effector candidates. In the original publication (Kleemann *et al*., 2008) these were named contig271 and 1-O01-T7 but herein they are re-named as *Colletotrichum higginsianum* effector candidate (ChEC) 1 and 2. ChEC1 and ChEC2 could also be recognized in the transcriptome of plant-penetrating appressoria and appressoria formed *in vitro*, which were deeply sequenced recently from independently prepared samples using 454-pyrosequencing (see below).

For 454-sequencing the transcriptome of *in vitro* appressoria, RNA populations were pooled in equal amounts from two different stages of appressorial morphogenesis. The rational behind this was to maximize gene discovery for annotation of the in house-sequenced *C. higginsianum* genome and to allow *in silico* discrimination of plant-induced genes from genes whose expression is developmentally regulated and coupled to appressorium morphogenesis (see below). The samples consisted of RNAs from mature appressoria at 18 h (as above) and from germlings formed after 5 h incubation on a polystyrene surface. Again, conidial germination was found to be well-

synchronized at this early time point, with most of the germ tubes having produced irregularly shaped apical swellings (Figure 3 D). These non-melanized appressoria initials and the associated cytoplasm-rich conidia and germ-tubes differed markedly from the mature appressoria at 18 h. The two samples therefore represent very distinct developmental stages.

3.2.2 Expressed sequence tags from plant-penetrating appressoria

3.2.2.1 EST generation and co-assembly with other ***in planta*** ESTs

Neither ESTs from *in vitro* appressoria nor from fully-mature biotrophic hyphae isolated by FACS allow the identification of early plant-induced genes. Therefore, attempts were made to obtain RNA from mature appressoria formed on the host leaf surface. However, at this early infection stage fungal biomass is very low, therefore, the contribution of fungal RNA to the total RNA isolated from whole infected leaves is almost negligable. For that reason, epidermal peels from heavily infected leaves were prepared between 20 and 22 hpi, representing the time frame in which *C. higginsianum* appressoria penetrate leaf epidermal cells of the highly susceptible *A. thaliana* ecotype Landsberg *erecta* (Ler-0). The PEN APP cDNA was generated with a mixture of RNA from epidermal strips with mostly unpenetrated appressoria (20 hpi) and mostly penetrated appressoria (22 hpi, Figure aa, E), followed by subtraction with cDNA obtained from mock-inoculated epidermis.

454-sequencing of the PEN APP cDNA resulted in 218,811 raw ESTs, and thus PEN APP was the least deeply sequenced of the four libraries, assuming similar transcriptome complexity for all sampled stages (Table 5). Despite enrichment of fungal RNA by preparing epidermal peels and subtractive hybridization with cDNA from mock-inoculated epidermis, 56.7 % of the ESTs were found to be of plant origin. Since the PEN APP library was subtracted with cDNAs from mock-infected epidermal peels, these plant ESTs constitute an invaluable resource to study *Arabidopsis* genes specifically upregulated in the tissue targeted by *C. higginsianum*. However, as a consequence, the PEN APP dataset provided the lowest number of high-quality fungal ESTs for a co-assembly with ESTs from the three other libraries (17.4 % of total raw ESTs, Table 5).

Table 5. The 454-sequenced transcriptome in numbers.

cDNA source[1)]	*In planta* ESTs			IV APP
	FACS BH	NECRO	PEN APP	
Raw reads	404,299	243,154	218,811	390,303
Contaminating plant sequences[2)]	124 (0.03 %)	25,389 (10.4 %)	123,978 (56.7 %)	-
Assembled fungal ESTs after clean-up[3)]	318,604 (78.8 %)	143,637 (59.1 %)	38,024 (17.4 %)	322,853 (82.7 %)
Contigs	35,500 (Co-assembly of *in planta* ESTs)			22,549
Transcriptional units[4)]	26,463			

[1)] FACS BH: biotrophic hyphae isolated from infected leaves by fluorescence-activated cell sorting, PEN APP: appressoria penetrating host cells, NECRO: leaf tissue heavily infested with necrotrophic hyphae, IV APP: mature and developing appressoria *in vitro*.
[2)] BLASTN against *Arabidopsis* genome.
[3)] Removal of reads <80 bp, terminal PolyN stretches and adaptors used for bar-coding, 454-sequencing and cDNA library preparation.
[4)] Transcriptional units are defined as EST contigs clustering together on the fungal genome by at least one base-pair overlap.

PEN APP ESTs were co-assembled with the other *in planta* ESTs (FACS BH and NECRO), resulting in 35,500 contigs. This clearly exceeds the number of genes expected from the *C. higginsianum* genome, which is estimated to be 50 Mb in size and to carry between 15,000 and 25,000 protein-coding genes, depending on the gene-calling program used (Emiel ver Loren van Themaat, personal communication). Many contigs matching to the same genomic region were found to be redundant, i. e. their ESTs were dissimilar enough to be assembled into separate contigs by the assembly program, due to the relatively high proportion of sequencing errors inherent to 454 sequencing (Wheat, 2010), and splice variants. In addition, redundancy was also caused by non-overlapping contigs or contigs with insufficient overlapping base pairs, as a result of the fragmentary nature of 454 data and the relatively low coverage (8x for the largest contigs). To reduce redundancy, contigs built from the *in planta* ESTs (35,500) and *in vitro* ESTs (22,549) were mapped onto the fungal genome and those overlapping by at least one basepair were defined as transcriptional units. This resulted in 26,463 ‘transcriptional units’. Although not all transcriptional units may encode proteins, and it is unlikely that all protein-coding genes are expressed in the sampled

transcriptomes, this number more closely approaches the number of protein-coding genes expected for a fungal genome of 50 Mb.

Figure 4 summarizes how many transcriptional units are shared by, or unique to, particular fungal stages. To calculate the proportion of transcriptional units specific to each fungal stage, those exclusively consisting of ESTs from one stage were referred to the number of transcriptional units having at least one EST from that stage. This was done to improve comparability between the libraries allowing for the fact that the libraries were sequenced to different depths and that all except the PEN APP library were normalized. The FACS BH and IV APP libraries have the highest proportion of stage-specific transcriptional units, with 34.3 % and 31.5 % respectively. Remarkably, PEN APP has the lowest proportion of stage-specific transcriptional units (6.9 %). However, this is not caused by a huge overlap with IV APP data since only 133 (31 %, sector B in Figure 4) out of 426 transcriptional units specifically expressed during early pathogenesis (sector A and B in Figure 4) contained IV APP ESTs and thus represent developmentally-regulated genes with their expression coupled to appressorium morphogenesis. Thus, the remaining 293 (69 %) can be considered as plant-induced transcriptional units in the sense that their genes are only expressed in appressoria formed on the plant surface but not in appressoria formed on an artificial substratum (plant-induced *sensu stricto*). Alternatively, their expression may be developmentally coupled to penetration peg and infection vesicle formation (plant-induced *sensu lato*).

On the other hand, 10,176 of 14,865 (68.5 %) transcriptional units containing IV APP ESTs also include ESTs from *in planta* infection stages. This suggests either that many *C. higginsianum* genes are already expressed by *in vitro* infection structures and/or that the IV APP library has been very efficiently normalized and deeply sequenced, so that even minute numbers of transcripts from genes showing very low or leaky transcription may be represented in this EST collection. Only 8.4 % of the total transcriptional units contain ESTs from all sampled infection stages and cell types and are thus likely to represent constitutively expressed genes.

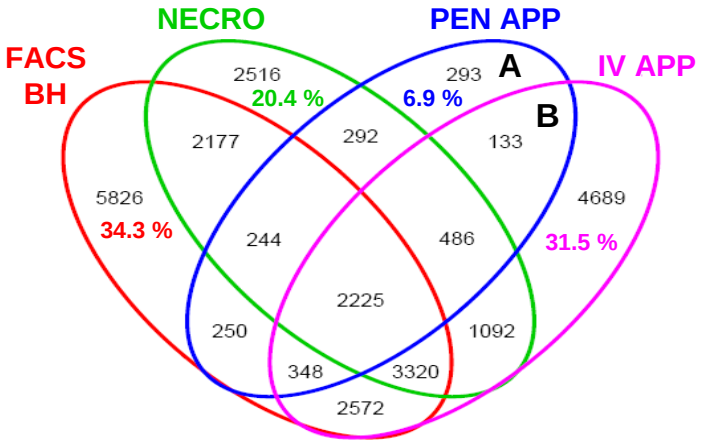

26463 grand total transcriptional units

16,962 transcriptional units with at least one FACS BH EST

12,352 transcriptional units with at least one NECRO EST

4,271 transcriptional units with at least one PEN APP EST

14,865 transcriptional units with at least one IV APP EST

Figure 4. Venn diagram showing transcriptional units (EST contigs that cluster together in the same genomic region) shared by, or unique to, the transcriptome of different infection stages or cell types. Indicated percentages specify the proportion of transcriptional units unique to the indicated stage, relative to the number of transcriptional units harbouring at least one EST of this stage. FACS BH, biotrophic hyphae isolated from infected leaves by fluorescence-activated cell sorting; PEN APP, appressoria penetrating host cells; NECRO, leaf tissue heavily infested with necrotrophic hyphae; IV APP, mature appressoria and appressorium initials formed *in vitro*. Sectors labelled with A and B represent transcriptional units which are unique to early *in planta* pathogenesis.

3.2.2.2 The transcriptome of plant-penetrating appressoria is enriched for secreted proteins, effector candidates and orphan sequences

From the co-assembly of *in planta* ESTs, 35,500 contiguous sequences were obtained. Contigs that purely consisted of NECRO ESTs and produced no match to the fungal genome assembly were likely to be derived from concomitant saprotrophic microbes, and were therefore removed. Furthermore, contigs that were less than 120 bp in size were not considered for further analysis, leaving a total of 32,794 contigs. Of these, 20,534 (63 %) were stage-specific, i. e. contained exclusively ESTs from one infection stage. As expected, the proportion of stage-specific contigs correlated with the number of stage-specific transcriptional units (see above). Again, the PEN APP library contained the lowest number of stage-specific contigs (12.4 %) compared to other *in planta* infection stages. (Tab. 6).

Both PEN APP-specific and NECRO-specific contigs contained a high proportion (71.3 % and 82.3 %, respectively) of contigs without any significant BLAST match to the nucleotide, protein and EST databases of GenBank and thus are likely to be *Colletotrichum*-specific ‘orphan’ sequences. For FACS BH-specific contigs and the grand total collection of contigs, the proportion of ‘orphan’ sequences was lower (45.7 % and 54.7 %, respectively).

Table 6: Characteristics of contigs from co-assembled *C. higginsianum in planta* ESTs.

		cDNA source[1)]			Total contigs
		FACS BH	PEN APP	NECRO	
	Contigs with at least one EST from the indicated cDNA source	25,900	5,348	16,322	
A	Stage-specific contigs composed of 100 % ESTs from the indicated cDNA source	14,869 (57.4 %)	662 (12.4 %)	5,003 (30.7 %)	32,794 [2)]
B	Proportion of A with no homology to entries in GenBank databases (%)	45.7	71.3	82.3	54.7
C	Proportion of B which have no homologue in *C. graminicola* (%)	63.0	85.6	83.5	71.0
	Proportion of A which are plant-induced (%)[3)]	46.0	48.6	48.1	38.4
	Proportion of A which encode secreted proteins (%)	0.7	3.0	0.9	1.0
	Proportion of C which are plant-induced (%)[3)]	54.4	80.0	60.5	45.8
D	Proportion of A which are considered ChECs (%)	0.4	2.3	0.6	0.6
	Proportion of D which are plant-induced (%)[3)]	60.4	80.0	58.6	49.3

[1)] FACS BH: biotrophic hyphae isolated from infected leaves by fluorescence-activated cell sorting, PEN APP: appressoria penetrating host epidermal cells, NECRO: leaf tissue heavily infested with necrotrophic hyphae.

[2)] Grand total of contigs from the co-assembly that are >120 bp, irrespective of cDNA source.

[3)] To determine plant-induced contigs, transcriptional units (i. e. all *in vitro* and *in planta* EST contigs that cluster together on the fungal genome with at least one base pair overlap), were checked for the presence or absence of ESTs from mature appressoria and developing appressoria formed *in vitro* (IV APP). Plant-induced contigs were defined as being part of a transcriptional unit entirely lacking IV APP ESTs.

To estimate how many of the identified *Colletotrichum* orphan sequences could be *higginsianum*-specific, their contigs were queried against the recently-sequenced genome of another *Colletotrichum* species, *C. graminicola*, the causal agent of maize anthracnose. PEN APP- and NECRO-specific orphan contigs were found to contain the highest proportion of contigs lacking *C. graminicola* homologues (85.6 % and 83.5 %, respectively), suggesting that these steps of crucifer anthracnose development require the highest proportion of diversified sequences and *higginsianum*-specific gene 'inventions'.

Out of the grand total of 32,794 *in planta* EST contigs, 330 (1.0 %) were predicted to encode solubly secreted proteins, i. e. to harbour ORFs that were stringently predicted by SignalP to contain a signal peptide for secretion but lacked any transmembrane-spanning α-helices. Of these, 168 (50.3 %) were found to be stage-specific. To test whether there is a preference for a particular fungal stage at which genes encoding secreted proteins are expressed, the proportion of stage-specific contigs encoding soluble secreted proteins was determined for each library. Remarkably, the highest proportion was present in the PEN APP-specific contigs (3.0 %). This was more than three times higher than for FACS BH-specific contigs (0.7 %) and NECRO-specific contigs (0.9 %) (Tab. 6).

Out of 330 soluble secreted proteins detectable in the entire *in planta* transcriptome, 201 (61 %) were considered as effector candidates (ChECs). Searches in the genome of *C. graminicola* revealed that 65 ChECs (32.3 %) had homologues in the maize anthracnose fungus. Sixty-nine ChECs were found to be depleted in NECRO ESTs (<15 %), and may therefore be preferentially expressed in biotrophy-relevant stages. Next, the proportion of stage-specific contigs encoding ChECs was determined. Again, PEN APP-specific contigs included a striking proportion that are predicted to encode ChECs (2.3 %), which was three to four times higher than for FACS BH-specific contigs (0.4 %) and NECRO-specific contigs (0.6 %) (Tab. 6). Taken together, these results suggest that the transcriptome of plant-penetrating appressoria is, in relative terms, enriched for transcripts encoding secreted proteins, including ChECs, providing a more complex secretome compared to other stages of pathogenesis.

The proportion of stage-specific contigs which are derived from plant-induced genes is similar for all three libraries. Thus, 46.0 %, 48.6 % and 48.1 % of the FACS BH-, PEN APP- and NECRO-specific contigs, respectively, lack contributing IV APP ESTs. However, these ratios change when this analysis is restricted to secreted proteins

and ChECs: 80 % of secreted proteins and ChECs that are specifically expressed in PEN APP are plant-induced. This proportion was considerably lower for FACS BH- and NECRO-specific secreted proteins and ChECs (between 54 and 60 %, Tab. 6). In other words, relative to the total number of secreted proteins and ChECs specific for each stage, there are more FACS BH- and NECRO-specific contigs that share IV APP ESTs than PEN APP-specific contigs.

3.2.2.3 The majority of highly expressed genes specific to plant-penetrating appressoria encode secreted proteins and ChECs

EST redundancy in non-normalized cDNA libraries provides an estimate of relative gene expression level, even after PCR amplification has been performed (Sacadura *et al*., 2003). Since the PEN APP library was not normalized, it was assumed that contigs enriched for PEN APP ESTs correspond to genes that were upregulated in appressoria *in planta*. Contigs consisting of more than 60 % PEN APP ESTs but less than 15 % NECRO ESTs were considered to be enriched for PEN APP ESTs without being constitutive genes expressed at high levels. The entries in Table 7 show the top 30 contigs with the highest absolute and relative numbers of PEN APP ESTs, containing an average of 92 % (± 12 %) PEN APP ESTs. These contigs accounted for 13 % of the total PEN APP ESTs that were available for co-assembly.

Remarkably, out of these 30 contigs, 18 (60 %) encode proteins predicted to be secreted. Furthermore, 12 (40 %) were considered to be ChECs. These included ChEC3 and ChEC3a, previously identified by analysis of the fungal genome and Sanger-sequenced ESTs from the FACS BH cDNA library (see 3.3.2), as well as ChEC4 and ChEC6, previously identified in a preliminary analysis of the PEN APP ESTs before the global co-assembly of *in planta* ESTs became available. The contig encoding ChEC6 contained the largest number of PEN APP ESTs (753).

Table 7. Redundancy of ESTs from plant-penetrating appressoria (PEN APP) as a measure for gene expression level: list of top 30 *in planta* EST contigs with the highest absolute and relative numbers of PEN APP ESTs.

Contig ID[1)]	PEN APP ESTs	IV APP ESTs?[2)]	Nearest informative homologue given by BLAST[3)]				Secreted?[4)]	ChEC[5)]		Remarks
			Description	Species	Accession No.	Expect value		Name[8)]	Amino acids[6)] /cysteines	
1152	753	N	-	-	-	-	Y	**6**	71/0	Contains an intron in the 3' UTR
28743	481		Retrotransposon *CgT1*	*Colletotrichum gloeosporioides*	L76169	2e-51	Y	7	69/8	Hybrid transcript with retrotransposon remnant, cysteine-rich
12272	310	N	-	-	-	-	Y[7)]	**4**	91/0	Contains a predicted nuclear localization signal
34725	257		Conserved hypothetical protein	*Sordaria macrospora*	CBI59290	5e-39		-	-	Many splice variants
32503	238		-	-	-	-	Y	8	102/1	
1281	231		Hypothetical secreted protein	*Colletotrichum higginsianum*	CAP17696	3e-16	Y	-	-	-
30751	215		-	-	-	-	-	-	-	-
30657	186	N	*CgDN3*	*Colletotrichum gloeosporioides*	AAB92221	3e-9	Y	**3**	47/2	Presumed effector of *Colletotrichum gloeosporioides*
6117	182		Hypothetical secreted protein	*Colletotrichum graminicola*	CAQ16226	4e-06	Y	-	-	-

Contig ID[1)]	PEN APP ESTs	IV APP ESTs?[2)]	Nearest informative homologue given by BLAST[3)]				Secreted?[4)]	ChEC[5)]		Remarks
			Description	Species	Accession No.	Expect value		Name[8)]	Amino acids[6)] /cysteines	
28307	167	N	-	-	-	-		-	-	Intergenic region between two otherwise not expressed polyketide synthase genes
1868	164	N	-	-	-	-	Y	9	283/0	Contains a predicted nuclear localization signal
1215	150	N	-	-	-	-		-	-	-
686	130	N	-	-	-	-		-	-	5'-UTR (?) of an otherwise unexpressed peptidase gene
2117	118		Cyclophilin	*Magnaporthe grisea*	AAG13968	2e-62		-	-	-
2898	113	N	Hypothetical protein	*Podospora anserina*	XP_001903723	3e-14	Y	-	-	-
3811	94		-	-	-	-		-	-	-
6505	89		Retrotransposon *Ccret2*	*Colletotrichum cereale*	DQ663512	2e-06	Y	10	52/0	Hybrid transcript with retrotransposon remnant, gene absent from genome assembly.
3306	83		-	-	-	-	Y	BEG6	66/8	Identified in pilot-scale EST analysis of FACS-isolated biotophic hyphae (Takahara *et al*., 2009), cysteine-rich

Contig ID[1)]	PEN APP ESTs	IV APP ESTs? [2)]	Nearest informative homologue given by BLAST[3)]				Secreted?[4)]	ChEC[5)]		Remarks
			Description	Species	Accession No.	Expect value		Name[8)]	Amino acids[6)] /cysteines	
10725	80	N	Cu/Zn superoxide dismutase	*Verticillium albo-atrum*	EEY18399	5e-46	Y	-	-	Gene located upstream of ChEC3
	74		-	-	-	-		-	-	-
131	71	N	Hypothetical protein	*Magnaporthe grisea*	XP_368940	1e-05	Y	-	-	-
6843	67		-	-	-	-	Y	11	28/6	Very small and cysteine-rich
28263	67	N	DNA transposase	*Ophiostoma novo-ulmi*	ABG26269	3e-09		-	-	-
29187	67	N	-	-	-	-	Y	12	82/6	Cysteine-rich
17128	67		-	-	-	-	Y	13	135/2	-
20127	65		Hypothetical protein	*Magnaporthe grisea*	XP_001409354	2e-08	Y	-	-	-
1153	64	N	Putative oxidoreductase	*Neosartorya fischeri*	XP_001267508	2e-56		-	-	-
8261	63		-	-	-	-		-	-	-

Contig ID[1)]	PEN APP ESTs	IV APP ESTs? [2)]	Nearest informative homologue given by BLAST[3)]				Secreted?[4)]	ChEC[5)]		Remarks
			Description	Species	Accession No.	Expect value		Name[8)]	Amino acids[6)] /cysteines	
5699	63		*CgDN3*	*Colletotrichum gloeosporioides*	AAB92221	5e-10	Y	**3a**	54/2	Paralogue of ChEC3
1627	62	N	Hypothetical protein	*Magnaporthe grisea*	XP_362922	1e-05		-	-	-

[1)] Contigs which were composed of at least 60 % PEN APP ESTs and less than 15 % ESTs from the necrotrophic stage (NECRO) are listed. There was no constraint for ESTs from FACS-isolated biotrophic hyphae (FACS BH). The mean composition for the listed contigs was 92 % (± 12 %) PEN APP ESTs, 6 % (± 10 %) FACS BH ESTs and 2 % (± 4 %) NECRO ESTs.

[2)] Transcriptional units, i. e. all EST contigs that cluster together on the fungal genome with at least one base pair overlap, were checked for the presence or absence of ESTs from mature appressoria and appressoria initials formed *in vitro* (IV APP).

[3)] BLASTN or BLASTP against the GenBank nr database

[4)] ORFs with predicted signal peptides and without transmembrane domains or GPI anchors were considered to encode solubly secreted extracellular proteins.

[5)] *C. higginsianum* effector candidates (ChECs) were defined as predicted ORFs with an N-terminal methionine which were predicted to be solubly secreted without having similarity to known proteins or having similarity to putative effectors of other fungal species.

[6)] Without signal peptide.

[7)] Experimentally verified to be secreted despite one qualifier of the SignalP program being below its threshold of significance (see text).

[8)] Numbers in bold face specify ChECs that were identified previously in a preliminary analysis of a subset of PEN APP ESTs and were chosen for further characterization.

Several of the identified ChECs were found to have notable features. For example, four ChECs were ‘cysteine-rich’, with ChEC11 having the remarkable number of six cysteines within a mature protein of only 28 amino acids. ChEC4 and ChEC9 contained predicted nuclear localization signals, and thus might be effectors that target the host nucleus for transcriptional re-programming. While ChEC4 is a relatively small protein with 91 amino acids and tandem amino acid repeats (see 3.5), ChEC9 is larger (238 amino acids). However, apart from their predicted nuclear localization signals, neither protein contains recognizable functional motifs or domains or has any significant match to entries in databases of plant transcription-related proteins.

Remarkably, two ChECs had transcripts containing remnants of retrotransposons. Contig 28743 is 1582 bp long, but only the 5’ half of the sequence encodes the ORF of ChEC7, whereas the 3’ half (the 3’ UTR with respect to the ChEC ORF) is occupied by the C-terminal part of the reverse transcriptase/RNaseH protein of CgT1, a non-LTR LINE-like element that was identified in *Colletotrichum gloeosporioides* (He *et al*., 1996) (Fig. 5 A). The retrotransposon remnant appeared to have undergone substantial truncation and mutations and thus is unlikely to encode a functional protein. The ChEC7 ORF is unlikely to be the result of an artifactual ORF prediction, since 2 further paralogues could be identified in the genome (Fig. 5 B). In *Blumeria graminis*, CgT1-like retrotransposons were recently found to have co-evolved with, and to be physically associated with, the AVR_{K1} effector gene family, which has undergone remarkable proliferation and diversification within the mildew genome (Sacristan *et al*., 2009). However, for the two identified *C. higginsianum* paralogues of ChEC7, no transposase-like sequences were found in close proximity (within 2 kb). Contig 6505 also contained a retrotransposon remnant in the 5’ UTR upstream of the predicted start codon of ChEC10. In contrast to the previous example, only a small sequence stretch of 46 bp matched to the retrotransposon Ccret2 (Crouch *et al*., 2008). Further analysis of this EST contig is complicated by the fact that the corresponding gene is absent from the draft *C. higginsianum* genome assembly, possibly due to the gene being located in a genomic region that is difficult to sequence and/or assemble. For ChEC10, no paralogues were found in the genome.

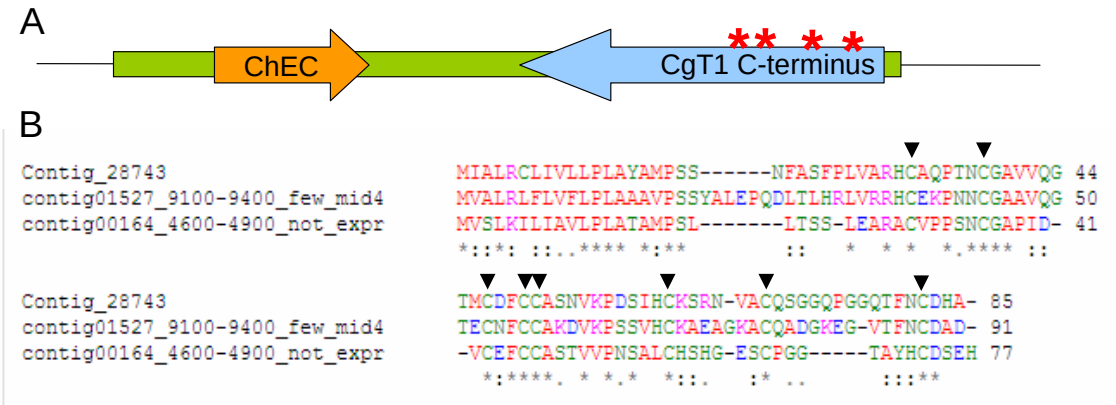

Figure 5. ChEC7 is encoded by a hybrid transcript containing a retrotransposon remnant.

A, Schematic representation of Contig 28743 (green box) with the ORF of ChEC7 (orange box). The retrotransposon remnant encoding the C-terminal half of the reverse transcriptase/RNase H protein from CgT1 (He *et al.*, 1996) is shown as a blue arrow. The weak similarity at protein level and the introduction of four stop codons (asterisks) into the protein-coding part suggests that the retrotransposon has been subjected to substantial mutations. Note the abrupt end of the region matching to CgT1, wich does not extend into the downstream genomic region (black line).

B, The ChEC encoded by contig 28743 (top sequence) has two paralogues in the fungal genome, for which either no ESTs (lower sequence) or only ESTs from appressoria *in planta* and *in vitro* could be found (middle sequence). Identical amino acids are labelled with asterisks below the sequence alignment. Arrowheads indicate eight conserved cysteines.

To test whether further ChECs with retrotransposon footprints were present in the *in planta* transcriptome, all EST contigs producing BLAST matches to transposons were extracted. Out of the 50 contigs identified, none, apart from the above-mentioned examples, contained ChEC-like ORFs. However, this does not rule out a close association of some ChECs with transposable elements within the genome that are not part of the transcript.

Out of the 30 contigs displayed in Table 7, 14 (47 %) are likely to be plant-induced genes, i. e. they lack any IV APP ESTs in their corresponding transcriptional units, consistent with results from the global analysis of PEN APP-specific contigs (Tab. 6). The contig encoding ChEC3a was also found to include many IV APP ESTs. Surprisingly, however, ChEC3a transcripts were not detectable in any *in vitro* infection structure by RT-PCR, in contrast to *in planta* appressoria (see 3.3.3). This suggests that the number of ESTs representing plant-induced genes may be even underestimated

because normalization may have resulted in artifactual amplification of rare transcripts present in *in vitro* appressoria which are negligable compared to the enormous upregulation observed by RT-PCR in plant-penetrating appressoria.

3.3 Characterization of selected ChECs

3.3.1 The identified ChECs lack a conserved amino acid motif and are not members of expanded gene families

To determine whether any of the secreted proteins identified from the *in planta* transcriptome (see 3.2.2) are member(s) of a gene family that may have expanded in the genome of *C. higginsianum,* BLAT (BLAST-like alignment tool) was used to identify EST contigs producing more than one match to the fungal genome. Most of the additional matches were artifacts, resulting from repetitive low quality sequences at the end of the contigs, and required that the ORFs corresponding to the secreted proteins were queried manually against the fungal genome using TBLASTN. The maximum number of detectable paralogues was eight for two secreted proteins resembling hypothetical secreted proteins common to various fungal species. For ChECs, the maximum number of paralogues found was only three, suggesting that if there are expanded gene families encoding secreted proteins, their members are not expressed in the *in planta* transcriptome.

Recently, the 'Y/W/FxC' motif was identified in a plethora of poorly-related effector candidates of *Blumeria graminis* f. sp. *hordei*, most of which showed stage-specific expression at high level (Godfrey *et al*., 2010). Inspired by this discovery, a motif search was conducted amoung the co-expressed ChECs. Analysis of the *in planta* transcriptome revealed that at least 69 *ChECs* appear to be preferentially expressed in biotrophy-relevant stages (see 3.2.2). The MEME software was used to identify *de novo* any possible amino acid motifs contained within this set of ChECs. However, no motif could be identified that was shared by more than three ChECs, indicating that there is no widespread protein motif within expressed ChECs.

3.3.2 ChEC genes diversified to different degrees within the genus *Colletotrichum*

ChEC1 and ChEC2 were initially identified by analysis of ESTs from appressoria formed *in vitro* (see 3.2.1; Kleemann *et al,* 2008). ChEC1 is predicted to be a very

small protein comprising only 44 amino acids after signal peptide cleavage, including six cysteines. In contrast, ChEC2 is larger and consists of 185 amino acids, of which 12 are cysteines. To estimate the degree of sequence conservation within *Colletotrichum* species, Southern blot analysis was carried out using the genomic DNA from 21 different *Colletotrichum* species and isolates. Hybridization was performed with the full-length cDNA of *ChEC1* and *ChEC2*, and the hybridization conditions allowed 25 % base pair mismatches. *ChEC2* was strongly conserved within the *C. destructivum* species aggregate, a group of closely related *Colletotrichum* species comprising *C. truncatum*, *C. destructivum*, *C. higginsianum* and *C. linicola* (Latunde-Dada and Lucas, 2007), but was not detected in any other species tested (Fig. 6). A similar distribution was obtained for *ChEC1*, except that it appeared to be conserved in *C. graminicola*, as inferred from a weakly hybridizing band.

When the *C. graminicola* genome sequence became available, both *ChEC1* and *ChEC2* were found to have orthologues in that genome. ChEC1 and its *C. graminicola* homologue only had 12 out 44 amino acids in common, none of which were cysteines. In line with the Southern analysis, an alignment at the DNA level was not possible. In contrast, ChEC2 and its *C. graminicola* homologue were more similar to each other, sharing 76 % identical amino acids and 76 % identical base-pairs, confirming the Southern analysis.

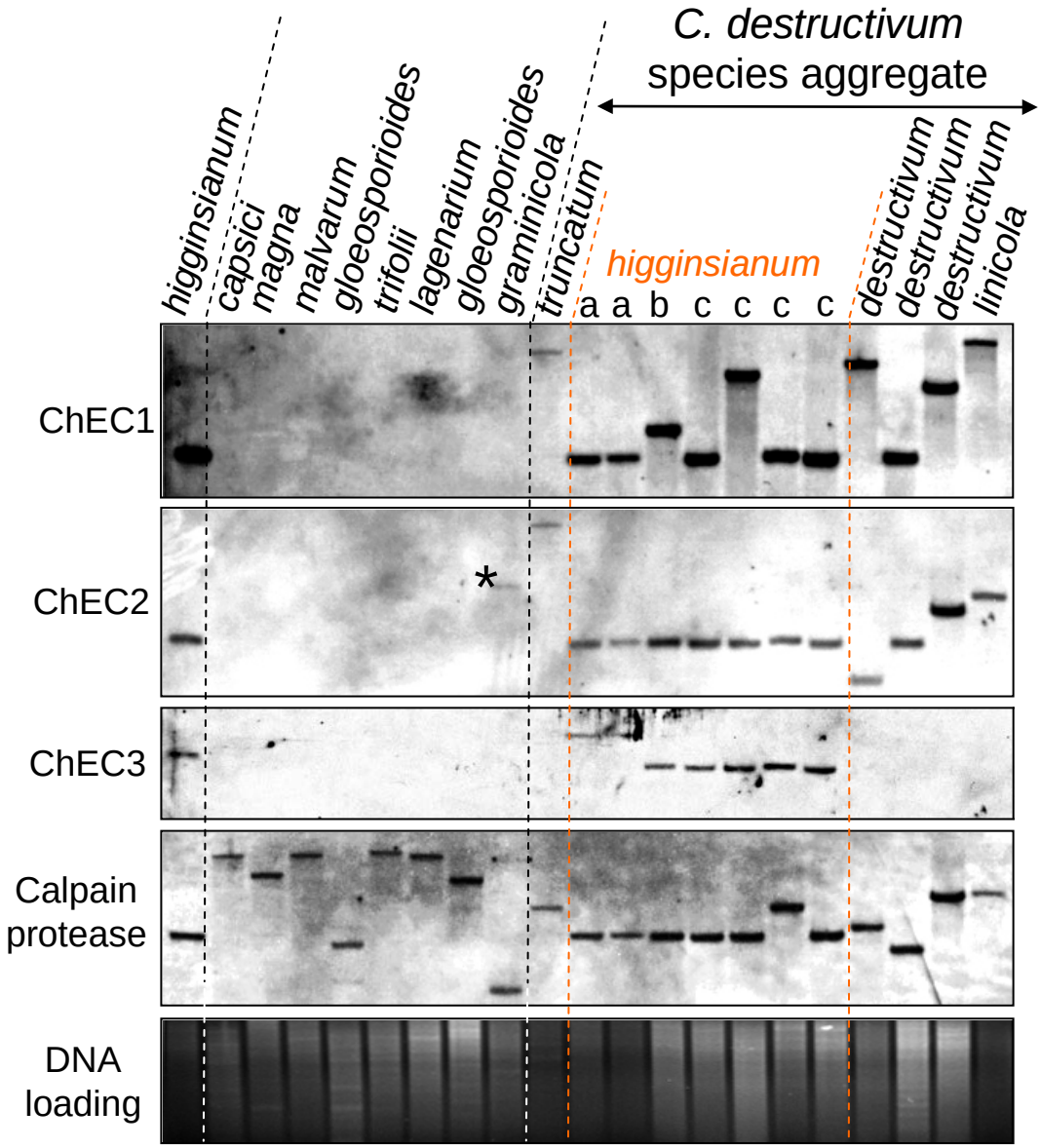

Figure 6. Sequence conservation of selected *ChEC* genes in the genus *Colletotrichum*. Digested genomic DNA of 21 different *Colletotrichum* species and isolates, respectively, was blotted onto a membrane and hybridized with labelled full-length ChEC cDNAs obtained from the *C. higginsianum* reference strain (left). Hybridization conditions allowed 25 % mismatches between orthologous sequences. Note the low sequence conservation or absence of *ChEC* genes outside the *C. destructivum* species aggregate Only ChEC1 was conserved outside the *C. destructivum* species aggregate, with a weakly hybridizing band in *C. graminicola* DNA (asterisk). *ChEC3* is only detectable in *C. higginsianum* strains, isolated from *Matthiola incana* (a), *Raphanus sativus* (b) and *Brassica spp.* (c). A gene encoding a non-secreted calpain protease, wich is the most highly expressed gene in mature appressoria and absent from most fungal genomes (Kleemann *et al*, 2008), is conserved in all the *Colletotrichum* species tested.

A photograph of the ethidium bromide-stained agarose gel before blotting is shown below to demonstrate DNA loading. From left to right, the following species and isolates were analyzed: *C. higginsianum* IMI349063A, *C. capsici* LARS 141, *Glomerella magna* LARS 688, *C. malvarum* LARS 629, *C. gloeosporioides* LARS 074, *C. trifolii* LARS 972, *C. lagenarium* 104-T, *C. gloeosporioides* LARS 224, *C. graminicola* M1.001, *C. truncatum* LARS 060, *C. higginsianum* Ch90-M3, CH93-M1, AR 3-1, NBRC6182, Abo 1-1, Abp 3-1 and MAFF 305968, *C. destructivum* N150, LARS 056 and LARS 709, *C. linicola* IMI103844.

Of all ChECs tested, ChEC3 appeared to be the least widely conserved in the southern analysis. A strong hybridization signal was only detectable in DNA from other *C. higginsianum* isolates, and not from any other close relatives in the *C. destructivum* species aggregate. ChEC3 and its paralogue ChEC3a were found initially in ESTs from biotrophic hyphae isolated by FACS and by searching a draft assembly of the *C. higginsianum* genome, respectively. Both show weak similarity to CgDN3, a presumed effector from *C. gloeosporioides* (Stephenson *et al*., 2000), and lack homologues in the *C. graminicola* genome. ChEC3 and its two homologues are small proteins (47 to 56 amino acids after signal peptide cleavage), and have only 17 amino acids in common. Interestingly, despite the high number of polymorphic amino acids, the potential of certain regions of the proteins to form short alpha helices, beta strands and coils was the same, suggesting that secondary structure has been conserved in these homologues (Fig. 7). Remarkably, also the exon-intron structure is conserved between these highly divergent effector genes.

The low degree of sequence conservation of *ChEC3* in the genus *Colletotrichum* prompted the question whether particular codons of that gene could be subject to positive selection, which is a frequent feature of pathogen effectors that are rapidly evolving as part of an arms race between pathogen and host (Aguileta *et al*., 2009). *ChEC3* and *ChEC3a* genes from 17 *C. higginsianum* isolates were sequenced, including those analysed by Southern hyridization shown in Figure 6. Surprisingly, a high degree of sequence conservation was found for both genes, even within intron sequences. In fact, neither synonymous nor non-synonymous polymorphisms were found, except for one SNP in *ChEC3a* leading to an amino acid exchange in *C. higginsianum* isolate AR3-1 (Fig. 7), suggesting that this amino acid residue could be under positive selection. The employed genomic DNAs showed substantial restriction fragment polymorphisms (Fig. 6), making it unlikely that the sampled fungal isolates

were identical. Taken together, ChEC3 appears to be interspecifically diversified or absent, but intraspecifically conserved.

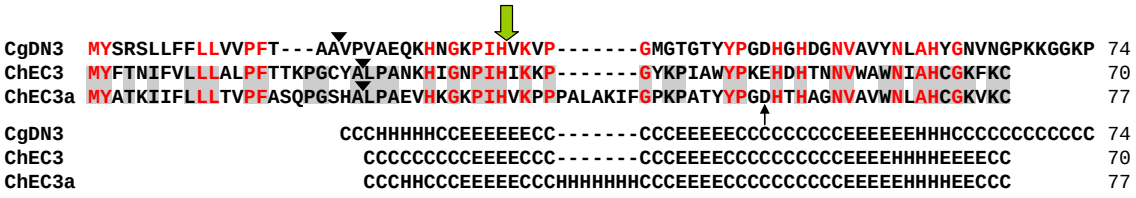

Figure 7. Alignment of ChEC3, ChEC3a and *C. gloeosporioides* (CgDN3) protein sequences after signal peptide cleavage (above) and corresponding secondary structure predictions of the mature proteins (below). Amino acid residues identical in all three proteins are indicated in red, those identical in ChEC3 and ChEC3a are shaded in grey. The predicted signal peptide cleavage site is marked with a triangle. The green arrow indicates the conserved position of a phase 2-intron, which splits the codon for the conserved histidine residue between the second and third base. A black arrow indicates the only identified SNP within ChEC3 and ChEC3a genes sequenced from 17 different *C. higginsianum* isolates, resulting in an exchange of the aspartate with asparagine in the protein sequence of ChEC3a in *C. higginsianum* isolate AR3-1. C, coil; E, strand; H, helix.

3.3.3 Most identified ChECs show strongly stage-specific expression *in planta*

The identification of ChEC1 to ChEC6 in collections of stage-specific ESTs does not rule out possible expression during other stages of fungal pathogenesis. Furthermore, ChEC genes that show a constitutive expression pattern, or are expressed also at the late necrotrophic stage, are unlikely to play a role in establishment or maintenance of the biotrophic interaction and would not be chosen for further characterization. To determine *ChEC* expression levels during fungal pathogenesis, RT-PCR was carried out using cDNA generated from four fungal cell types produced *in vitro* (namely ungerminated spores, germ tubes with appressorial initials, mature appressoria and saprophytic mycelium) and five different stages of fungal development *in planta*, ranging from early germination to the late necrotrophic phase.

As expected, *ChEC5*, which was identified in a proteomic analysis of the secretome of *in vitro* appressoria as well as *ChEC1* and *ChEC2*, identified from *in vitro* appressoria ESTs, were expressed in germ tubes and appressoria developing *in vitro* (Fig. 8). For *ChEC5* and *ChEC1*, their expression patterns *in vitro* and *in planta*

were different. ChEC1 appeared to be most highly expressed in mature appressoria *in vitro*, whereas highest transcript accumulation was found at the germ tube stage *in planta*. *ChEC5* was highly expressed in germ tubes and appressoria formed on a polystyrene substratum but, surprisingly, not in germ tubes and appressoria *in planta*. Interestingly, genes encoding *ChEC3*, *ChEC3a*, *ChEC4* and *ChEC6* were all highly upregulated, or exclusively expressed, in appressoria penetrating the leaf epidermis but transcripts were not detectable in any infection structures formed *in vitro* (Fig. 8), suggesting that these genes are induced by plant-derived cues or that their expression is linked to penetration peg and infection vesicle morphogenesis. Their expression pattern is consistent with the finding that EST contigs corresponding to these genes predominantly consisted of PEN APP ESTs.

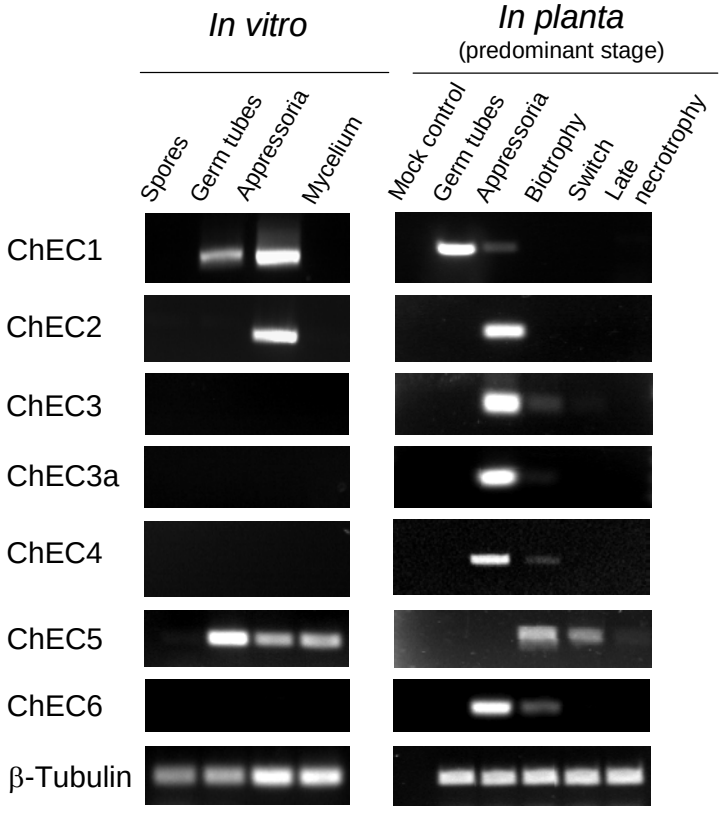

Figure 8. Detection of transcripts of *Colletotrichum higginsianum* effector candidates (ChECs) in four different cell types and at five stages of plant infection using RT-PCR. Total RNA was extracted from ungerminated and germinated conidia, appressoria formed *in vitro* and saprophytic mycelium as well as from epidermal peels of infected *Arabidopsis thaliana* leaves representing pre- and post-penetration phases of infection. The β-Tubulin amplicon was used to adjust cycle numbers and loading of individual PCR reactions to allow for variation of fungal biomass. A representative picture of 3 experimental replicates with similar results is shown**.**

With the exception of *ChEC1* and *ChEC5*, most *ChEC* genes are expressed predominantly at one stage, as revealed by a strong amplicon band. Only a minor amplicon band was found in the subsequent infection stage. This may reflect the relatively poor synchronization of fungal development *in planta*, whereby the development of some propagules lags behind the majority of infection structures. Overall, the expression of most *ChEC* genes analyzed in this study was highly stage-specific and appears, within the sampled intervals, to be induced only transiently, suggesting tight gene regulation.

3.4 Functional analysis of effector candidates by targeted gene replacement

A targeted gene knockout in *Colletotrichum gloeosporioides* allowed the identification of the sole *Colletotrichum* secreted effector protein known to date and provided unambiguous genetic evidence that the gene is required for full pathogenicity (Stephenson *et al*., 2000). Given the genetic tractability of *C. higginsianum*, this approach could likewise be used to test directly whether the identified ChECs make a measurable contribution measurably to fungal virulence. Since ChEC1 and ChEC2 were the first *C. higginsianum* effector candidates to be identified (Kleemann *et al*., 2008), these as well as the subsequently discovered ChEC3 were chosen for targeted gene replacement.

3.4.1 Establishing targeted gene replacement for *C. higginsianum* and deletion of effector candidate genes *ChEC1* and *ChEC2*

When this project was initiated, no methods for targeted gene knockout in *C. higginsianum* had been reported in the literature. Thus, gene knockout strategies previously applied to other fungal species had to be adapted. Initial attempts using PEG-mediated protoplast transformation with split hygromycin-marker constructs (Venard *et al*., 2008; Szewczyk *et al*., 2006) failed because no hygromycin-resistant transformants could be recovered (not shown). In an alternative approach, *Agrobacterium tumefaciens*-mediated transformation was used. For this, the flanking sequences surrounding the target gene were fused upstream and downstream of a bacterial hygromycin phosphotransferase (*Hph*) gene and cloned into a binary vector (Fig. 9). After co-cultivation with agrobacteria, the resulting hygromycin-resistant colonies were screened in a multiplex PCR which allowed the identification of transformants that had undergone double, single or no cross-over with the incoming T-DNA. Hereafter, transformants that had undergone double cross-over are referred to as targeted mutants, whereas those in which homologous recombination had failed are referred to as ectopic mutants.

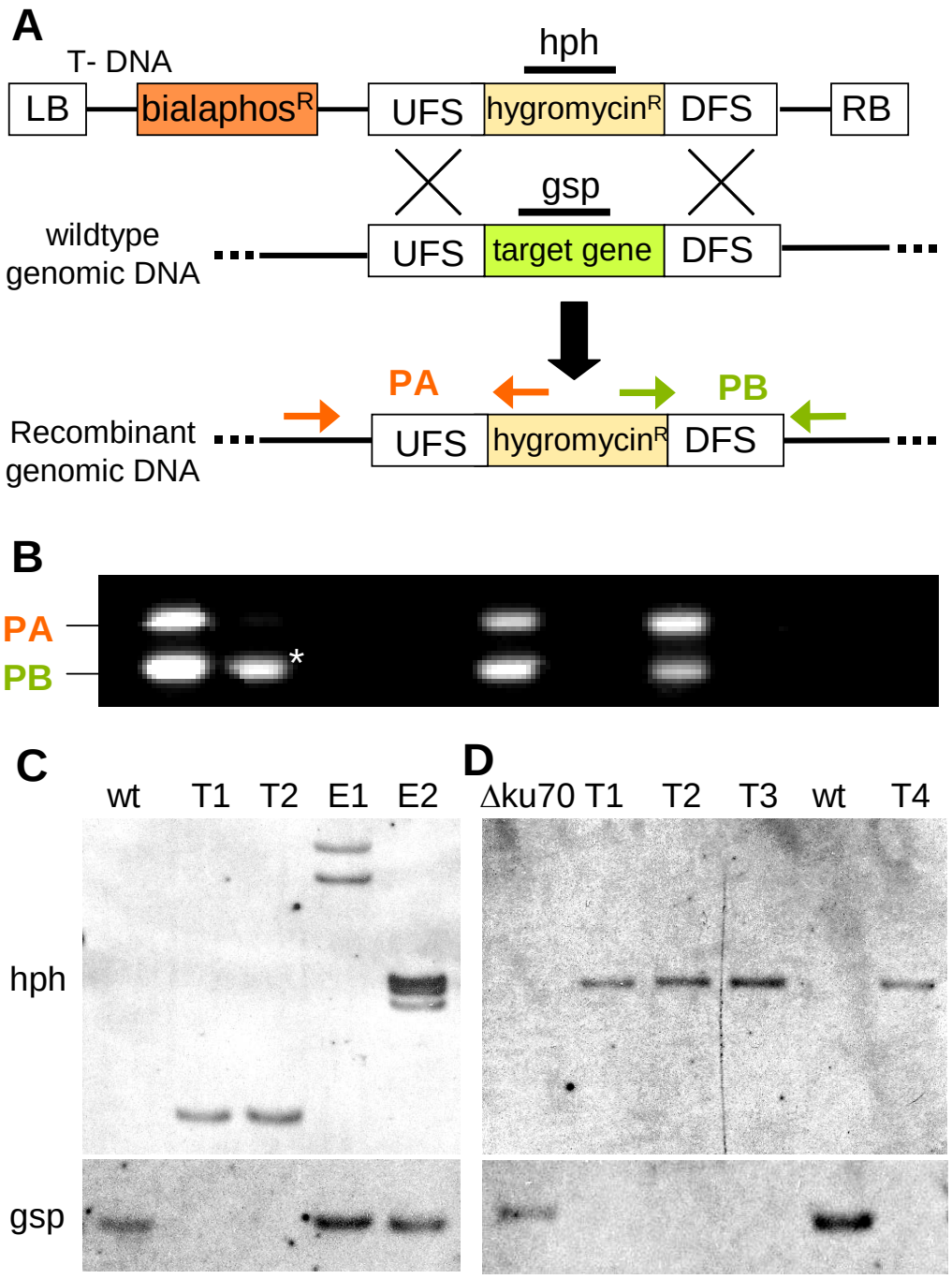

Figure 9. Targeted gene-replacement in *Colletotrichum higginsianum*.

(A) The upstream (UFS) and downstream (DFS) flanking sequence of a target gene are cloned into the T-DNA of a binary vector adjoining a hygromycin resistance cassette containing the hygromycin phosphotransferase gene (hygromycin^R). The UFS and DFS of the incoming T-DNA undergo double cross-over homologous recombination with target sequences, resulting in hygromycin-resistant mutants lacking the target gene. Ectopic mutants are resistant to bialaphos, while targeted mutants are not.

(B) Primer combinations PA and PB, each having one primer matching to the genomic backbone, allow screening of hygromycin-resistant transformants for double cross-over events

in a Multiplex PCR. Note that some transfomants have only undergone single cross-over (asterisk).

(C) and (D) Southern blot analyses to confirm loss of the target genes *ChEC2* (C) and *ChEC1* (D). T, targeted mutants. E, ectopic mutants. wt, wild-type. Δku70, mutant impaired in non-homologous end-joining (Krappmann, 2007). gsp, target gene-specific probe. hph, probe located in the hygromycin resistance cassette. Note that E1 and E2 in (C) contain multiple ectopic insertions of the T-DNA.

Table 8. Efficiency of targeted gene replacement in *Colletotrichum higginsianum.*

	Length of cloned sequence flanking the target locus (bp)			Genetic background of recipient fungal strain					
				Δ*ku70*			Wild-type		
Targeted locus	Up-stream	Down-stream	Total	KO[1)]	Hyg^R colonies	%[2)]	KO[1)]	Hyg^R colonies	%[2)]
ChEC1	883	682	1565	6	29	20,7	1	40	2,5
ChEC2	937	707	1644	25	36	69,4	2	60	3,3
ChEC3 - construct A[3)]	859	846	1705	0	52	0	0	80	0
ChEC3 - construct B[4)]	279	515	794	0	54	0	0	~650[5)]	0

[1)] Successful gene replacement of targeted transformants (KO) was determined by Multiplex PCR using two primer pairs spanning the left and right junctions between fungal DNA and integrated T-DNA.

[2)] Proportion of targeted transformants among hygromycin-resistant (Hyg^R) colonies.

[3)] The flanking sequence of construct A was found to contain remnants of a fungal transposase appearing at several positions in the draft fungal genome assembly.

[4)] Construct B was shortened to portions unique in the fungal genome.

[5)] Approx. 400 Hyg^R colonies were pooled for a bulk DNA extraction and 250 Hyg^R colonies were pre-screened for loss of bialaphos resistance, which should indicate a targeted gene replacement.

Using a total of 1565 bp flanking sequence, *ChEC1* was found to be successfully replaced in 2.5 % of the hygromycin-resistant transformants in a wild-type background (Table 8). Similarly, *ChEC2*-lacking mutants were obtained with a success rate of 3.3 % using a total of 1644 bp flanking sequence. However, an extraordinary increase in the rates of targeted gene replacement could be observed when a Δ*KU70* strain of *C. higginsianum* (G. Tsuji, unpublished) was employed as T-DNA recipient strain. KU70 is a protein required for the non-homologous end-joining pathway of DNA double-strand break repair which competes with the pathway of homologous integration

(Krappmann, 2007). Interfering with the non-homologous end-joining pathway of *C. higginsianum* by mutating *ChKU70* allowed targeted mutants to be recovered ten to twenty times more frequently compared to wild type background (Tab. 8).

After the initial multiplex PCR screen, selected targeted mutants of *ChEC1* and *ChEC2* and corresponding ectopic transformants were confirmed by Southern blot analyses (Fig. 9 C, D). As expected, targeted mutants lacked the target gene. In contrast, ectopic mutants were wild-type with respect to the target locus, but contained one or several ectopic integrations of the T-DNA. Mutant conidia that were obtained after subculturing twice on non-selective medium still gave rise to hygromycin-resistant colonies lacking the target gene, suggesting a stable integration of the antibiotic resistance marker and stable asexual propagation into subsequent generations.

3.4.2 The *ChEC3* locus is recalcitrant to homologous recombination

The *ChEC3* locus turned out to be a remarkably difficult target for homologous recombination. In a first transformation attempt, no targeted mutants could be obtained in either wild-type or Δ*KU70* backgrounds, although the cloned flanking sequence was slightly longer (1705 bp) than for the previously described mutants. After a first draft assembly of the *C. higginsianum* became available, it was possible to estimate the uniqueness of the cloned flanking sequences in the genome. In contrast to the flanking sequences employed for *ChEC1* and *ChEC2* targeting, a short portion of each of the cloned up- and downstream sequences flanking *ChEC3* were not unique in the fungal genome. The upstream flanking sequence contained a 188 bp stretch which occured three times elsewhere in the genome, whereas the downstream flanking sequence carried a 112 bp segment matching to as many as 24 paraloguous sequences (e value < $1e^{-5}$). In both cases, there was 88 % nucleotide identity between the best-matching paralogous sequences. To test whether these proliferated sequences were part of a known transposable element, BLAST against NCBI's non-redundant nucleotide and protein databases and against RepBase, a database hosting repetitive DNA elements, was conducted but without revealing any significant match. However, when queried against the assembled, 454-sequenced *C. higginsianum* transcriptome (see 3.2.2), the 112 bp-long DNA sequence matched significantly (e value $1e^{-18}$) to the UTR of an OPHIO2-like transposable element (Bouvet *et al*., 2007). This suggests, that at least

the sequence stretch in the cloned downstream targeting sequence is a remnant of a transposition event, which occurred at many locations in the genome.

It is plausible that the lack of uniqueness of the cloned flanking sequences accounted for the failure of homologous recombination required for replacement of *ChEC3* with the hygromycin resistance cassette. To test this, the flanking sequences were shortened to unique portions with a total length of 794 bp. Approximately 650 transformants in the wild-type background were analyzed, of which 250 were pre-screened for the loss of bialaphos resistance, which should result from a targeted gene replacement event (Fig. 9 A) The candidates obtained from pre-screening and a bulk DNA extraction from approximately 400 pooled transformants were analyzed by multiplex PCR. In addition, 54 hygromycin-resistant colonies in the Δ*KU70* background were individually tested. Despite the extremely high number of tested transformants, none gave rise to amplicons indicative of single or double cross-over events. To rule out false negative results resulting from PCR failure, the initially-used larger construct, containing all binding sites for the employed multiplex-primers, was included as a positive control. When the bulk DNA extract was supplemented with 10 pg/µL of the longer construct, the expected amplicons were obtained, confirming that the lack of targeted mutants was due to a failure of homologous recombination between the incoming T-DNA and the genomic locus. Thus, the transposase footprint appeared not to be responsible for failure of targeted gene replacement. Taken together, the *ChEC3* locus proved to be recalcitrant to gene targeting by homologous recombination.

3.4.3 Characterization of Δ*ChEC1* and Δ*ChEC2* mutants

Two independent mutants lacking *ChEC1* or *ChEC2* and mutants showing ectopic integration of the corresponding T-DNA were selected for phenotypic characterization. Both mutants grew and sporulated normally *in vitro* and neither gene was required for spore germination and appressorium morphogenesis (Fig. 10). Furthermore, neither of these genes seem to contribute to formation of the proteinaceous matrix surrounding germinating conidia and appressoria formed *in vitro* (Fig. 10). The overall mycelial growth rate of the mutants was not different from wild-type *C. higginsianum* (not shown).

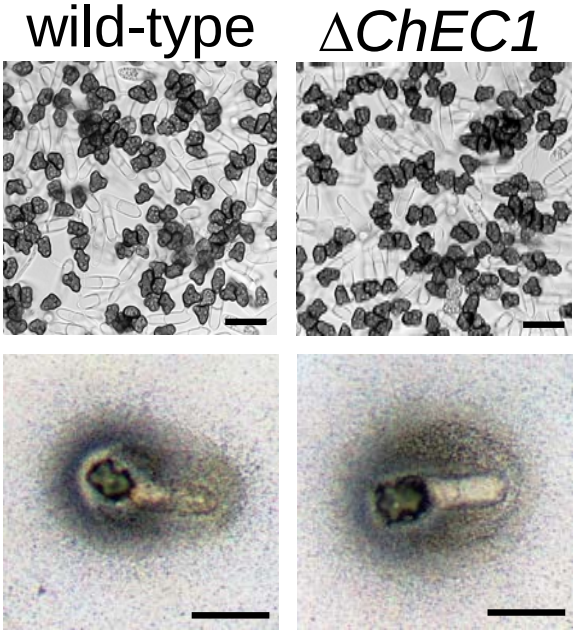

Figure 10. *Colletotrichum higginsianum* mutants lacking *ChEC1* are not impaired in appressorium development (top). ChEC1 is not a major constituent of the extracellular matrix surrounding appressoria (bottom). Protein haloes of the extracellular matrix around both wild-type and mutant label intensely with a sensitive total protein stain (silver-enhanced colloidal gold). Similar results were obtained with mutants lacking *ChEC2*. Scale bars: 10 µm.

When inoculated onto *Arabidopsis* Ler-*er* plants at $5x10^5$ spores per mL, no obvious reduction in pathogenicity was observed between wild-type and mutant strains in terms of symptom severity or timing of symptom development (Fig. 11). Infected plants appeared completely macerated six days after inoculation. However, similar symptoms on Ler-*er* plants could be obtained with wild-type spores using a five- to ten-fold lower spore concentration (not shown), indicating that this accession is extremely susceptible to *C. higginsianum* infection. Therefore, in subsequent experiments the intermediate susceptible accession Col-0 (O'Connell *et al*., 2004; Birker *et al*., 2009) was chosen in order to reveal subtle pathogenicity phenotypes.

ChEC1 and *ChEC2* mutants showed reduced symptoms compared to wild-type inoculations in three out of six experiments. However, the two independent mutants in each gene did not behave in a consistent manner in all experiments (Fig. 11). Remarkably, such inconsistent behaviour was never observed for the wild-type strain or any of the three ectopic mutants. Similar results were obtained by inoculating seedlings of various *Brassica* cultivars.

It is known that a moderate increase in temperature (to 28 °C) can impair basal and R-gene mediated defence in *Arabidopsis* (Wang *et al*., 2009). *Colletotrichum higginsianum* requires relatively high temperatures for optimal growth (O'Connell *et al*., 2004) and pathogenicity assays were routinely performed at 25 °C. To rule out the possibility that the incubation temperature weakened plant immunity to such an extent that it would be impossible to reveal subtle differences in fungal virulence, inoculation assays were repeated at 20 °C and 14 °C. Although symptom development took considerably longer (up to 10 days at 14 °C), no difference between wild-type and mutants became obvious (results not shown).

Transcription of the genes encoding *ChEC1* and *ChEC2* is upregulated in mature appressoria *in planta*, i. e. before or during host penetration. Thus, mutants lacking these genes could conceivably show impaired penetration frequency or weakly delayed penetration, but without this translating into a visible difference in symptom severity at later stages of infection. To test this possibility, penetration efficiency of appressoria from targeted and ectopic mutants as well as from the wild-type strain was determined on spray-inoculated Col-0 cotyledons. Since the penetration efficiency of *C. higginsianum* appressoria can differ across the lamina of mature rosette leaves and is strongly dependent on leaf age (Liu *et al*., 2007), cotyledons of synchronously germinated seedlings were used for determining fungal entry rate. Penetration was scored by counting appressoria that had elaborated infection vesicles or fully-expanded biotrophic hyphae inside epidermal cells at 42 and 54 hpi using light microscopy. Figure 11 D shows the individual and mean appressorial entry rates for three independent experiments for mutants lacking *ChEC1*, corresponding ectopic mutants and the wild-type strain. Twenty-five percent of wild-type appressoria successfully penetrated the host epidermis at 42 hpi. Compared to this, the penetration rate of ectopic mutants was not statistically different ($P>0.12$). In contrast, appressoria of two independent *ChEC1* knockout mutants penetrated with significantly lower frequency compared to wild-type ($P<0.02$). The mean increase in entry rate occurring between 42 and 54 hpi was not significantly different ($P=0.8$) between targeted mutants (12.7 % ± 0.8) and ectopic mutants/wild type (10.5 % ± 8.8). This suggests that the targeted mutants display a penetration delay rather then a penetration failure *per se*. However, although mean entry rates of the ectopic mutants were higher at 42 hpi than those of targeted mutants, this difference was not or only weakly significant ($P>0.2$ against ectopic mutants E1 and E2, $P>0.06$ against E3). This suggests that enumerating the

penetration frequency of *C. higginsianum* appressoria on wild-type hosts is not sensitive enough to detect small reductions in penetration due to the high level of background variability.

Similar results were also obtained for mutants lacking *ChEC2* (not shown). Taken together, these results suggest that deletion of *ChEC1* and *ChEC2* individually does not produce a virulence phenotype that is consistent and reproducible under laboratory conditions.

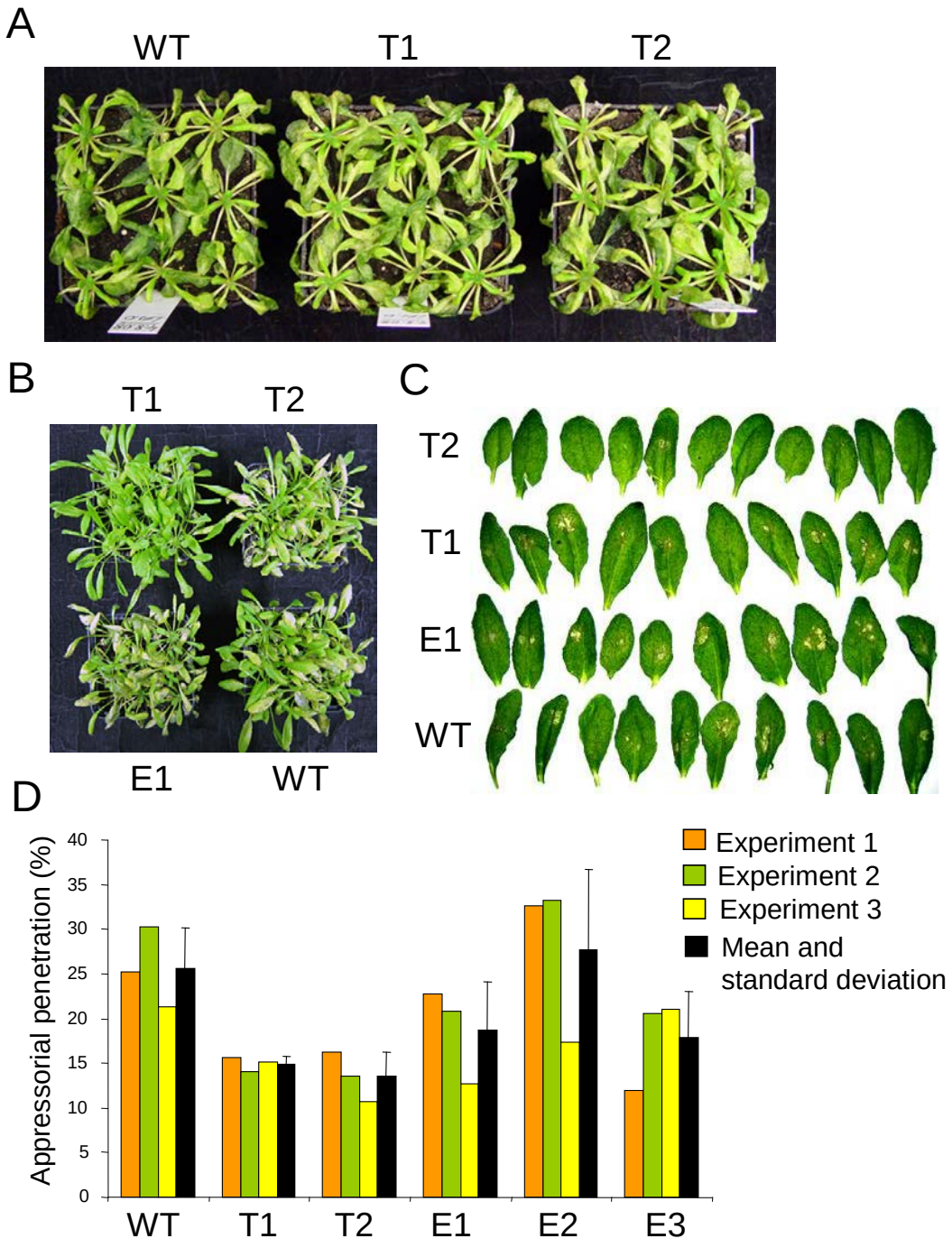

Figure 11. *C. higginsianum* mutants lacking ChEC1 fail to give a consistent and reproducible virulence phenotype in infection assays and penetration counts.

(A) The highly susceptible *Arabidopsis* accession Ler-*er* is completely macerated at 6 dpi after spray-inoculation with mutants lacking *ChEC1* (T1 and T2) or wild-type strain (WT). Similar results were obtained for mutants lacking *ChEC2*.

(B) and (C), Infection phenotypes of targeted mutants lacking *ChEC1* (T1, T2), corresponding ectopic mutant (E1) and wild-type (WT) on intermediate susceptible Col-0 plants. (B), Plants were photographed at seven days after spray inoculation. Note that targeted mutant KO1 gave rise to less severe symptoms than KO2. (C) Leaves of Col-0 plants after droplet inoculation with targeted mutants, ectopic mutants and wild-type, detached and photographed 6 dpi on a light screen. Water-soaked lesions, indicative of extensive necrotrophic proliferation, appear as bright patches on the leaf lamina. Note that in this experiment T2 gave rise to less severe symptoms than T1.

(D) Appressorial entry rates of mutants and wild-type. Col-0 plants were spray-inoculated with conidial suspensions and after 42 hpi, cotyledons of synchronously germinated seedlings were prepared for microscopy and appressoria scored for presence of infection vesicles and biotrophic hyphae. For each fungal strain and experiment, at least 300 appressoria on at least 20 seedlings were inspected

3.5 ChEC4 – a putative reprogrammer of host gene expression

ChEC4 was found through 454-sequencing of the fungal transcriptome during plant penetration. ChEC4 ESTs were the third-most abundant in the pentration-associated cDNA library, indicative of a strong gene expression or mRNA stability. The predicted protein encoded by ChEC4 consisted of only 107 amino acids (11 kDa, including signal peptide) and displayed a remarkable modular structure: three nearly identical tandem amino acid repeats of 27 amino acids encompassing a predicted bipartite nuclear localization signal (Fig. 12). It is noteworthy that the SignalP program did not reveal a strong signal peptide prediction, with the score for the cleavage site probability of the SignalP-NN algorithm just below its threshold of significance. However, several other signal peptide prediction programs, including Sosui and WolfPsort predicted a signal peptide for secretion. It was therefore hypothesized that ChEC4 may be transferred to the extracellular space following the classical fungal secretory pathway with subsequent transfer into the plant cell, where it may enter the plant nucleus to interfere with host gene expression.

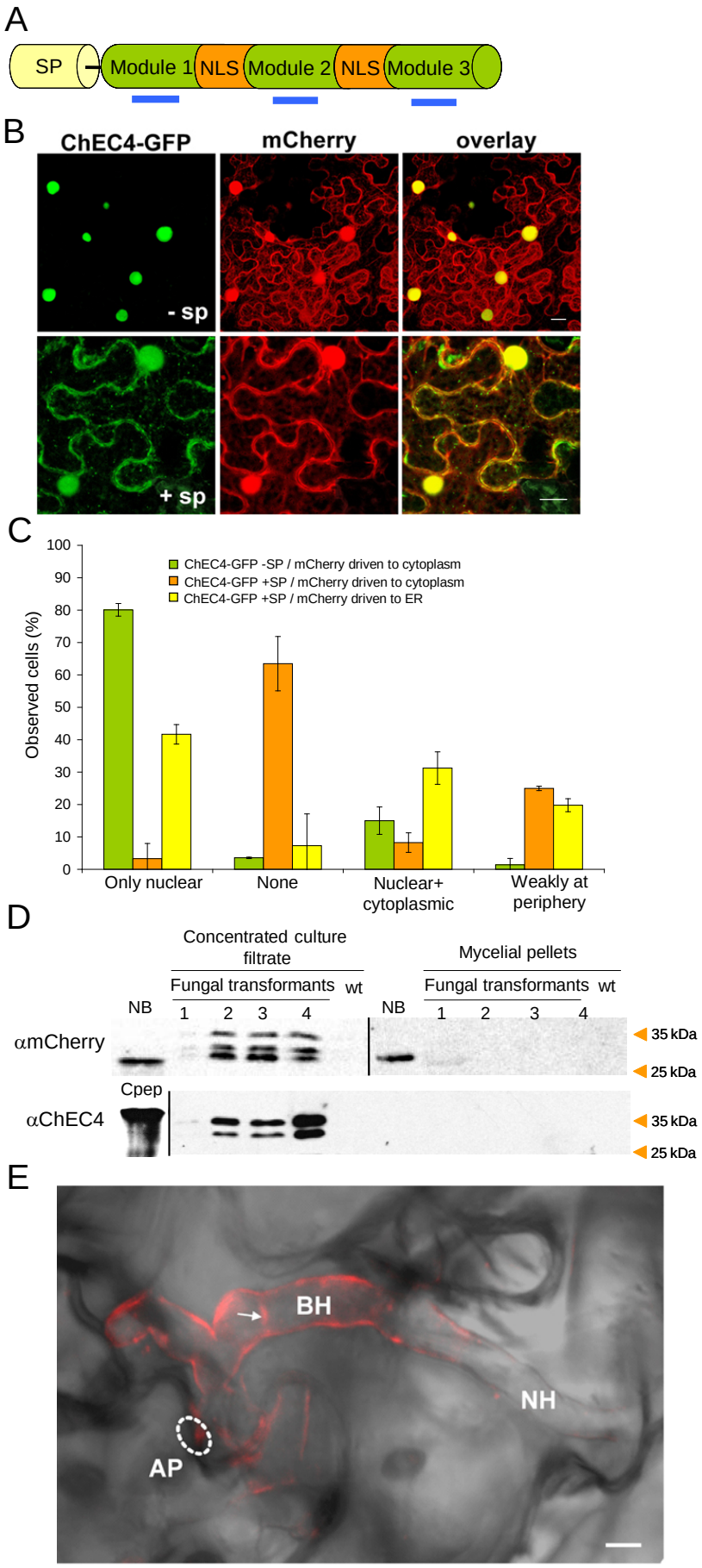
A
SP
Module 1
NLS
Module 2
NLS
Module 3
B
ChEC4-GFP
mCherry
overlay
- sp
+ sp
C
ChEC4-GFP -SP / mCherry driven to cytoplasm
ChEC4-GFP +SP / mCherry driven to cytoplasm
ChEC4-GFP +SP / mCherry driven to ER
Observed cells (%)
100
90
80
70
60
50
40
30
20
10
0
Only nuclear
None
Nuclear+ cytoplasmic
Weakly at periphery
D
Concentrated culture filtrate
Mycelial pellets
Fungal transformants
wt
NB
1
2
3
4
αmCherry
Cpep
αChEC4
35 kDa
25 kDa
E
BH
NH
AP

Figure 12. ChEC4 contains a functional nuclear localization signal and a functional signal peptide for secretion.

(A), Schematic protein structure. ChEC4 is predicted to be a small (11 kDa) protein with three nearly identical tandem amino acid repeats forming modules which encompass a predicted bipartite nuclear localization signal (NLS). SP, predicted signal peptide for secretion. Blue lines indicate identical regions of the protein which were chemically synthesized as a peptide against which a polyclonal antibody was raised.

(B), Transient over-expression of ChEC4-GFP in *Nicotiana benthamiana* by agroinfiltration. ChEC4-GFP lacking its predicted signal peptide (-SP, top) shows strong accumulation in cell nuclei in contrast to the similar-sized mCherry. Nuclear accumulation is abolished by expression of the full-length fusion protein including its signal peptide (+SP, bottom). Note that the plant cytoplasm contains pin-point speckles of GFP fluorescence. Scale bar: 10 µm

(C), Biolistic delivery of ChEC4-GFP and mCherry as transformation marker into epidermal cells of *Arabidopsis thaliana* Col-O. Indicated is the proportion of mCherry-expressing cells which displayed the GFP localization specified below the columns.

(D), Western blot analysis of fungal mutants constitutively expressing a ChEC4-mCherry fusion protein. Following SDS-PAGE, concentrated culture supernatants and total protein extracts from mycelium of transformants and wild-type (wt) were blotted onto a membrane and probed with an antibody against mCherry and ChEC4, respectively. Note that the total amount of loaded protein was four times higher for the mycelial samples. Total protein extract from *N. benthamiana* expressing mCherry (NB) and the synthetic ChEC4 peptide coupled to a carrier protein (Cpep, 400 kDa) were used as positive controls.

(E), Confocal microscopy of fungal transformants constitutively expressing ChEC4-mCherry and infecting the host epidermis reveals extracellular mCherry labeling of cell walls of biotrophic hyphae (BH). The fluorescence signal is retained in the fungal cell walls after the switch to necrotrophy. AP, appressorium (indicated by dotted line). NH, necrotrophic hypha. Arrow, cell wall septum between two biotrophic hypha cells. Wild-type biotrophic hyphae were found to be devoid of any fluorescence (not shown). Scale bar: 5 µm.

3.5.1 ChEC4 contains a functional nuclear localization signal

To test whether ChEC4 contains a functional NLS, ChEC4 was C-terminally fused to GFP and expressed transiently in *Nicotiana benthamiana* leaves *via Agrobacterium* infiltration (Fig. 12 B). Expression without its predicted signal peptide resulted in strong nuclear accumulation, as revealed by exclusively nuclear GFP fluorescence. In contrast, co-expressed mCherry protein, which has a similar molecular size, was found

throughout the plant cytoplasm, including nuclei. This nuclear localization of mCherry is the result of its small size (~30 kDa) which allows passive diffusion through nuclear pores (Weigel and Glazebrook, 2002). Expression of ChEC4-GFP including the fungal signal peptide abolished nuclear accumulation of GFP and resulted in a fluorescence distribution similar to mCherry. However, in rare cases, the plant cytoplasm contained pin-point speckles of GFP fluorescence, as exemplified in Figure 12 B (bottom panel)

Biolistic transformation of *Arabidopsis thaliana* Col-0 epidermal cells was used to confirm these results in a true host of *C. higginsianum*. ChEC4-GFP was co-expressed with (+SP) and without (-SP) the fungal signal peptide, together with mCherry targeted either to the ER or cytosol, repectively, as transformation marker. As expected, when transformed with ChEC4-GFP -SP most (80.1 %) of the cells positive for the mCherry transformation marker also displayed a strong and exclusively nuclear GFP fluorescence (Fig. 12 C) However, in contrast to *N. benthamiana*, inclusion of the fungal signal peptide into the ChEC4-GFP construct resulted in no visible GFP fluorescence in most (63.5 %) of the cells. Interestingly, co-expression of ER-targeted mCherry with ChEC4-GFP +SP increased the proportion of cells showing GFP exclusively in nuclei, possibly as a result of two strongly over-expressed proteins being targeted to the secretory pathway and thereby saturating co-translational ER-import.

3.5.2 ChEC4 is a genuine secreted protein

To verify whether ChEC4 carries a functional signal peptide for secretion, *C. higginsianum* transformants were generated to constitutively express a ChEC4-mCherry fusion protein under the control of the *Aspergillus nidulans* trpC promoter. mCherry was chosen because of its better performance compared to GFP in the acidic environment of the plant apoplast (Zheng *et al*., 2004; Shaner *et al*., 2005; Doehlemann *et al*., 2009), although the pH of the interfacial matrix between *C. higginsianum* biotrophic hyphae and plant plasma membrane is unknown. Fungal transformants were recovered which transcribed full-length transcripts of the synthetic gene (not shown). Western blot analysis of concentrated culture filtrates of saprophytic mycelia using a mCherry-specific antibody allowed the detection of three protein bands which were absent in wild-type samples. One out of four transformants appeared to express the fusion protein only weakly. No hybridizing bands could be detected in

total protein extracts derived from the corresponding mycelial pellets (Fig. 12 D). In addition to the full-length fusion protein (39 kDa expected size), two smaller bands could also be observed, indicative of partial degradation into protein fragments containing the mCherry epitope. All three fragments had a higher apparent molecular weight than mCherry. Recording of fluorescence emission revealed that culture filtrates from transformant but not wild-type cultures exhibited an emission spectrum typical for mCherry (see Supplementary Figure 1), corroborating the results of the Western blot analysis and demonstrating that ChEC4-driven mCherry secretion can be readily monitored via its fluorescence.

To track the distribution of the fusion protein *in planta*, transformants constitutively expressing ChEC4-mCherry were inoculated onto *A. thaliana* leaves. No red fluorescence was visible surrounding penetrating appressoria, and cell walls of very young biotrophic hyphae rarely displayed a weak mCherry signal. However, strong mCherry accumulation was found in cell walls of mature biotrophic hyphae and in biotrophic hyphae that had undergone the switch to necrotrophy (Fig. 12 E). Remarkably, the mCherry signal was specific to the biotrophic cell walls despite constitutive transgene expression and was retained in fungal cell walls even after death of the host cell had occurred. In contrast, no fluorescence was detectable in hyphae from untransformed fungus. Taken together, these results strongly suggest that ChEC4 carries a functional signal peptide for secretion.

However, no fluorescence was detectable in plant nuclei at any infection stages. This suggests that either ChEC4 is not translocated into host cells, or that the relatively large mCherry tag could interfere with effector translocation. To allow tag-independent localization of native ChEC4, a polyclonal antibody was raised against a synthetic peptide derived from an amino acid sequence which appears three times in the tandem repeat modules. (Fig. 12 A). To evaluate its performance, the antibody was used in Western blot analysis of concentrated culture filtrates and mycelial extracts as described above. As expected, using anti-ChEC4 antibody, the full-length fusion protein could be detected in culture supernatants but not mycelial extracts. However, only one additional smaller band was found, which corresponded to the middle band appearing on the membrane probed with anti-mCherry antibody. Thus, the smallest of the three bands that hybridized with the anti-mCherry antibody contained the mCherry epitope but was lacking the epitope of the ChEC4-specific antibody. Initial attempts to localize native ChEC4 with the ChEC4-specific antibody *in planta* by

immunofluorescence labelling of epidermal peels failed, probably due to sub-optimal fixation or the peptide epitopes being unavailable on the native protein. Whether un-tagged ChEC4 accumulates to detectable levels at all during infection needs to be determined by Western blot analysis of infected epidermal peels.

Taken together, ChEC4 contains a functional signal peptide for secretion and a functional nuclear localization signal, suggesting a high potential for this effector to be translocated into the host nucleus. However, internalization of the protein into the host cell still needs to be elucidated.

3.6 Effector candidates antagonizing plant cell death

Assigning virulence-related functions to individual *C. higginsianum* effector candidates (ChECs) remains a challenging task, especially given that certain ChEC genes are not amenable to genetic inactivation or do not display detectable phenotypes, possibly as a result of functional redundancy (see 3.4.3). However, direct expression of fungal proteins in plant cells allows, for example, the ability of ChECs to interfere with host cell death to be evaluated in isolation from other fungal effectors. As a starting point, we selected two necrosis-eliciting proteins for this assay which are likely to have two different modes of action, namely INF1 from *P. infestans* (Kanneganti *et al*., 2006) and NLP1 from *C. higginsianum*.

3.6.1 Identification of cell death-inducing proteins of *C. higginsianum*

Necrosis- and ethylene inducing peptide 1-like proteins (NLPs) were considered as suitable elicitors to be used in such a cell death suppression assay. NLPs provoke plant responses similar to MAMPS by interfering with plasma membrane integrity, finally resulting in strong cell death, thereby promoting the virulence of hemibiotrophic and necrotrophic fungal, bacterial and oomycete pathogens (Ottmann *et al*, 2009). However, to date NLPs have not been reported from any *Colletotrichum* species. To identify *C. higginisianum* homologues of NLPs (ChNLPs), the well-characterized NLP from *Phytophthora sojae* (Kanneganti *et al*., 2006) was used to query a draft genome assembly of *C. higginsianum* by BLAST. This resulted in the identification of six homologous sequences in *C. higginsianum*, with ChNLP1 being the most similar (e value: $5e^{-44}$) and ChNLP6 being the least similar homologue (e value: $3e^{-9}$). Iterative searches using the identified ChNLP paralogues or NLPs from other organisms did not

reveal any further homologues, suggesting that the *C. higginsianum* genome harbours six NLP-like genes.

The genes for ChNLP5 and ChNLP6 were found to be located at the outer margins of genomic contigs of the draft genome assembly, resulting in N-terminally incomplete coding sequences. However, for ChNLP5 it was possible to identify the genomic contig encoding the N-terminus via its best BLAST match obtained from querying public databases. This could be confirmed experimentally with primers located in the N-terminal and C-terminal half of the protein, resulting in a bridging amplicon. The missing sequence appeared to be an intron containing 18 consecutive cytosines, probably resulting in mis-assembly or 454-sequencing failure. In contrast, this strategy proved unsuccessful for ChNLP6, making signal peptide predictions and full-length sequence alignments impossible.

Certain amino acids of the highly conserved central heptapeptide motif 'GHRHDWE', a hallmark of nearly all known NLPs, were recently found to be required for full biological activity of a bacterial and oomycete NLP (Ottmann *et al*., 2009). Figure 13 A shows an alignment of the amino acids surrounding this motif, which was detectable in all six ChNLPs. However, none of the ChNLPs contained this consensus motif in its entirety. ChNLP3 and ChNLP5 lacked three, and ChNLP6 lacked one of the amino acid residues demonstrated to be crucial for NLP activity. In contrast, ChNLP1, ChNLP2 and ChNLP4 contained all of these important amino acids, suggesting that these homologues have the potential to exert necrosis-inducing activity.

To estimate whether ChNLPs may play a role during pathogenesis, their expression *in planta* and in several fungal cell types was determined by RT-PCR (Fig. 13 C). ChNLP1 and ChNLP2 were found to be exclusively expressed during the switch from biotrophy to necrotrophy, when pin-point water-soaked lesions first became apparent on inoculated leaves (Fig. 13 B). Neither ChNLP4 nor ChNLP6 were expressed during pathogenesis or at any developmental stage *in vitro*, at least under the laboratory conditions used. Remarkably, ChNLP3 and ChNLP5 were strongly upregulated in appressoria penetrating host cells, with transcripts still detectable during biotrophy. ChNLP3, but not ChNLP5, was also strongly upregulated in appressoria formed *in vitro*. Taken together, ChNLP1 and ChNLP2 were considered most likely to have necrosis-inducing activity during plant infection.

To test whether ChNLP1 could be used as a cell death inducer, the cDNA was cloned into a binary vector providing overexpression under the control of the

cauliflower mosaic virus 35S promoter. Agroinfiltration of *N. benthamiana* leaves resulted in strong confluent necrotic lesions in infiltrated parts of the leaf lamina six days after infiltration. Visible necrosis could be obtained with bacterial densities (OD_{600}) as low as 0.01 (Fig. 13 D), suggesting that ChNLP1 is a potent cell death inducer.

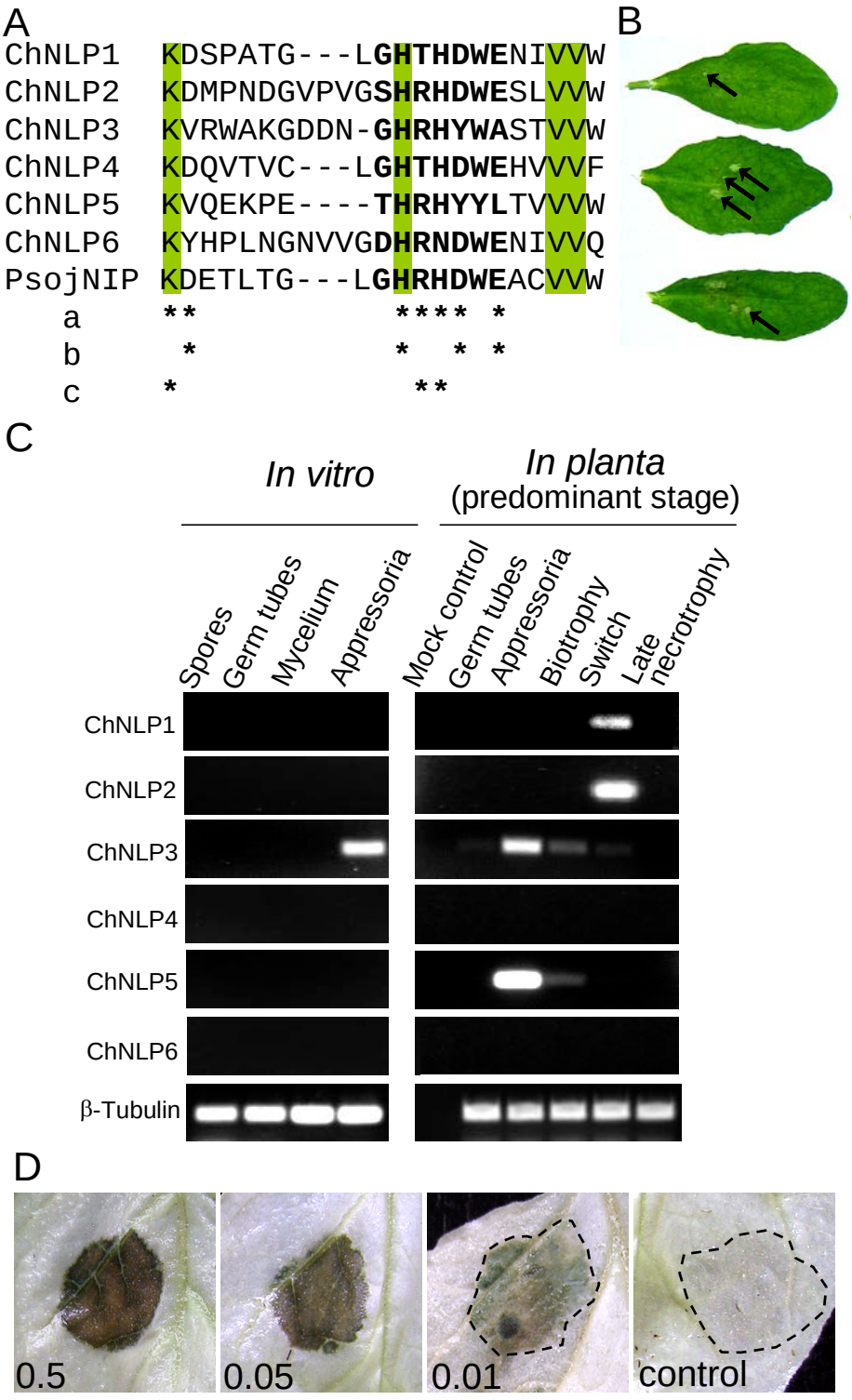

Fig. 13. Necrosis and ethylene-inducing peptide1-like proteins of *Colletotrichum higginisianum* (ChNLPs).

A, Alignment of amino acids encompassing the conserved consensus motif "GHRHDWE" (Gijzen and Nürnberger, 2006) of the six ChNLPs found in the fungal genome and a reference NLP from *Phytophthora sojae* (Qutob *et al*., 2002). Asterisks indicate amino acid residues crucial for NLP activity. a, amino acid residues investigated by Ottmann *et al*., 2009 by alanine replacements. Replacement of these amino acids abolished (b) or reduced (c) biological activity of an oomycete and bacterial NLP. Conserved amino acid residues are shaded in green.

B, Detection of ChNLP1 and ChNLP2 transcripts requires material from a distinct stage of pathogenesis: to obtain RNA from the switch between biotrophy and necrotrophy, densly inoculated leaves were harvested at 55 h after inoculation, when pin-point water-soaked lesions (arrows) first appeared.

C, Detection of transcripts of ChNLPs in four different cell types and at five stages of plant infection using RT-PCR. Total RNA was extracted from ungerminated and germinated conidia, saprophytic mycelium and appressoria formed *in vitro* as well as from epidermal peels or whole infected leaves of *Arabidopsis thaliana* representing pre- and post-penetration phases of infection, including the switch between biotrophy and necrotrophy. The β-tubulin amplicon was used to adjust cycle numbers and loading of individual PCR reactions to allow for variation of fungal biomass.

D, ChNLP1 causes severe necrosis in *Nicotiana benthaminana* leaf tissue. An *A. tumefaciens* strain carrying a construct for transient over-expression of ChNLP1 was infiltrated with the indicated optical densities (at 600 nm) into fully-expanded leaves of *N. benthamiana*. Pictures were taken 6 days after infiltration and clearing of the leaf tissue by ethanol. An *A. tumefaciens* strain carrying a construct for ChEC3 expression was included as a control. Dotted lines indicate infiltrated areas.

3.6.2 ChEC3, ChEC3a and ChEC5 suppress ChNLP-, but not INF1-induced necrosis

The *CgDN3* gene of *Colletotrichum gloeosporioides*, encoding a predicted secreted protein, is considered to be the only *Colletotrichum* secreted effector protein reported to date. A *CgDN3* disruption mutant provoked a strong hypersensitive response in the host plant *Stylosanthes* (Stephenson *et al*., 2000). ChEC3 and its paralogue ChEC3a were found to be weakly similar to CgDN3 (see 3.3.2). To test whether ChEC3 and ChEC3a are able to suppress ChNLP1-induced cell death, both were co-expressed transiently with ChNLP1 in *N. benthamiana*. Similarly, ChEC5, a cerato-platanin

domain-containing protein identified in the secretome of mature *in vitro* appressoria (3.1.2), was also included in this assay.

In brief, an *A. tumefaciens* strain containing a construct for ChEC over-expression was mixed with one carrying a ChNLP1 over-expression construct and infiltrated into one half of fully-expanded leaves of *N. benthamiana*. As a control mixture, the ChEC-carrying *A. tumefaciens* strain was replaced by one harbouring a construct for expression of the yellow fluorescent protein (YFP). The control mixture was infiltrated into the other half of the leaf (Fig. 14 A). This allowed side-by-side comparisons within the same leaf, to take account of leaf-to-leaf variation in transgene expression levels, and thus necrosis intensity, within and between individual plants, which was found to be a significant source of variability in preliminary experiments. Six to eight days after infiltration, sites co-expressing YFP and ChNLP1 showed a very strong cell death response leading to confluent necrosis.

However, co-expression of ChEC3, ChEC3a and ChEC5, respectively, impaired the ChNLP1-induced cell death and prevented the manifestation of a confluent tissue necrosis in most of the infiltrated sites. To quantify cell death suppression, the proportion of infiltration site pairs in which ChEC-expressing sites showed reduced necrosis (exemplified in Fig. 14 B) or no reduction in necrosis (exemplified in Fig.14 C) was determined six to eight days after infiltration. Co-expression of full-length proteins of ChEC5, ChEC3 and ChEC3a significantly reduced necrosis in 70 to 80 % of the inspected infiltration site pairs (Fig. 14 D). Co-expression of both ChEC3 and ChEC3a together with ChNLP resulted in a small additive effect, but this further increase in sites showing necrosis suppression was not statistically significant. In contrast, co-expression of a putative secreted chitinase of *C. higginsianum*, a gene which was found to be strongly upregulated during biotrophy (Takahara *et al*., unpublished results), resulted in significantly fewer sites showing reduced necrosis in pair-wise comparisons (26 ± 16 %, $P<0.02$, Student's t-test). This suggests that co-expression of *C. higginsianum* proteins *per se* does not interfere with ChNLP1-induced necrosis in *N. benthamiana*. The background variability in necrosis induction inherent in this assay was evaluated by infiltrating an *Agrobacterium* strain mixture carrying constructs for YFP and ChNLP1 expression into both left and right halves of the leaf lamina. After applying the same scoring strategy as above, only ten percent (± 3.3 %) of the infiltration site pairs showed differences in necrosis severity. The data obtained from the negative control (chitinase/ChNLP1 expression) and background control

(double-sided YFP/ChNLP1 expression) were not significantly different (P = 0.2), confirming that the chitinase protein lacks any detectable cell death-suppressing activity in this assay. ChEC5, ChEC3, ChEC3a and a combination of the latter two failed to suppress necrosis induced by the INF1 elicitin from *Phytophthora infestans* (Fig. 14 D). In contrast, co-expression of $Avr3a^{KI}$, a well-characterized suppressor of INF1-induced cell death (Bos *et al*., 2006; Bos *et al*., 2010), resulted in necrosis reduction in 88 (± 5) % of the infiltration site pairs.

Next, the effect of the fungal signal peptide for secretion on suppression of ChNLP1-induced necrosis was investigated by omitting the coding sequence for the N-terminal signal peptide (except for the start codon) from the expression constructs. Interestingly, the data obtained with these constructs (Fig. 14 E) were not significantly different from those derived from full-length constructs. Taken together, these results suggest that ChEC3, ChEC3a and ChEC5 interfere with ChNLP-induced necrosis, but not INF1-induced necrosis, independent of the presence of the fungal signal peptide.

3.6.3 Co-expression of ChECs has no impact on ChNLP1 expression level

To exclude the possibility that the observed necrosis reduction is due to failure of ChNLP1 protein expression, ChNLP1 was cloned into an expression vector providing C-terminal translational fusions with a hemagglutinin (HA) tag (ChNLP1-HA). Similar to untagged ChNLP1, ChNLP1-HA was able to induce severe necrosis when over-expressed in *N. benthamiana* (not shown). ChNLP1-HA expression levels in plant extracts pooled from sites expressing either ChEC3/ChNLP1-HA or ChEC5/ChNLP1-HA were compared to corresponding YFP/ChNLP1-HA site pairs by Western blot analysis. ChEC3 and ChEC5 were expressed either with or without their signal peptides for secretion. Using an anti-HA antibody, the full-length protein (30 kDa expected molecular mass) could be detected, as well as three additional bands between 25 and 30 kDa which indicates partial protein cleavage (Fig. 14 F). Plant extracts expressing untagged ChNLP produced no detectable signal in Western blots. However, more importantly, there was no major difference in ChNLP1-HA protein band intensity between ChEC- and YFP-expressing infiltration site pairs, suggesting that co-expression of ChECs, with or without signal peptide, has no impact on ChNLP protein level *per se.* Thus, the observed necrosis reduction must be a genuine effect of ChEC activity.

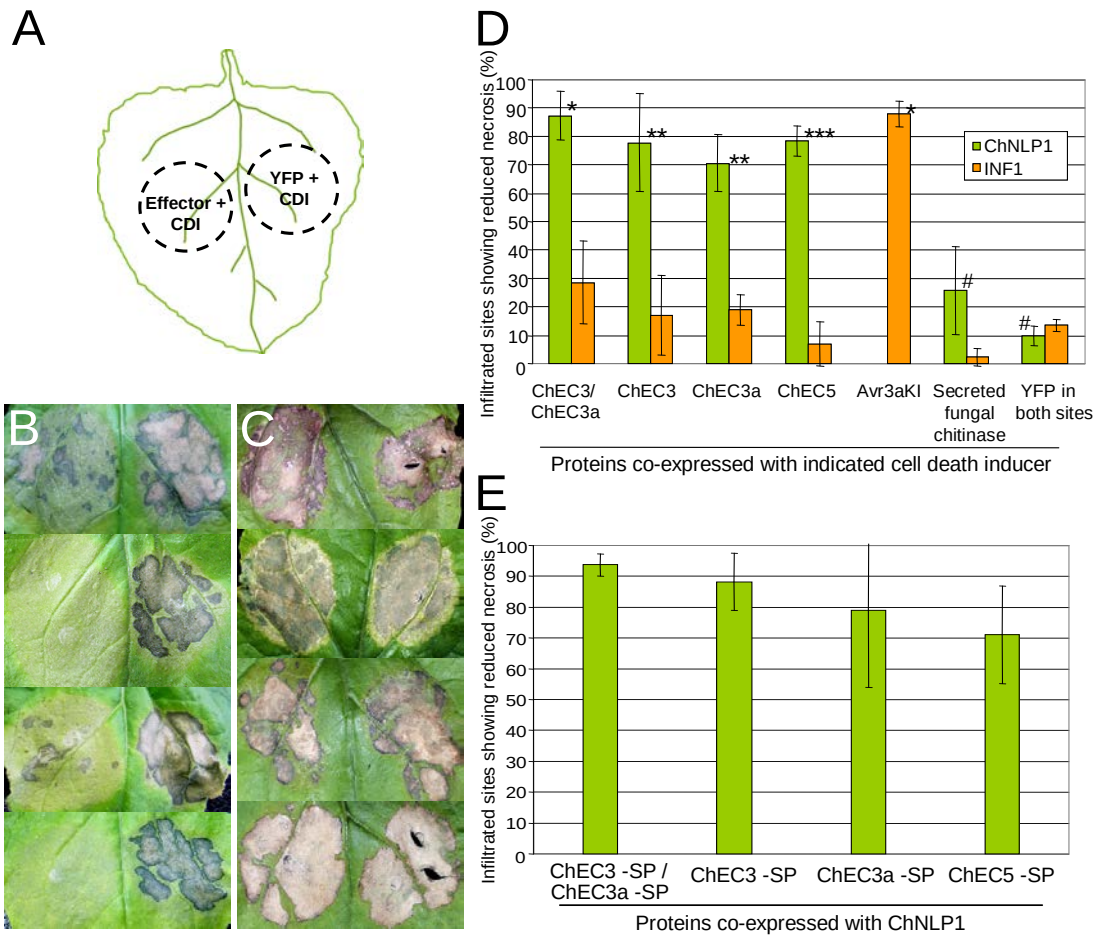
A
Effector + CDI
YFP + CDI
B
C
D
Infiltrated sites showing reduced necrosis (%)
ChNLP1
INF1
ChEC3/ ChEC3a
ChEC3
ChEC3a
ChEC5
Avr3aKI
Secreted fungal chitinase
YFP in both sites
Proteins co-expressed with indicated cell death inducer
E
Infiltrated sites showing reduced necrosis (%)
ChEC3 -SP / ChEC3a -SP
ChEC3 -SP
ChEC3a -SP
ChEC5 -SP
Proteins co-expressed with ChNLP1

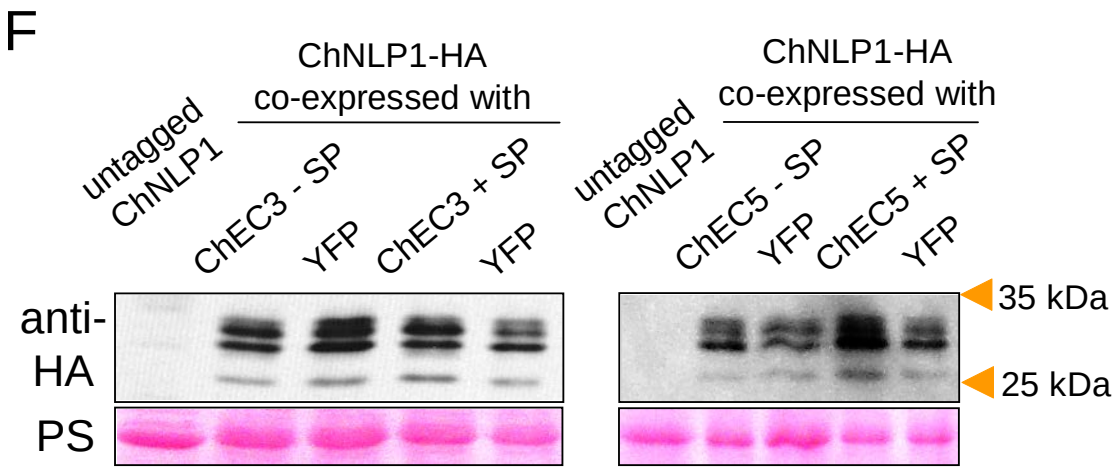
F
ChNLP1-HA co-expressed with
untagged ChNLP1
ChEC3 - SP
YFP
ChEC3 + SP
YFP
ChNLP1-HA co-expressed with
untagged ChNLP1
ChEC5 - SP
YFP
ChEC5 + SP
YFP
anti-HA
PS
35 kDa
25 kDa

Figure 14. *Agrobacterium tumefaciens*-based transient expression assay to explore cell death-suppressing capability of *Colletotrichum higginsianum* effector candidates (ChECs).

(A), Infiltration scheme. Agrobacteria containing constructs for ChECs or YFP expression were mixed with those carrying cell death-inducing proteins (CDIs). These mixtures were infiltrated into two sites on the same leaf to allow pair-wise comparisons and to overcome leaf-to-leaf variation in necrosis manifestation. (B, C), Typical examples of infiltration site pairs six days after infiltration in which the site co-expressing ChECs (left) was scored as showing reduced necrosis (B) or no reduction in necrosis (C).

(D, E), Cell death-suppressing activity of ChEC3, ChEC3a and ChEC5 expressed either with (D) and without (E) their predicted signal peptides for secretion. The proportion of sites showing reduced necrosis upon co-expression with CDIs was determined and statistical significance was tested by employing Student's *t*-test. In each experiment, at least 20 leaves were inspected per co-expression combination. Data were obtained from at least 3 independent experiments.

(D), a fungal secreted chitinase found to be strongly upregulated during biotrophy (Takahara *et al*., unpublished) was included as a negative control. *, ** and *** indicate significant difference from the negative control at P <0.0005, <0.02 and <0.005, respectively. The infiltration mixture containing CDI and YFP was also infiltrated into both sides of the leaf to reveal the intrinsic background variability of necrosis manifestation within the same leaf. Note that there was no statistically significant difference (P=0.2) between the negative control and the background control (#). Data obtained from sites co-expressing ChECs and *Phytophthora infestans* INF1 were not significantly different from the background control (P>0.3). The *P. infestans* effector $Avr3a^{KI}$ was used as a positive control for the suppression of INF1-induced cell death but was not tested in conjunction with ChNLP1.

(E), Ability of ChECs to suppress ChNLP1-induced cell death was not significantly affected by the lack of their signal peptides (P>0.2, pair-wise comparisons with the respective data shown in C).

(F), Co-expression of ChECs has no impact on ChNLP1 protein expression level *per se*. Western blot analysis of plant extracts pooled from sites co-expressing HA-tagged ChNLP1 together with ChEC3, ChEC5 or YFP using an anti-HA antibody. Plant material was harvested before onset of visible necrotic symptoms after three days *post* infiltration. PS, Ponceau red stain. The expected size of mature HA-tagged ChNLP1 is 30 kDa.

4 Discussion

In this study, the repertoire of *Colletotrichum higginsianum* secreted effector proteins expressed during plant pathogenesis was defined. Furthermore, the contribution of selected *C. higginsianum* effector candidates (ChECs) to fungal virulence was explored either directly by targeted gene replacement or indirectly using a transient expression assay for suppression of particular forms of plant cell death.

ChEC discovery was accomplished by computational mining of EST collections from different stages of plant infection, including mature and developing appressoria formed *in vitro*, appressoria penetrating host cells and biotrophic hyphae isolated from infected host tissue by fluorescence-activated cell sorting. Comparison to ESTs from *in vitro* infection structures allowed the discrimination of plant-induced ChECs, whereas ESTs from the necrotrophic stage permitted a set of 69 *ChEC* genes that are preferentially expressed in biotrophy-relevant stages to be defined. The trancriptome of plant-penetrating appressoria generally appeared to be enriched for genes encoding *higginsianum*-specific proteins as well as plant-induced secreted proteins, including ChECs. One further ChEC was identified in a complementary proteomic analysis of secreted proteins from conidial germlings developing *in vitro*, whose immediate secretory activities upon contact with the inductive artificial surface could be traced using a sensitive protein stain.

The expression of most of the *ChECs* chosen for further study was highly stage-specific, with *ChEC3*, *ChEC3a*, *ChEC4* and *ChEC6* being plant-induced. Targeted gene replacement showed that neither ChEC1 nor ChEC2 contribute measurably to fungal virulence in a reproducible manner. ChEC4 was found to contain a functional nuclear localization signal and a functional signal peptide to enter the fungal secretory pathway, raising the possibility that this effector candidate is translocated into the host nucleus for transcriptional re-programming. ChEC3, ChEC3a and ChEC5 suppressed plant cell death evoked by a *C. higginsianum* homologue of a Necrosis and Ethylene-inducing Peptide1-like protein, but not necrosis induced by *Phytophthora infestans* INF1, indicating possible functional redundancy between *C. higginsianum* effectors.

4.1 The extracellular proteome of *in vitro*-formed germlings and appressoria of *Colletotrichum higginsianum*

Knowledge about the composition of the extracellular matrices surrounding conidia, germ tubes and appressoria of *Colletotrichum* spp. and their developmental regulation during infection structure morphogenesis has been largely obtained from cell biological studies with monoclonal antibodies and other cytochemical probes (Green *et al*., 1995; O'Connell *et al*, 1996; Perfect *et al*., 1999). The extracellular matrices of *Colletotrichum* infection structures are heterogenous in composition, mostly consisting of proteins with a high apparent molecular weight and high degree of glycosylation (O'Connell *et al*., 1996; Sugui *et al*., 1998; Hutchison *et al*., 2002) and some were shown to be involved in conidial adhesion to hydrophobic substrata (Hughes *et al*., 1999). However, the cloning and identification of the epitope-containing proteins was technically challenging and laborious. Apart from bioinformatic predictions based on EST data (this study, Kleemann *et al*., 2008; Takahara *et al*., 2009), neither soluble secreted proteins nor extracellular matrix proteins produced by *C. higginsianum* pre-invasive infection structures have been identified to date. To complement the purely EST-based approach for identification of secreted proteins and ChECs, a direct proteomic analysis of proteins secreted from conidia developing appressoria *in vitro* was conducted.

Conidia, emerging germ tubes and developing appressoria secreted distinct haloes of proteinaceous material onto the substratum, which could be revealed with a sensitive protein stain based on silver-enhancement of colloidal gold particles. The haloes were resistant to trypsin and V8 protease digestion. This suggests that these proteins lack the corresponding cleavage sites targeted by these enzymes or that cross-linking of proteins to the melanin layer and/or extensive glycosylation protected them against protease attack. However, high concentrations of the less selective pronase E could dissolve these haloes, suggesting that the constituent proteins are enriched for consecutive hydrophobic amino acids (the preferred cleavage sites of pronase E). It is plausible that such secreted proteins are enriched with hydrophobic amino acid residues, wich could mediate interaction with the hydrophobic substratum. Ungerminated *Colletotrichum* spores are known to adhere within 30 min to hydrophobic substrata (Hughes *et al*., 1999). Kuo and Hoch (1995) reported that the extracellular matrix surrounding germlings and appressoria of *Phyllosticta ampelicida* were digestable with trypsin and pronase E, but not with other enzymes.

Since pronase E-digested proteins were considered to be unsuitable for liquid chromatography-coupled mass spectrometry analyses, a gel-based proteomic analysis of the solubly secreted proteins released during conidial germination and appressoria formation was performed instead. This cumulative secretome appeared to be enriched for proteins with a high apparent molecular weight and a low isoelectric point, which appears to be a hallmark of many fungal secretomes (Suarez *et al*., 2005; Espino *et al*., 2010) although this may be influenced by the extraction method used (Vincent *et al*., 2009).

Interestingly, two paralogous chitin deacetylases were identified in the secretome of germlings and developing appressoria. Conversion of chitin into chitosan by means of secreted chitin deacetylases (Siegrist and Kauss, 1990; Deising and Siegrist, 1995, El Gueddari *et al*., 2002) as well as the secretion of chitin-sequestering effectors (de Jonge *et al*., 2010) are involved in minimizing PAMP release in order to evade recognition by the plant (Miya *et al*., 2007; Wan *et al*., 2008, Shimizu *et al*., 2010). However, depending on the degeree of de-acetylation, chitosan can also act as a PAMP (Iriti and Faoro, 2009; Petutschnig *et al*., 2010).

There was remarkably little overlap between the proteins identified by proteomic analysis and the proteins predicted to be secreted based on EST data (Kleemann *et al*., 2008). This is probably a reflection of the small datasets, due to the relatively low success rate of protein identification on one hand and the low sequencing depth of the cDNA library on the other hand, and may improve when the larger EST collection derived from 454-sequencing of *in vitro* infection stages is used for comparison. Also the nature of the biological samples may account for the small overlap: the solubly secreted proteins accumulated from early germination until harvest at the mature appressorium stage. In contrast, the RNA extracted for cDNA library construction was highly stage-specific for mature, fully-melanized appressoria (Kleemann *et al*., 2008). Furthermore, the structure of appressoria may partly account for this discrepancy: heavily melanized cell walls of appressoria are considered to be impermeable to solutes, which is thought to be a prerequisite for the generation of turgor pressure (Deising *et al*., 2000). Thus, mature appressoria are unlikely to secrete proteins through their melanized cell walls. However, the penetration pore in the basal cell wall, through which the penetration peg emerges to pierce the host cuticle and cell wall, remains unmelanized (Kleemann *et al*., 2008). Thus, it is conceivable that secreted proteins which are required for invasive growth are focally secreted through

the penetration pore. This is supported by the finding that proteins were detected underneath penetration pores after removal of appresoria (Fig. 1). However, those proteins are unlikely to be present in the liquid film surrounding mature appressoria but could be identified in an EST-based approach, demonstrating the value of utilizing these two complementary approaches.

Remarkably, 18 % of the identified proteins lacked a predicted signal peptide. These included mainly enzymes involved in basic house-keeping cellular processes, e. g. transaldolase, malate dehydrogenase, esterase and cyclophilin. Additionally, a 190 kDa protein homologous to fungal copper radical oxidases also failed signal peptide prediction. Two further proteins also gave weak signal peptide predictions, with cleavage site probability score of the SignalP-NN algorithm falling just below its threshold of significance. This is similar to the situation with ChEC4, which also provided a weak signal peptide cleavage site prediction, despite the fact that this protein was experimentally demonstrated to be solubly secreted by the fungus. Proteins with no or weak signal peptide predictions would have evaded bioinformatic mining of the *C. higginsianum* EST data, which employed stringent SignalP settings. This suggests that the *C. higginsianum* secretome was underestimated. EST mining with stringent SignalP settings identified 330 solubly secreted proteins, of which 201 are ChECs. However, relaxed SignalP settings, allowing the above-mentioned qualifier to fall below the threshold of significance, resulted in the identification of 376 secreted proteins of which 232 were ChECs. However, these totals are probably still underestimates, given the fragmentary nature of the EST contigs commonly obtained from 454 sequence data (Cheung *et al*., 2008; Wheat, 2010), leading to a large amount of N-terminally incomplete ORFs. The proportion of non-classically secreted proteins cannot be estimated computationally but may be extrapolated from the proteomics study.

There is increasing evidence that mammalian proteins as well as those from *Saccharomyces*, *Candida* and *Aspergillus*, can be secreted *via* pathways that function independently of signal peptides (Lee *et al*., 2003; Denikus *et al*., 2005; Nickel, 2005; Nombela *et al*., 2006). It remains unclear how these proteins reach the cell wall or extracellular space. Unlike their bacterial and mammalian counterparts, there is no bioinformatic tool available for the prediction of fungal non-conventionally secreted proteins, possibly due to their diversity (Bendtsen *et al*., 2004; Nombela *et al*., 2006). It is debatable whether non-classical secretion occurs in filamentous phytopathogenic

fungi. The release of exosomes has been suggested for human pathogenic fungi including *Cryptococcus neoformans*, *Histoplasma capsulatum* and *Candida* spp. to be an alternative route for the delivery of virulence and pathogenicity factors (Rodrigues *et al*., 2008; Casadevall *et al*., 2009). Signal peptide-less secreted proteins of plant pathogenic fungi, especially proteins with assumed house-keeping functions, are ubiquitous in proteomic studies (Paper *et al*., 2007; Shah *et al*., 2009) as well as yeast-based functional screens of cDNA libraries ('signal sequence traps'), which are based on the complementation of a reporter gene lacking a signal peptide (Krijger *et al*., 2008; Lee *et al*., 2006). Whether these proteins represent multifunctional proteins ('moonlighting proteins') and whether their extracellular localisation is an experimental artifact or the result of non-classical secretion, is a source of an ongoing debate (Nombela *et al*., 2006; Agrawal *et al*., 2010). However, it was shown recently that two AVR proteins lacking signal peptides from the powdery mildew fungus *B. graminis* f sp *hordei* are recognized and induce cell death when transiently expressed in barley plants carrying matching R proteins with assumed cytoplasmic localization (Ridout *et al*., 2006). This suggests the existence of an alternative route for secretion in this fungus, as well as an uptake mechanism for these proteins at the plant cell periphery.

Unfortunately, novel *Colletotrichum*-specific proteins were not identified in the present proteomics study. This may reflect the low success rate with which small (<25 kDa) proteins could be recovered from two-dimensional gels in sufficient amounts for MS analysis. In addition, secreted proteins encoded by plant-induced genes were absent from this *in vitro* sample, whereas such genes were a prominent component of the transcripome of plant-penetrating appressoria. However, one of the most abundant proteins secreted by germinating conidia and developing appressoria contained a cerato-platanin domain, present in some plant response-eliciting effectors from phytopathogenic fungi (see below). This protein, named ChEC5, was chosen for further characterization.

4.2 Remarkable features of the host invasion transcriptome

The present study provided the first global analysis of the *in planta* transcriptome for any *Colletotrichum* species. Stages of *C. higginsianum* pathogenesis that were sampled for cDNA generation and pyrosequencing included early invasive growth, biotrophy and late necrotrophy. Enrichment for RNA from plant-penetrating appressoria

involved peeling off infected *Arabidopsis* leaf epidermis, a technique that has not been employed previously for any *Arabidopsis* pathogen to my knowledge. In a similar approach, Mosquera and co-workers (2009) used infected rice leaf sheath to enrich for the biotrophic intracellular hyphae of *Magnaporthe*. This allowed extraction of a high proportion of fungal RNA and allowed the microarray-based identification of genes that were specifically up-regulated in intracellular hyphae, providing a first insight into the plant-interaction transcriptome of *Magnaporthe*.

In silico barcoding of the obtained *C. higginsianum in planta* ESTs allowed the examination of EST composition of individual contigs. Analysis of the global assembly of all *in planta* ESTs from *C. higginsianum* revealed that ESTs from plant-penetrating appressoria provided the lowest proportion of stage-specific contigs (12.4 %) and transcriptional units (6.9 %). This may reflect the narrow time window in which the RNA samples were collected (within 2 hours between 18-20 h after infection), providing a 'snapshot' of the penetration process. The other infection phases (necrotrophy and biotrophy) may represent a broader range of developmental stages resulting from the poor synchronization of fungal growth *in planta*. However, it should be noted that this low number of stage-specific contigs probably also reflects the low sequencing depth of this library; the fact that this library was the only one derived from non-normalized cDNAs further complicates comparative analyses.

Whatever the reason for their relatively low number, contigs composed only of ESTs from plant-penetrating appressoria had remarkable features when compared to those of the other stages. For example, they had the highest proportion of secreted proteins, ChECs and *higginsianum*-specific genes. This suggests that the early penetration stage of fungal pathogenesis requires the highest proportion of diversified sequences and *higginsianum*-specific gene 'inventions'. It is conceivable that this is the result of *C. higginsianum* having evolved 'localized biotrophy', i. e. confinement of the biotrophic phase to the first invaded epidermal cell. This localized biotrophy is the hallmark of an aggregate of very closely related *Colletotrichum* species (Latunde-Dada and Lucas, 2007) for which publicly available sequences are sparse.

From all the fungal stages employed for EST generation, *in vitro* appressoria and plant-penetrating appressoria are the most similar stages, with regard to morphology and developmental state. However, this superficial similarity is not reflected in their transcriptomes: within transcriptional units specific for early *in planta* pathogenesis (sector A and B in Fig. 4), the proportion of transcriptional units

containing ESTs from *in vitro* appressoria (sector B in Fig. 4) was remarkably low. Similarly, 80 % of the EST contigs specific for plant-penetrating appressoria encoding secreted proteins and ChECs lacked any *in vitro* ESTs. Thus, these genes appear to require plant-derived cues (plant-induced genes *sensu stricto*) or are linked to penetration peg and infection vesicle formation (plant-induced genes *sensu lato*). It may be possible to distinguish these possibilities for particular genes by using promoter fusions with fluorescent proteins and comparing appressoria penetrating a plant surface or artificial substrata, e. g. cellophane.

These findings prompt the question whether *in vitro* infection structures are a suitable surrogate for studying gene expression in *in planta* infection structures. However, almost 70 % of transcriptional units containing ESTs from developing and mature appressoria formed *in vitro* are shared with *in planta* infection stages. Overall, ESTs from *in planta* appressoria undergoing invasive growth proved to be a rich resource for discovery of biotrophy-relevant genes and ChECs. The remarkable properties of the host invasion transcriptome support the hypothesis, that, given the very short and transient nature of the biotrophic phase, plant-penetrating appressoria are the most crucial stage for the biotrophic interaction between *C. higginsianum* and its host. This is consistent with the finding that penetration peg formation of *C. lindemuthianum* appressoria is sufficient and necessary to trigger an R-gene mediated hypersensitive response on resistant bean cultivars (Veneault-Fourrey *et al*., 2005), suggesting the secretion of an avirulence effector during host invasion. Similarly, appressoria of *C. higginsianum* but not those of non-adapted *Colletotrichum* species appear able to suppress the deposition of papillary callose (Shimada *et al*., 2006).

4.3 *ChEC3, ChEC7* and *ChEC10* are associated with transposable elements

There appeared to be a conspicuous association of transposable elements with ChECs. Thus, the genomic sequence flanking *ChEC3* contained a footprint of the un-translated region (UTR) of a transposable element with similarity to *OPHIO2*, a DNA transposon of the dutch elm disease pathogens *Ophiostoma ulmi* and *O. novo-ulmi* (Bouvet *et al*., 2007). Furthermore, for ChEC7 and ChEC10 (Tab. 7), which were both identified as being highly expressed in plant-penetrating appressoria, the immediate proximity to retrotransposon remnants resulted in hybrid transcripts in which the transposon remnant even formed part of the ChEC transcript UTR. ChEC10 contained a small

stretch of *Ccret2*, a retrotransposon of *Colletotrichum cereale* (Crouch *et al*., 2008), whereas ChEC7 was accompanied by the non-LTR LINE-like retrotransposon *CgT1*, originally identified in *Colletotrichum gloeosporioides* (He *et al*., 1996).

Transposable elements of plant pathogenic fungi are thought to play roles in effector gene expansion/diversification, in abolishing the expression of avirulence genes, or in inactivation of avirulence genes by creating truncated proteins. Transposon-mediated truncation of avirulence proteins has been described for *Avr2* from *Cladosporium fulvum* (Luderer *et al*., 2002) and *ACE1* from *Magnaporthe grisea* (Fudal *et al*., 2005), whereas insertion of a Pot3 transposon into the promotor *Avr-Pita* of *M. grisea* was thought to abrogate *Avr-Pita* expression (Kang *et al*., 2001).

There are two remarkable examples known in which *CgT1*-like retrotransposons are thought to act as evolutionary driving forces for adaptation of plant pathogens. In the first instance, it was recently discovered that nearly 60 % of the AVR_{K1} effector paralogues that have extensively colonized the genome of *Blumeria graminis* f. sp. *hordei* are consistently associated, and have co-evolved, with CgT1-like retrotransposons, with some even occurring as hybrid transcripts providing translational fusions (Ridout *et al*., 2006; Sacristan *et al*., 2009). This work provided the first evidence for co-evolution of effector genes and a retrotransposon, suggesting a mutual benefit for this association, in which retrotransposon-driven effector proliferation contributes to fitness of the pathogen facing a range of host resistance genes, while simultaneously satisfying the ‘selfish’ demands of the retrotransposon to multiply in its host genome.

In the second example, a truncated CgT1-like retrotransposon was found to be inserted into the upstream region of *CYP51* of sterol demethylation inhibitor-resistant isolates of *Blumeriella jaapii*, the causal agent of cherry leaf spot (Ma *et al*., 2006). This gene is a target of sterol demethylation inhibitors, commonly employed in fungicides. The retrotransposon insertion correlated with a considerable increase in *CYP51* expression levels, thereby compensating for the enzyme inhibition. In general, LINE retrotransposons carry promoter and enhancer motifs and are also known to modulate mammalian gene expression, although mainly cases of attenuated or ectopic expression of genes are described (Han and Boeke , 2005).

Although the retrotransposon remnant is not located in the promoter region of ChEC7 but rather in its 3’ UTR, it is still conceivable that the retrotransposon remnant maybe responsible for the high expression level of ChEC7. The similarity of the

retrotransposon remnant to *CgT1* ended abruptly, without extending into the genomic region downstream of the aligning EST contig (Fig. 5). This suggests that the inserted transposon underwent ectopic recombination with another transposon copy located elsewhere in the fungal genome. Transposon-mediated genome rearrangements have been frequently observed in fungi (Daboussi and Capy, 2003), including chromosomal rearrangements leading to truncated avirulence genes of *Magnaporthe grisea* and *F. oxysporum* f. sp. *lycopersici* (Khang *et al*., 2008, Rep *et al*., 2005b). It could be envisaged that such a rearrangement resulted in a new 3' UTR providing high mRNA stability, or could have carried *ChEC7* into a chromatin region with high transcriptional activity. In this context, it is noteworthy that *ChEC6*, the gene providing the most abundant ESTs from plant-penetrating appressoria, contains an intron in its 3' UTR. Introns in UTRs are known to be involved in post-transcriptional gene regulation (Roy *et al*., 2007 and references herein), revealing a further possible link between high ChEC expression levels and 'unusual' UTR structure.

Analysis of the transcriptome did not reveal any further examples of ChEC transcripts containing transposon footprints. However, this does not rule out a close association of ChECs with transposable elements in the fungal genome. It would be interesting to examine in a genome-wide analysis whether *ChEC* loci are in genomic regions that are enriched for transposable elements or their relics.

4.4 ChEC1 and ChEC2 – examples of effector candidates that do not contribute measurably to fungal virulence

The targeted gene knock-out of an effector gene provides unambiguous genetic evidence for whether it contributes to fungal virulence (or avirulence, in case of matching R genes). There are several examples known where deleting, disrupting or silencing effector genes of filamentous plant pathogens lead to a measurable decrease in pathogen virulence or even complete loss of pathogenicity (Tab. 9).

Table 9. Secreted effector proteins of filamentous pathogens making an experimentally confirmed contribution to virulence.

Effector name	Species	Host	Phenotype/Function	Reference
CgDN3	*Colletotrichum gloeosporioides*	*Stylosanthes guianensis*	Mutants elicit host response	Stephenson *et al*., 2000
Avr2	*Cladosporium fulvum*	Tomato	Protease Inhibitor	van Esse *et al*., 2008
Avr4	*Cladosporium fulvum*	Tomato	Protection against chitinases	van Esse *et al*., 2007
Ecp6	*Cladosporium fulvum*	Tomato	Chitin sequestration	Bolton *et al*., 2008
Pep1	*Ustilago maydis*	Maize	Mutants elicit host response	Doehlemann *et al*., 2009
Avr3a	*Phytophthora infestans*	Potato	Reduced virulence	Bos *et al*., 2010
Avr3 (Six1)	*Fusarium oxysporum* f. sp. *lycopersici*	Tomato	Required for full virulence	Rep *et al*., 2005a
Avr2 (Six3)	*Fusarium oxysporum* f. sp. *lycopersici*	Tomato	Required for full virulence	Houterman *et al*., 2009

Inspired by these examples, it was aimed to test the contribution of ChECs to virulence genetically by taking advantage of the fact that *C. higginsianum* can be stably transformed (O'Connell *et al*., 2004; Huser *et al*., 2009). The present study showed that mutants lacking ChEC1 and ChEC2 did not contribute to virulence in a measurable and reproducible manner. This is reminiscent of the highly-expressed biotrophy-associated secreted (BAS) proteins of *M. grisea*, of which some are translocated into the cytoplasm of infected cells and adjacent uninfected cells (Khang *et al*., 2010). Targeted gene knockouts of four *BAS* genes failed to give a pathogenicity phenotype, although for *BAS1* mutants "*three out of six independent whole-plant assays showed quantitative decreases in lesion numbers and lesion sizes in mutants relative to the wild-type*" (Mosquera *et al*., 2009).

Although care was taken in the present study to standardize infection assays with regard to plant cultivation conditions, inoculum density and infection time point, it cannot be ruled out that the conditions used may have caused (maybe even uncontrollable) environmental or physiological states that resulted in the observed inconsistent behaviour of fungal mutants, maybe as a result of a conditional phenotype. It is also conceivable that mutants lacking *ChEC1* and *ChEC2* may show decreased fitness in the field, where the pathogen has to cope with multiple abiotic and biotic stresses, e. g. competing microbes.

One reason frequently proposed for the lack of detectable phenotypes in effector mutants is their functional redundancy (Stergiopolous and Wit, 2009). Functional redundancy of effectors is considered to be a strategy for pathogens to evade recognition by the host because it allows avirulence effectors to be jettisoned (Godfrey *et al*., 2010). In the present study, it was shown that ChEC3, ChEC3a and ChEC5 all suppressed a specific type of plant cell death, demonstrating that *C. higginsianum* possesses functionally redundant effectors for cell death suppression. *ChEC1* and *ChEC2* do not have obvious paralogues in the fungal genome. Similarly, for the expressed ChECs identified from the *in planta* transcriptome, the presence of paralogues in the genome was more the exception than the rule: three genes was the maximum number of paralogous sequences detected. However, pathogen effectors can be diversified beyond recognizable sequence similarity although there is evidence for a common ancestral gene, as proposed recently for expanded families of oomycete and powdery mildew effector genes (Jiang *et al*., 2008; Godfrey *et al*., 2010). However, it was recently discovered that the RXLR effector AVR3a from *P. infestans* is required

for full virulence on a susceptible host (Bos *et al*., 2010), suggesting that this effector is not functionally redundant, despite the fact that the RXLR effector superfamily has extensively proliferated within the genome of *P. infestans* (Jiang *et al*., 2008; Haas *et al*. 2009). This suggests that functional redundancy of effectors is not necessarily correlated with members of gene families, which probably rapidly evolve to co-opt different functions. In the case of essential effector genes, gene loss and the resulting presence/absence polymorphisms in pathogen populations, which is frequently observed for candidate effector loci in *M. grisea* (Yoshida *et al*., 2009), are not an option to evade recognition by the host. Instead, as a consequence, sequence polymorphisms that allow effectors to escape detection by R genes, will be ultimately selected for by positive selection.

4.5 Chromatin status may affect efficiency of homologous recombination in *C. higginsianum*

The gene encoding ChEC3 was found to be remarkably recalcitrant to targeted gene replacement by homologous recombination, even when a Δ*KU70* strain of *C. higginsianum* was employed as T-DNA recipient. This is reminiscent of the avirulence gene *ACE1* of *M. grisea,* which was shown to undergo homologous recombination very infrequently (Böhnert *et al*., 2004). ACE1 is a hybrid between a polyketide synthase and a nonribosomal peptide synthetase and is involved in the synthesis of a secondary metabolite which is recognized by resistant rice cultivars carrying the resistance gene Pi33 (Böhnert *et al*., 2004). *ACE1* was found to be part of a cluster of genes that are all putatively involved in secondary metabolite synthesis. Interestingly, all genes of that cluster displayed a reduced ability to undergo homologous recombination as indicated by the low frequency of targeted gene replacements, with two genes being completely recalcitrant to gene disruption (Collemare *et al*., 2008). It was suggested that locus-specific chromatin modifications may enable stage-specific co-expression of genes that are part of that cluster and that these modifications could account for the reduced frequency of targeted gene replacement. In this context it is noteworthy that mutants of *M. oryzae* lacking *Tig1*, which is part of a conserved histone deacetylase transcriptional co-repressor complex, were defective in their ability to overcome plant defense responses and maintain biotrophic growth after penetration (Ding *et al*., 2010), indicating that chromatin modification and structure is a crucial regulatory mechanism controlling invasive growth. Another effector example in which

the frequency of homologous recombination turned out to be extremely low was for targeted knockout of Avr1 from *Fusarium oxysporum* f. sp. *lycopersici* (Houterman *et al*., 2008).

The expression patterns of *ChEC3* and *ACE1* are remarkably similar: both are exclusively expressed during appressorial penetration of plant cells (this study, Böhnert *et al*., 2004, Collemare *et al*., 2008) but lack any transcriptional activity in appressoria formed on un-penetratable substrata (this study, Fudal *et al*., 2007). In line with this, analysis of the 454-sequenced *C. higginsianum* transcriptome revealed that neither the EST contig encoding the ChEC3 ORF nor its corresponding transcriptional unit contained ESTs from developing and mature appressoria formed *in vitro*. Remarkably, ESTs of several genes located on the same genomic contig as *ChEC3* appeared to be highly enriched for ESTs from plant-penetrating appressoria but lacked almost completely ESTs from *in vitro* infection structures (not shown). This also included the gene immediately upstream of ChEC3, encoding a predicted secreted superoxide dismutase (Tab. 7). Taken together, these findings suggest that this genomic region is enriched for genes that are co-expressed during plant penetration. This supports the hypothesis that chromatin at this locus may be in a silent state during any other developmental stage, including conidial germination *in vitro*. *Agrobacterium tumefaciens*-mediated transformation of *C. higginsianum* was conducted *in vitro* by co-cultivation of the bacteria with fungal spores, which germinated on rich nutrient medium to produce undifferentiated hyphae. It is conceivable that accessibility of the chromatin for homologous recombination with the incoming T-DNA is limited at this stage, resulting in the observed failure of *ChEC3* targeting. This raises the possibility that fungal transformation *in planta* may be a better strategy to target *C. higginsianum* genes that are specifically expressed during plant colonization.

4.6 ChEC4 – a putative re-programmer of host gene expression

Analysis of EST redundancy suggested that *ChEC4* was the third most highly expressed gene in plant-penetrating appressoria (Tab. 7). The predicted protein sequence of ChEC4 had a repetitive structure and contained a weakly predicted signal peptide for secretion and a predicted nuclear localization signal. Despite its modular structure, ChEC4 lacks the repeats and C-terminal cysteine motif typical for covalently bound cell wall proteins with internal repeats (PIR proteins) (Klis *et al*., 2010). Nuclear accumulation was demonstrated experimentally by transient expression of a

GFP-tagged fusion protein in *N. benthamiana* and *A. thaliana*. Using a similar approach, Kelley and co-workers (2010) demonstrated that SNE1 from *P. infestans* contains a nuclear localization signal. Likewise, Nuk6 and Nuk7 of *P. infestans* were shown recently to accumulate in plant nuclei upon transient expression in a plant importin-dependent manner (Kanneganti *et al*., 2007). RTP1, a protein secreted by haustoria of *Uromyces fabae* was detected within the extrahaustorial matrix and inside infected plant cells, including host nuclei, by immunofluorescence and electron microscopy, providing direct evidence that this protein translocates into host cells during colonization of broad bean plants by the rust fungus (Kemen *et al*. 2005). A remarkable example of transcriptional re-programming of host genes is provided by AvrBs3, an effector of *Xanthomonas campestris* pv. *vesicatoria* which is injected into the host cell *via* the bacterial type III secretion system and mimics a plant transcription factor (Kay *et al*., 2007; Römer *et al*., 2007).

ChEC4 was shown in this study to be solubly secreted. Western blot analysis revealed that secreted mCherry-tagged ChEC4 constitutively expressed by *C. higginsianum* transformants in liquid culture is subject to partial cleavage. The only report in which fungal effector tagging with mCherry was surveyed by Western blotting is from Doehlemann and co-workers (2009). Tagging *Ustilago maydis* Pep1 and other effectors with mCherry resulted in partial cleavage, which was not observed when a HA-tag was used (Doehlemann *et al*., 2009; Regine Kahmann, personal communication). Whether the observed partial cleavage of ChEC4-mCherry is an artefact of the foreign protein tag or the constitutive expression by saprophytic mycelium, or whether it occurs normally during plant infection, remains to be elucidated.

Despite the constitutive expression of ChEC4-mCherry in fungal transformants, fluorescent labelling was only detectable on the cell walls of fully-mature biotrophic hyphae, confirming that ChEC4 is secreted to the plant-fungal interface during infection. This specific labelling of biotrophic cell walls was retained even after the fungus had entered the necrotrophic phase of pathogenesis. This also raises the possibility that ChEC4 might be a cell wall protein and only biotrophic hypha cell walls may incorporate it. Alternatively, it may be that the constitutive *trpC* promoter from *Aspergillus nidulans* used in this experiment provides low levels of transgene expression. As a result, the protein may become detectable in late-stage biotrophic hypha cell walls only because the relatively large mCherry tag interferes with effector

translocation into the host cell. In support of this notion, the *A. nidulans trpC* promoter was found to be a weak promotor in *M. oryzae* (Marc-Henri Lebrun, personal communication). Expression from its native promoter may be required for proper ChEC4 localization. Interestingly, it was recently discovered that the native promoter and/or the signal peptide of *M. oryzae* effectors impact on the localization of effector fusion proteins (Khang *et al*., 2010).

4.7 *C. higginsianum* effector candidates antagonize a specific type of plant cell death

ChEC3, ChEC3a and ChEC5 were found to suppress cell death induced by a *C. higginsianum* homolog of a Necrosis- and Ethylene-inducing Peptide1-Like protein (NLP) in *N. benthamiana*, but not the cell death induced by *P. infestans* INF1. It was previously demonstrated by virus-induced gene silencing in *N. benthamiana* that components of jasmonic acid-mediated signalling (COI1), mitogen-activated protein kinase relays (MEK2) and salicylic acid-mediated signalling (NPR1 and TGA2.2) are required for NLP-, but not INF1-induced cell death in, suggesting that distinct signalling pathways mediate each type of cell death (Kanneganti *et al*., 2006). It is conceivable that *C. higginsianum* effectors interfere with plant components that are required for the NLP-induced cell death pathway but which are also shared by other cell death pathways. This also implies that these plant components are sufficiently conserved between *Brassica* (the original host of *C. higginsianum*) and *N. benthamiana* to be targeted by the same effector.

The plant responses evoked by NLPs share certain characteristics with microbe-associated molecular patterns (PAMP)-triggered immunity. NLPs mediate the activation of MAPKs, induction of ion fluxes, the production of phytoalexins and reactive oxygen species, callose deposition and the induction of defense-related genes (Qutob *et al*., 2006; Bae *et al*., 2006). These responses resemble to a great extent those triggered by the well-studied PAMP flg22, the minimal elicitor-active amino acid motif of bacterial flagellin. Also the broad taxonomic distribution of NLPs, including true fungi, oomycetes and bacteria, and the relatively high sequence conservation of NLPs is consistent with the classical concept of PAMPs (Gijzen and Nürnberger, 2006). However, NLPs also clearly differ from true PAMPs in some respects: first, NLPs are not expressed constitutively (this study, Qutob *et al*., 2002). Second, their elicitor activity cannot be restricted to a peptide motif (like flg22) (Fellbrich *et al*.,

2002, Schouten *et al*., 2008). Third, they are not essential for microbial life, as demonstrated by the viability of a *Mycosphaerella graminicola* mutant lacking the only NLP of its genome (Motteram *et al*., 2009) and fourth, genuine PAMPs trigger the programmed cell death associated with the hypersensitive response only in exceptional cases (Bittel and Robatzek, 2007), whereas NLPs cause necrotic lesions in all dicotyledonous (but not monocotyledonous) plants tested (Gijzen and Nürnberger, 2006; Pemberton and Salmond, 2004). It was shown recently that the same structural properties of a *Phytophthora parasitica* NLP are required for both plant plasma membrane disruption and cross-kingdom complementation of a NLP-deficient *Pectobacterium carotovorum* mutant (Ottmann *et al*., 2009). Moreover, the same structural properties were responsible for the onset of plant defence responses, suggesting that plant cells recognize the NLP action but not the molecule itself. NLP-mediated membrane disruption may result in the release of endogenous damage-associated molecular patterns (DAMPs). In this view, ChEC3, ChEC3a and ChEC5 may not interfere with the action of NLPs *per se* but rather with a signal amplification loop provided by DAMPs. In support of this notion, single dead cells were observed upon co-expression of ChECs and ChNLP1, whereas expression of ChNLP1 with a control protein resulted in a confluent tissue necrosis, as revealed by Trypan blue staining (data not shown).

Until very recently, no pathogen effector has been described which suppressed NLP-induced cell death. Kelley and co-workers (2010) provided the first evidence that such effectors exist. In this study, it was shown that *P. infestans* SNE1 broadly suppresses cell death induced by NLPs as well as by co-expressed avirulence-resistance protein pairs in *N. benthamiana*. Remarkably, SNE1 showed this effect after being directly expressed in the plant cytosol, without its signal peptide for secretion. SNE1 carries the motif RXLX at its N-terminus. This motif resembles a variant of the oomycete host translocation motif RXLR (Whisson *et al*., 2007) and this variant was determined experimentally to mediate effector uptake (Dou *et al*., 2008). Similarly, ChEC3, ChEC3a and ChEC5 also exert their cell death-suppressing activity without their signal peptides. Despite the lack of any RXLR-like or other shared amino acid motif in these proteins, this finding suggests that they act intracellularly after being translocated into the host cell. The cell death-suppressing effect of full-length ChEC proteins expressed with their signal peptides could be interpreted as resulting from their re-entry after being secreted by the plant cell. However, it cannot be excluded that

the fungal signal peptide is not functional in *N. benthamiana* or that overexpression bypasses the plant secretory pathway resulting in protein leakage into the cytosol.

Based on the extremely stage-specific, reciprocal expression pattern of ChNLP1 and ChEC3, ChEC3a and, to a lesser extend ChEC5, it is tempting to speculate that with the onset of necrotrophic growth the fungus triggers and exploits the same type of programmed cell death that it is aiming to suppress during biotrophic pathogenesis. This scenario would imply that effector-targeted components of the signalling cascade required for NLP-induced cell death potentially become compatibility factors for the late necrotrophic stage of anthracnose development. A similar scenario was envisaged recently by Bos and co-workers (2010) for the interaction of *P. infestans* AVR3^{KI} with the ubiquitin E3-ligase CMPG of *N. benthamiana*, which is required for the cell death mediated by INF1. AVR3^{KI} was shown to stabilize CMPG, which was correlated with its altered activity. Remarkably, virus-induced silencing of CMPG in *N. benthamiana* resulted in reduced sporulation and lesion severity when challenged with *P. infestans*, thereby providing direct evidence that CMPG-mediated cell death contributes to the necrotrophic stage of this pathogen and is a prerequisite for its successful multiplication.

The strong upregulation of two genes resembling NLPs during host penetration and biotrophy (Fig. 13 C) is intriguing. This clearly shows that expression of NLP-homologues during host penetration and biotrophic pathogenesis is not detrimental to the biotrophic lifestyle *per se*. Consistent with this, these early-expressed NLP homologues lacked three out of four highly conserved amino acid residues that were shown to be essential for full NLP activity (Ottmann *et al*., 2009), suggesting that these proteins may have adopted new pathogenicity functions. This is supported by the fact that obligate biotrophic pathogens like *Hyaloperonospora arabidopsidis* contain several NLP-like genes (cited as personal communication in Ottmann *et al*., 2009).

4.8 ChEC3 and its homologues: *Colletotrichum*-specific suppressors of host defence responses

ChEC3 and its paralogue ChEC3a both have weak similarity to *Colletotrichum gloeosporioides DN3* (Stephenson *et al*., 2000). Using a CgDN3 promotor-GFP fusion, this gene was found to be exclusively expressed in infection vesicles during the biotrophic phase of *C. gloeosporioides* infection. The mutant generated by targeted gene disruption proved non-pathogenic on intact leaves of the host *Stylosanthes*, but

retained the ability to grow necrotrophically on wounded leaves. The *CgDN3*-mutant appressoria elicited a hypersensitive-like response in attacked host cells and it was suggested that this gene plays a role in establishing a biotrophic interaction by suppressing host defence resoponses. A comparison of ChEC3, ChEC3a and CgDN3 revealed a large number of polymorphic amino acids and only few conserved residues. Database searches using the conserved consensus sequence (amino acid residues labelled red in Fig. 7) with pattern-hit-initiated (PHI)- BLAST did not reaveal any similar proteins sharing this sequence pattern. The (unsignificant) BLAST match proposed by Stephenson and co-workers to the extracellular domain of an *Arabidopsis* cell wall receptor kinase *wak3* was not reproducible with the *C. higginsianum* homologues, confirming its unsignificance.

C. higginsianum and *C. gloeosporioides* are located in phylogenetically distinct clades within the genus *Colletotrichum* (Latunde-Dada and Lucas, 2007), with *C. gloeosporioides* itself being a very heterogeneous species complex (Sutton, 1992). Despite their low level of overall sequence similarity, ChEC3, ChEC3a and CgDN3 have some remarkable features in common: First, all homologues are expressed very specifically at early stages of the biotrophic interaction, suggesting their importance for biotrophy. Second, despite many polymorphisms in the primary amino acid sequence, the physico-chemical properties of most residues appear to be conserved, as indicated by their predicted secondary structure. Third, the exon-intron structure (but not the actual intron sequences) is conserved, probably as a result of pressure to conserve the 'split' histidine residue (Fig. 7), suggesting a single origin of these genes (Betts *et al*., 2001). This situation is reminiscent of recently identified effectors of *Blumeria graminis* f. sp. *hordei* which are poorly related but share a common motif and exon-intron structure (Godfrey *et al*., 2010).

Remarkably, a survey of *ChEC3* and *ChEC3a* genes of 17 different *C. higginsianum* isolates only revealed one SNP in the *ChEC3a* allele of one isolate, resulting in an amino acid exchange. This isolate (*C. higginsianum* AR3-1) was the only one that was analyzed from a group of isolates from *Raphanus sativus* (small radish). Work is underway to determine whether this amino acid exchange holds true for other available *Raphanus* isolates and whether it is correlated with a differential host range. A high degree of sequence conservation within effector genes carrying few SNPs exclusively resulting in amino acid changes has also been observed in *Fusarium*

oxysporum f. sp. *lycopersici* isolates, leading to either increased virulence (Rep *et al*., 2005a) or loss of avirulence (but not virulence) function (Houterman *et al*., 2009). The low level of sequence polymorphism was shown to be a result from a recent spread of these effectors within polyphyletic clonal lines of *Fusarium oxysporum* f. sp. *lycopersici* through horizontal transfer of a mobile pathogenicity chromosome, on which all these effector genes reside (van der Does *et al*., 2008; Ma *et al*., 2010).

4.9 Cell death-suppression is a novel function for cerato-platanin domain-containing proteins

ChEC5 contains a cerato-platanin domain and homologous sequences of ChEC5 are found in several other fungal pathogen genomes. The founding member of this protein family, cerato-platanin from *Ceratocystis fimbriata* f. sp. *platani*, the causal agent of canker stain of plane trees, induces cell death when infiltrated into *N. tabacum* leaves, but not when infiltrated into plane leaves (Pazzagli *et al*., 1999) and induces phytoalexin synthesis in host and non-host plants (Scala *et al*., 2004). This protein was also found to be located in cell walls of several fungal structures (Boddi *et al*., 2004). However, ChEC5 was discovered in this study by a proteomics approach as a soluble secreted protein released by appressoria developing *in vitro*. Similarly, MSP1 of *Magnaporthe grisea* was not associated with the fungal cell wall and was solubly secreted into the culture medium when expressed from a constitutive promoter (Jeong *et al*., 2007). In contrast to cerato-platanin from *Ceratocystis*, Sm1 of the biocontrol fungus *Trichoderma virens* lacks any toxic or necrosis-inducing activity against a range of microbes and plants, but instead triggers production of reactive oxygen species in monocot and dicot seedlings and induces the expression of defense-related genes both locally and systemically in cotton (Djonovic *et al*, 2006). No phytotoxicity was observed for the purified cerato-platanins SnodProt1 from *Stagonospora nodorum* (Hall *et al*., 1999) and MSP1 from *Magnaporthe grisesa* (Jeong *et al*., 2007). The latter was required for pathogenicity in *M. grisea*, but Sp1 from *Leptosphaeria maculans* was not (Wilson *et al*., 2002). Remarkably, the expression of *Bcspl1* encoding a cerato-platanin of *Botrytis cinerea* was found to be regulated by host-derived ethylene (Chague *et al*., 2005).

Taken together, cerato-platanin domain-containing proteins appear to have varied and sometimes contrasting activities, depending on the fungal pathogen and host species. It appears that these proteins represent a diversified protein family

specific to, and broadly distributed within the Ascomycete lineage. With the exception of the saprophyte *Neurospora crassa* (Galagan *et al*., 2003) and the opportunistic human pathogens *Aspergillus fumigatus* and *Coccioides immitis* (Pan and Cole, 1995), most cerato-platanins are present in genomes of plant pathogens, ranging from obligate necrotrophs like *Botrytis cinerea* (Chague *et al*., 2005; Shah *et al*., 2009) to obligate biotrophs like *Blumeria graminis* f. sp. *hordei* (Bindschedler *et al*., 2009). This prevalence in genomes of plant pathogenic fungi suggests an important function of these secreted proteins during plant colonization, although their mechanism during pathogenesis remains to be determined.

The present study provides first evidence that a cerato-platanin domain-containing secreted protein of *C. higginsianum* may act as a suppressor of a specific type of cell death, induced by an NLP, adding another level of complexity to the cerato-platanin family. This suggests that certain members may have co-opted functions to suppress or elicit host cell death, depending on the pathogen's lifestyle. The maintenance of cerato-platanins in genomes of obligate biotrophic fungi (Bindschedler *et al*., 2009) or ectomycorhizal fungi (Peter *et al*., 2003) is intriguing, and suggests that these proteins do not have a phytotoxic or cell death-inducing activity *per se*. Similarly, the failure of appressorial penetration and abortion of early pathogenesis of *M. grisea* mutants lacking *MSP1*, the closest homologue of *ChEC5*, shows that this cerato-platanin could be involved in the establishment of a biotrophic interaction with the host. This is further corroborated by the finding that expression of fluorescent protein-tagged MSP1 in *M. grisea* results in fluorescence accumulation in biotrophic interfacial complexes, a pathogen-induced compartment to which effector proteins are focally secreted (Mosquera *et al*., 2009; Khang *et al*., 2010), and appeared subsequently transferred into the cytoplasm of living host cells and from there into uninfected adjacent cells (Mark Farman, personal communication)

.

5 Concluding remarks and future perspectives

The present study has provided the first global analysis of the *in planta* transcriptome for any *Colletotrichum* species and allowed an inventory of *C. higginsianum* effector candidates to be defined *via* the computational analysis of ESTs. Although the overall number of ESTs obtained from appressoria during host invasion was relatively small compared to other stages, this infection stage turned out to be a rich resource for ChEC discovery. These ChECs provide the basis for ongoing and future research on effector function in this model pathosystem. The experimentally determined expression pattern of the ChECs was remarkably consistent with the observed EST contig composition, suggesting that a purely *in silico* analysis of ESTs can provide sufficient information for prioritizing ChECs, without the need for expression profiling with microarrays or qPCR. The extreme stage-specificity of *ChEC* transcription, as well as phenomena such as the presence of transposable elements or introns in *ChEC* UTRs and highly transcribed intergenic regions, suggest that gene regulation during host invasion is complex. Thus, further exploration of the host invasion transcriptome could provide important insights into gene regulation mechanisms in *Colletotrichum*.

The demonstrated interference of some ChECs with NLP-induced plant cell death points to a possible role of these effectors in suppressing PAMP-triggered immunity, since NLP-induced plant responses overlap significantly with those evoked by canonical PAMPs like flg22 (Qutob *et al*., 2006; Bae *et al*., 2006). To confirm and extend these findings, transgenic *A. thaliana* are being generated for stable, ectopic expression of ChECs in a true host for *C. higginsianum*. These plants will be used to determine whether *in planta* expression of ChECs interferes with classical PAMP responses, e.g. callose deposition or ROS production, and whether it primes the plant to allow ingress of non-adapted pathogens. Expression in transgenic *Arabidopsis* plants will also reveal whether ChECs with predicted NLS are involved in transcriptional reprogramming of plant cells, e.g. *via* array profiling.

It is currently unknown whether any races of *C. higginsianum* exist that can overcome the resistance observed in some *A. thaliana* accessions (Narusaka *et al*., 2004; Narusaka *et al*., 2009; Birker *et al*., 2009). Screening a world-wide collection of 40 *C. higginsianum* strains recently assembled at the MPIPZ will help to address this question. Once identified, re-sequencing the genome of such a race may reveal intraspecies sequence polymorphisms that could account for the differential phenotype

on resistant plants, and ultimately lead to the identification of *C. higginsianum* avirulence genes.

6 Supplementary data

Supplementary Table 1. Unique sequences from Sanger-sequenced appressorial ESTs with similarity to verified pathogenicity and virulence genes (Kleemann *et al*., 2008)

Unique sequence ID	Function/Gene name	Organism	*E* value
Contig 35	Polyketide synthase *PKS1*	*Colletotrichum lagenarium*	1E-144
Contig 132	Phosphoenolpyruvate carboxykinase *PCK1*	*Cryptococcus neoformans*	1E-137
Contig 140	Copper transporting ATPase *CLAP1*	*Colletotrichum lindemuthianum*	1E-132
Contig 37	Polyketide synthase *PKS1*	*Colletotrichum lagenarium*	1E-126
1-M17-T7	Polyketide synthase *PKS1*	*Colletotrichum lagenarium*	1E-116
2-B11-SP6	Ste12-like transcription factor *CST1*	*Colletotrichum lagenarium*	1E-112
Contig 127	Topoisomerase *TOP1*	*Candida albicans*	1E-104
Contig 72	Class I chitin synthase *WdCHS2*	*Wangiella dermatitidis*	1E-104
Contig 247	PAK family kinase *CHM1*	*Magnaporthe grisea*	1E-103
3-K21-SP6*	Methionine synthase *MSY1*	*Fusarium graminearum*	4E-84
Contig 100	G-protein α subunit *MAGC*	*Magnaporthe grisea*	2E-81
Contig 220	Virulence factor *GAS1*	*Magnaporthe grisea*	1E-78
2-K02-T7	Methylcitrate synthase *MCSA*	*Aspergillus fumigatus*	2E-77
2-H18-SP6	Superoxide dismutase *SOD1*	*Botrytis cinerea*	9E-72
2-H08-T7	CREB-like transcription factor *CPTF1*	*Claviceps purpurea*	3E-67
2-C10-T7	Virulence *GAS1*	*Magnaporthe grisea*	1E-65
2-O08-T7	Transcription factor *ZIF1*	*Fusarium graminearum*	3E-62
Contig 128	Cyclophilin A *BCP1*	*Botrytis cinerea*	4E-62
Contig 80	Virulence factor *GAS2*	*Magnaporthe grisea*	2E-48
1-D04-SP6	Laccase *BcLCC2*	*Botrytis cinerea*	2E-41
Contig 134	Cell surface hydrophobicity protein *CSH1*	*Candida albicans*	8E-39
Contig 31	Virulence factor *CAP20*	*Colletotrichum gloeosporioides*	2E-34
Contig 15	GTP-binding protein *RAS2*	*Ustilago maydis*	4E-34
Contig 233	Laccase *BcLCC2*	*Botrytis cinerea*	6E-30
2-B02-SP6	Kinesin *KIN2*	*Ustilago maydis*	6E-28
3-C09-T7	ATPase *ssaN*	*Salmonella enterica*	4E-27
1-P06-SP6	Major facilitator superfamily transporter *BcMFS1*	*Botrytis cinerea*	3E-24
2-E21-SP6	Cell surface hydrophobicity protein *CSH1*	*Candida albicans*	9E-23
3-K21-T7*	Methionine synthase *MSY1*	*Fusarium graminearum*	1E-22
Contig 221	G-protein β subunit *CGB1*	*Cochliobolus heterostrophus*	2E-20
1-A08-T7	pH response regulator *RIM8* (*PRR1*, *palF*)	*Candida albicans*	3E-20
Contig 190	Secreted aspartyl protease *SAP3*	*Candida albicans*	9E-12
1-L01-T7	Calcineurin binding protein *CBP1*	*Cryptococcus neoformans*	1E-13
1-L21-SP6	MAPKKK *STE11a*	*Cryptococcus neoformans*	1E-13
3-G12-SP6	Transcription factor *NRG1*	*Cryptococcus neoformans*	9E-13
2-A10-SP6	pH response regulator *RIM8* (*PRR1*, *palF*)	*Candida albicans*	1E-12
1-B24-T7	Fructose transporter *FRT1*	*Botrytis cinerea*	2E-12
Contig 168	P-type ATPase *PMR1*	*Candida albicans*	7E-12
Contig 113	Secreted aspartyl protease *SAP3*	*Candida albicans*	9E-12
Contig 70	Peroxin *PEX6*	*Magnaporthe grisea*	2E-10
Contig 68	Plasma membrane protein *PTH11*	*Magnaporthe grisea*	6E-10
Contig 34	Virulence factor *ORP1*	*Magnaporthe grisea*	9E-10
Contig 193	Cytochrome P450 monooxygenase *BcBOT1*	*Botrytis cinerea*	3E-09

1-I09-T7	Methionine synthase *MSY1*	*Fusarium graminearum*	2E-08
Contig 171	Oxidoreductase *THR1*	*Colletotrichum lagenarium*	2E-06
Contig 241	PAK family kinase *CLA4*	*Ustilago maydis*	5E-06
Contig 199	*SCH9* protein kinase homologue	*Cryptococcus neoformans*	8E-06
3-M06-T7	Pectin methyl esterase *BcPME1*	*Botrytis cinerea*	1E-05
1-L06-SP6	Lysine/glutamate-rich plasma membrane protein *KER1*	*Candida albicans*	1E-05

* Two unique sequences from non-matching paired reads of one cDNA clone.

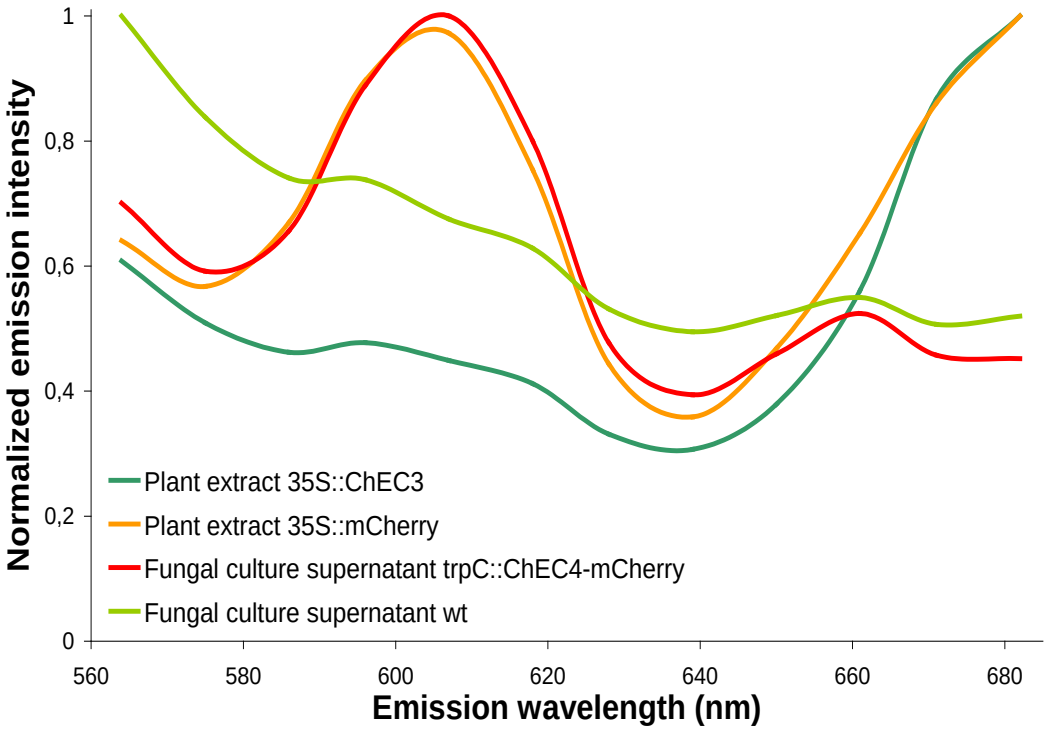

Supplementary Figure 1. ChEC4 targets functional mCherry to the fungal culture supernatant. The fluorescence spectra of supernatants of fungal transformant mycelium expressing ChEC4-mCherry and wild-type mycelium were recorded after excitation at 435 nm. Extracts from *N. benthamiana* leaves expressing mCherry or ChEC3 were used as positive and negative control, respectively. Note the mCherry-specific emission maximum at 610 nm.

7 List of abbreviations

Avr	avirulence
CC	coiled coil
ChEC	*Colletotrichum higginsianum* effector candidate
dai	days after inoculation
dpi	days post inoculation
E	ectopic mutant
FACS BH	biotrophic hyphae isolated by fluorescence-activated cell sorting
hpi	hours post inoculation
HR	hypersensitive response
IV APP	developing and mature appressoria formed *in vitro*
LRR	leucine-rich repeat
NBS	nucleotide binding site
NECRO	late necrotrophic stage
N-terminus	amino terminus
p35S	35S Cauliflower mosaic virus promoter
PAMP	pathogen associated molecular pattern
PEN APP	appressoria penetrating the plant epidermis
R	resistance
ROS	reactive oxygen species
SNP	single nucleotide polymorphism
Ss	single-stranded
T	targeted mutant
T-DNA	transfer DNA of *Agrobacterium tumefaciens*
TIR	Toll-interleukine-1 receptor
wt	wild-type

8 References

Abramovitch, R. B., Kim, Y.-J., Chen, S., Dickman, M. B. and Martin, G. M. (2003). Pseudomonas type III effector AvrPtoB induces plant disease susceptibility by inhibition of host programmed cell death. The EMBO Journal, **22**, 60-69

Agrawal, G. K., Jwa, N.-S. (2010). Plant secretome: unlocking secrets of the secreted proteins. Proteomics, **10**, 799-827.

Aguileta, G., Refrégier, G., Yockteng, R., Fournier, E., Giraud, T. (2009). Rapidly evolving genes in pathogens: methods for detecting positive selection and examples among fungi, bacteria, viruses and protists. Infection, Genetics and Evolution**, 9**, 656-670.

Akira, S., Uematsu, S. And Takeuchi, O. (2006). Pathogen recognition and innate immunity. Cell, **124**, 783-801.

Altschul, S. F., Gish, W., Miller, W., Myers, E. W. and Lipman, D. J. (1990). Basic local alignment search tool. Journal of Molecular Biology, **215**, 403-410.

Altschul, S. F., Madden, T. L., Schaffer, A. A., Zhang, J., Zhang, Z., Miller, W. and Lipman, D. J. (1997). Gapped BLAST and PSI-BLAST: a new generation of protein database search programs. Nucleic Acids Research, **25**, 3389-3402.

Asai, T., Tena, D., Plotnikova, J., Willmann, M. R., Chiu, W.-L., Gomez-Gomez, L., Boller, T., Ausubel, F. M., Sheen, J. (2002). MAP kinase signalling cascade in *Arabidopsis* innate immunity. Nature, **415**, 977-983.

Asakura, M., Ninomiya, S., Sugimoto, M., Oku, M., Yamashita, S., Okuno, T., Sakai, Y. and Takano, Y. (2009). Atg26-Mediated pexophagy is required for host invasion by the plant pathogenic fungus *Colletotrichum orbiculare*. Plant Cell, **21**, 1291-1304.

Asakura, M., Okuno, T. and Takan. Y. (2006). Multiple contributions of peroxisomal metabolic function to fungal pathogenicity in *Colletotrichum lagenarium*. Applied and Environmental Microbiology, **72**, 6345-6354.

Assaad, F.F., Qiu, J.L., Youngs, H., Ehrhardt, D., Zimmerli, L., Kalde, M., Wanner, G., Peck, S.C., Edwards, H., Ramonell, K., Somerville, C.R. and Thordal-Christensen, H. (2004). The PEN1 syntaxin defines a novel cellular compartment upon fungal attack and is required for the timely assembly of papillae. Molecular Biology of the Cell, **15,** 5118-5129.

Axtell, M. J. and Staskawicz, B. J. (2003). Initiation of RPS2-specified disease resistance in *Arabidopsis* is coupled to the AvrRpt2-directed elimination of RIN4. Cell, **112**, 369-377.

Bae H., Kim, M. S., Sicher, R. C., Bae, H. J., Bailey, B.A. (2006). Necrosis- and ethylene-inducing peptide from *Fusarium oxysporum* induces a complex cascade of transcripts associated with signal transduction and cell death in *Arabidopsis*. Plant Physiology, **3**, 1056-1067.

Bailey, J. A., Jeger, M., J, editors. (1992).*Colletotrichum*: biology, pathology and control. Wallingford: Commonwealth Mycological Institute; 1992. p. 388.

Bartetzko, V., Sonnewald, S., Vogel, F., Hartner, K., Stadler, R., Hammes, U. Z., Boernke, F. (2009). The *Xanthomonas campestri*s pv. *vesicatoria* type III effector protein XopJ inhibits protein secretion: evidence for interference with cell wall-associated defense responses. Molecular Plant-Microbe Interactions**, 22**, 655-664.

Bechinger, C., Giebel, K. F., Schnell, M., Leiderer, P., Deising, H. B. and Bastmeyer, M. (1999). Optical measurements of invasive forces exerted by appressoria of a plant pathogenic fungus. Science, **285,** 1896-1899.

Bendtsen, J. D., Jensen, L. J., Blom, N., von Heijne, G. and Brunak, S. (2004). Feature-based prediction of non-classical and leaderless protein secretion. Protein Engineering Design and Selection, **17**, 349-356.

Betts, M. J., Guigó, R., Agarwal, P. and Russell, R. B. (2001). Exon structure conservation despite low sequence similarity: a relic of dramatic events in evolution? EMBO Journal, 20, 5354 – 5360

Bhat, R.A., Miklis, M., Schmelzer, E., Schulze-Lefert, P. and Panstruga, R. (2005). Recruitment and interaction dynamics of plant penetration resistance components in a plasma membrane microdomain. Proceedings of the National Academy of Sciences ot the United States of America ,**102,** 3135-3140.

Bhattacharjee, S., Hiller, N.L., Liolios, K., Win, J., Kanneganti, T.D., Young, C., Kamoun, S., and Haldar, K. (2006). The malarial host-targeting signal is conserved in the Irish potato famine pathogen. PLoS Pathog 2, e50.

Bindschedler, L. V., Burgis, T. A., Mills, D. J. S., Ho, J. T. C., Cramer, R. and Spanu, P. D. (2009). In planta proteomics and proteogenomics of the biotrophic barley fungal pathogen *Blumeria graminis* f. sp. *hordei*. Molecular and Cellular Proteomics, **8**, 2368-2381.

Birker, D., Heidrich, K., Takahara, H., Narusaka, M., Deslandes, L., Narusaka, Y., Reymond, M., Parker, J. E. O'Connell, R. (2009). A locus conferring resistance to *Colletotrichum higginsianum* is shared by four geographically distinct *Arabidopsis* accessions. Plant Journal, **60**, 602-613.

Bittel, P., Robatzek, S. (2007). Microbe-associated molecular patterns (MAMPs) probe plant immunity. Current Opinion in Plant Biology, **10**, 335-341.

Boddi, S., Comparini, C., Calamassi, R., Pazzagli, L., Cappugi, G., Scala, A. (2004). *Cerato-platanin* protein is located in the cell walls of ascospores, conidia and hyphae of *Ceratocystis fimbriata* f. sp. *platani.* FEMS Microbiology Letters, **233**, 341-346.

Boehnert, H. U., Fudal, I., Dioh, W., Tharreau, D., Notteghem, J. L. and Lebrun, M. H. (2004). A putative polyketide synthase/peptide synthetase from *Magnaporthe grisea* signals pathogen attack to resistant rice. Plant Cell, **16**. 2499-2513.

Bolton, M. D., van Esse, H. P., Vossen, J. H., de Jonge, R., Stergiopoulos, I., Stulemeijer, I. J. E., van Den Berg, G. C. M., Borrás-Hidalgo, O., Dekker, H. L., de Koster, C. G., de Wit, P. J. G. M., Joosten, M. H. A. J., Thomma, B. P. H. J. (2008). The novel *Cladosporium fulvum lysin* motif effector Ecp6 is a virulence factor with orthologues in other fungal species. Molecular Microbiology, **69**, 119-136.

Bos, J. I. B., Armstrong, M. R., Gilroy, E. M., Boevink, P. C., Hein, I. Taylor, R. M., Zhendong, T., Engelhardt, S., Vetukuri, R. R., Harrower, B., Dixelius, CV., Bryan, G., Sadanandom, A., Whisson, S. C., Kamoun, S. and Birch, P. R. J. (2010). *Phytophthora infestans* effector AVR3a is essential for virulence and manipulates plant immunity by stabilizing host E3 ligase CMPG1. Proceedings of the National Academy of Sciences of the United States of America, **107**, 9909-9914.

Bos, J. I. B., Kanneganti, T.-B., Young, C., Cakir, C., Huitema, E., Win, J., Armstrong, M. R., Birch, P. R. J., Kamoun, S. (2006). The C-terminal half of *Phytophthora infestans* RXLR effector AVR3a is sufficient to trigger R3a-mediated hypersensitivity and suppress INF1-induced cell death in *Nicotiana benthamiana*. Plant Journal, **48**, 165–176.

Bouvet, G. F., Jacobi, V. and Bernier, L. (2007). Characterization of three DNA transposons in the Dutch elm disease fungi and evidence of repeat-induced point (RIP) mutations. Fungal Genetics and Biology, **44**, 430-443.

Bushnell, W. and Bergquist, S. (1975). Aggregation of host cytoplasm and formation of papillae and haustoria in powdery mildew of barley. Phytopathology ,**65,** 310-318.

Caracuel-Rios, Z. and Talbot, N. J. (2007). Cellular differentiation and host invasion by the rice blast fungus *Magnaporthe grisea*. Current Opinion in Microbiology, **10**, 339-345.

Casadevall, A., Nosanchuk, J. D., Williamson, P., Rodrigues, M. L. (2009). Vesicular transport across the fungal cell wall. Trends in Microbiology, **17**, 58-62.

Catanzariti, A.-M., Dodds, P. N., Lawrence, G. J., Ayliffe, M. A. and Ellis, J. G. (2006**).** Haustorially expressed secreted proteins from flax rust are highly enriched for avirulence elicitors. Plant Cell, **18,** 243-256.

Chagué, V., Danit, L.-V., Siewers, V., Schulze Gronover, C., Tudzynski, P., Tudzynski, B. and Sharon A. (2005). Ethylene sensing and gene activation in *Botrytis cinerea*: a missing link in ethylene regulation of fungus-plant interactions? Molecular Plant-Microbe Interactions **19**, 33-42.

Chaure, P., Gurr, S.J. and Spanu, P. (2000). Stable transformation of *Erysiphe graminis* an obligate biotrophic pathogen of barley. Nature Biotechnology, **18,** 205-207.

Chen, N., Hsiang, T. and Goodwin, P.H. (2003). Use of green fluorescent protein to quantify the growth of *Colletotrichum* during infection of tobacco. Journal of Microbiological Methods, **53,** 113-122.

Cheung, F., Win, J., Lang, J. M., Hamilton, J., Vuong,.H., Leach, J. E., Kamoun, S., Lévesque, C. A., Tisserat, N. and Buell, C. R. (2008). Analysis of the *pythium ultimum* transcriptome using Sanger and pyrosequencing approaches. BMC Genomics, **9**, doi:10.1186/1471-2164-9-542.

Chisholm, S. T., Coaker, G., Day, B. and Staskawicz, B. J. (2006). Host-microbe interactions: shaping the evolution of the plant immune response. Cell, **124**, 803-814.

Collemare, J., Pianfetti, M., Houlle, A.-E., Morin, D., Camborde, L., Gagey, M.-J., Barbisan, C., Fudal, I., Lebrun, M. H., Boehnert, H. U. (2008). *Magnaporthe grisea* avirulence gene ACE1 belongs to an infection-specific gene cluster involved in secondary metabolism. New Phytologist, **179**, 196-208.

Collins, N.C., Thordal-Christensen, H., Lipka, V., Bau, S., Kombrink, E., Qiu, J.L., Huckelhoven, R., Stein, M., Freialdenhoven, A., Somerville, S.C. and Schulze-Lefert, P. (2003). SNARE-protein-mediated disease resistance at the plant cell wall. Nature, **425,** 973-977.

Crouch, J. A., Glasheen, B. M., Giunta, M. A., Clarke, B. B. and Hillman, B.I. (2008). The evolution of transposon repeat-induced point mutation in the genome of *Colletotrichum cereale*: reconciling sex, recombination and homoplasy in an ”asexual” pathogen. Fungal Genetics and Biology, **45**, 190-206.

Daboussi, M. J., Capy, P. (2003). Transposable elements in filamentous fungi. Annual Review of Microbiology, **57**, 275-299.

Da Cunha, L., Sreerekha, M. V., Mackey, D., (2007). Defense suppression by virulence effectors of bacterial phytopathogens. Current Opinion in Plant Biology, **10**, 349-357.

Dangl, J. L. and Jones, J. D. G. (2001). Plant pathogens and integrated defence responses to infection. Nature, **411**, 826-833.

Deising, H. and Siegrist, J. (1995). Chitin deacetylase activity of the rust *Uromyces viciae-fabae* is controlled by fungal morphogenesis. FEMS Microbiology Letters, **127**, 207-211.

Deising, H. B., Werner, S. and Wernitz, M. (2000). The role of fungal appressoria in plant infection. Microbes Infect, **2**, 1631-1641.

De Jonge, R., van Esse, H. P., Kombrink, A., Shinya, T., Desaki, Y., Bours, R., van der Krol, S., Shibuya, N., Joosten, M. H. A. J., Thomma B. P. H. J. (2010). Conserved fungal LysM effector Ecp6 prevents chitin-triggered immunity in plants. Science, **329**, 953-955.

Denikus, N., Orfaniotou, F., Wulf, G., Lehmann, P.F., Monod, M. and Reichard, U. (2005). Fungal antigens expressed during invasive aspergillosis. Infection and Immunity, **73**, 4704-4713.

Deslandes, L., Olivier, J., Peeters, N., Feng, D. X., Khounlotham, M., Boucher, C., Somssich, I., Genin, S. and Marco, Y. (2003). Physical interaction between RRS1-R, a protein conferring resistance to bacterial wilt and PopP2, a type III effector targeted to the plant nucleus. Proceedings of the National Academy of Sciences of the United States of America, **100**, 8024-8029.

Ding, S.-L., Liu, W., Iliuk, A., Ribot, C., Vallet, J., Tao, A., Wang, Y., Lebrun, M. H. and Xu, J.-R. (2010). The Tig1 histone deacetylase complex regulates infectious growth in the rice blast fungus *Magnaporthe oryz*ae. Plant Cell, **22**, 2495-2508.

Djonović, S., Pozo, M. J., Dangott, L. J., Howell, C. R., Kenerley, C. M. (2006). Sm1, a proteinaceous elicitor secreted by the biocontrol fungus *Trichoderma virens* induces plant defense responses and systemic resistance. Molecular Plant-Microbe Interactions, **19**, 838-853.

Dodds, P. N., Lawrence, G. J., Catanzariti A. M., Teh, T., Wang, C. I. A. *et al*. (2006). Direct protein interaction underlies gene-for-gene spcificity and coevolution of the flax resistance genes and flax rust avirulence genes. Proc. Natl. Acad. Sci. USA 103:8888-93.

Doehlemann, G., van der Linde, K., Aßmann, D., Schwammbach, D., Hof, A., Mohanty, A., Jackson, D., Kahmann, R. (2009). Pep1, a secreted effector protein of *ustilago maydis*, is required for successful invasion of plant cells. PLoS Pathogens, **5**, e1000290. doi:10.1371/journal.ppat.1000290.

Doehlemann, G., Wahl, R., Horst, R. J., Voll, L. M., Usadel, B., Poree, F., Stitt, M., Pons-Kuehnemann, J., Sonnewald, U., Kahmann, R., Kämper, J. (2008). Reprogramming a maize plant: transcriptional and metabolic changes induced by the fungal biotroph *Ustilago maydis*. Plant Journal, **56**, 181–195.

Dou, D., Kale, S. D., Wang, X., Jiang, R. H. Y., Bruce, N. A., Arredondo, F. D., Zhang, X. and Tyler, B. M. (2008). RXLR-Mediated entry of *Phytophthora sojae* effector Avr1b into soybean cells does not require pathogen-encoded machinery. Plant Cell, **20**, 1930-1947.

Driouich, A., Jauneau, A., Staehelin, L. A. (1997), 7-Dehydrobrefeldin A, a naturally occurring brefeldin A derivative, inhibits secretion and causes a cis-to-trans breakdown of Golgi stacks in plant cells. Plant Physiology, **113**, 487-492.

Eisenhaber, B., Schneider, G., Wildpaner, M. and Eisenhaber, F. (2004). A sensitive predictor for potential GPI lipid modification sites in fungal protein sequences and its application to genome-wide studies for *Aspergillus nidulans*, *Candida albicans*, *Neurospora crassa*, *Saccharomyces cerevisiae* and *Schizosaccharomyces pombe*. Journal of Molecular Biology **337**, 243-253.

El Gueddari, N. E., Rauchhaus, U., Moerschbacher, B. M., Deising, H. B. (2002). Developmentally regulated conversion of surface-exposed chitin to chitosan in cell walls of plant pathogenic fungi. New Phytologist, **156**, 103-112.

Ellis, J. (2006). Insights into nonhost disease resistance: can they assist disease control in agriculture? Plant Cell, **18**, 523-528.

Emanuelsson, O., Brunak, S., von Heijne, G., Nielsen, H. (2007). Locating proteins in the cell using TargetP, SignalP and related tools. Nature Protocols, **2**, 953-971.

Epstein, L., Lusnak, K. and Kaur, S. (1998). Transformation-mediated developmental mutants of *Glomerella graminicola* (*Colletotrichum graminicola*). Fungal Genetics and Biology **23,** 189-203.

Espino, J. J., Gutiérrez-Sánchez, G., Brito, N., Shah, P., Orlando, R., González, C. (2010). The *Botrytis cinerea* early secretome. Proteomics, **10**, 3020-3034.

Farman, M. L. (2007). Telomeres in the rice blast fungus *Magnaporthe oryzae*: the world of the end as we know it. FEMS Microbiological Letter, 273, 125-132.

Fellbrich, G., Romanski, A., Varet, A., Blume, B., Brunner, F., Engelhardt, S., Felix, G., Kemmerling, B., Krzymowska, M., Nuernberger, T. (2002). NPP1, a P*hytophthora*-associated trigger of plant defense in parsley and *Arabidopsis.* Plant Journal, **32**, 375-390.

Feys, B. J., Wiermer, M., Bhat, R. A., Moisan, L. J., Medina-Escobar, N., Neu, C., Cabral, A. and Parker, J. E. (2005). Arabidopsis senescence-associated gene101 stabilizes and signals within an enhanced disease susceptibility1 complex in plant innate immunity. Plant Cell, 17, 2601-2613.

Flor, H. (1971). Current status of the gene-for-gene concept. Annual Review Phytopathology, **9**, 275-296.

Frans, M., Klis, F. M., Brul, S., de Groot, P. W. J. (2010). Covalently linked wall proteins in ascomycetous fungi. Yeast, **27**, 489-493.

Fudal, I., Boehnert, H. U., Tharreau, D. and Lebrun, M.-H. (2005). Transposition of MINE, a composite retrotransposon, in the avirulence gene ACE1 of the rice blast fungus *Magnaporthe grisea*. Fungal Genetics and Biology, **42**, 761-772.

Fudal, I., Collemare, J., Boehnert, H. U. Melayah, D., Lebrun, M. H. (2007). Expression of *Magnaporthe grisea* avirulence gene ACE1 is connected to the initiation of appressorium-mediated penetration. Eukaryotic Cell, **6,** 546–554.

Fujihara, N., Sakaguchi, A., Tanaka, S., Fujii, S., Tsuji, G., Shiraishi, T., O'Connell, R., Kubo, Y. (2010). Peroxisome biogenesis factor PEX13 is required for appressorium-mediated plant infection by the anthracnose fungus *Colletotrichum orbiculare*. Molecular Plant-Microbe Interaction, **23**, 436-445.

Galagan, J. E., Calvo, S. E., Borkovich, K. A., Selker, E. U., Read, N. D., Jaffe, D., FitzHugh, W., Ma, L.-J., Smirnov, S., Purcell, S. *et al*. (75 authors) (2003).The genome sequence of the filamentous fungus *Neurospora crassa*. Nature **422**, 859-868.

Ganem, S., Lu, S. W., Lee, B. N., Chou, D. Y., Hadar, R., Turgeon, B. G., Horwitz, B. A. (2004). G-protein beta subunit of *Cochliobolus heterostrophus* involved in virulence, asexual and sexual reproductive ability, and morphogenesis. Eukaryotic Cell., **3**, 1653-1663.

Gijzen, M., Nuernberger, T. (2006). Nep1-like proteins from plant pathogens: recruitment and diversification of the NPP1 domain across taxa. Phytochemistry, **67**, 1800-1807.

Godfrey, D., Boehlenius, H., Pedersen, C., Zhang, Z., Emmersen, J. and Thordal-Christensen, H. (2010). Powdery mildew fungal effector candidates share N-terminal Y/F/WxC-motif. BMC Genomics, **11**, doi:10.1186/1471-2164-11-317.

Goehre, V. and Robatzek, S. (2008). Breaking the barriers: microbial effector molecules subvert plant immunity. Annual Reviews of Phytopathology, **46**, 89-215.

Gómez-Gómez, L., Boller, T. (2002). Flagellin perception: a paradigm for innate immunity. Trends in Plant Science, **7**, 251-256.

Gout, L., Fudal, I., Kuhn, M. L., Blaise, F., Eckert, M., Cattolico, L., Balesdent, M. H., Rouxel, T. (2006). Lost in the middle of nowhere: the AvrLm1 avirulence gene of the *Dothideomycete Leptosphaeria maculans*. Molecular Microbiology, **60**, 67-80.

Gout, L., Kuhn, M. L., Vincenot, L., Bernard-Samain, S., Cattolico, L., Barbetti, M., Moreno-Rico, O., Balesdent, M. H., Rouxel, T. (2007). Genome structure impacts molecular evolution at the AvrLm1 avirulence locus of the plant pathogen *Leptosphaeria maculans*. Environmental Microbiology, **9,** 2978-2992.

Green, J. R., Pain, N. A., Cannell, M. E., Jones, G. L., Leckie, C. P., McCready, S., Mendgen, K., Mitchell, A. J., Callow, J. A. & O'Connell, R. J. (1995). Analysis of differentiation and development of the specialized infection structures formed by biotrophic fungal pathogens using monoclonal antibodies. Canadian Journal of Botany, **73**, 408–417.

Grouffaud, S., van West, P., Avrova, A. O., Birch, P. R. J. and Whisson, S. C. (2008). Plasmodium falciparum and *Hyaloperonospora parasitica* effector translocation motifs are functional in *Phytophthora infestans.* Microbiology, **154**, 3743-3751.

Guo, M., Tian, F., Wamboldt, Y., Alfano, J. R. (2009). The majority of the type III effector inventory of *Pseudomonas syringae* pv. tomato DC3000 can suppress plant immunity. Molecular Plant-Microbe Interaction, **22**, 1069-1080.

Haas, B. J., Kamoun, S., Zody, M. C., Jiang, R. H. Y., Handsaker, R. E., Cano, L. M., Grabherr, M., Kodira, C. D., Raffaele, S., Torto-Alalibo, T., *et al*. (96 authors) (2009). Genome sequence and analysis of the Irish potato famine pathogen *Phytophthora infestans*. Nature**, 461**, 393-398.

Hall, N., Keon, J. P. R. and Hagreaves, J. A. (1999). A homologue of a gene implicated in the virulence of human fungal diseases is present in a plant fungal pathogen and is expressed during infection. Physiological and Molecular Plant Pathology, **55,** 69-73.

Halterman, D. A., Chen, Y., Sopee, J., Berduo-Sandoval, J., Sánchez-Pérez, A, (2010). Competition between *Phytophthora infestans* effectors leads to increased aggressiveness on plants containing broad-spectrum late blight resistance. PLoS ONE 5, e10536. doi:10.1371.

Han, J.S., Boeke J.D. (2005). LINE-1 retrotransposons: modulators of quantity and quality of mammalian gene expression? Bioessays, **27**, 775-784.

He, C., Nourse, J. P., Kelemu, S., Irwin, J. A. and Manners, J. M. (1996). CgT1: a non-LTR retrotransposon with restricted distribution in the fungal phytopathogen *Colletotrichum gloeosporioides*. Molecular and General Genetics, **252**, 320-331.

Hogenhout, S. A., van der Hoorn, R. A. L., Terauchi, R. and Kamoun; S. (2009). Emerging concepts in effector biology of plant-associated organisms. Molecular Plant-Microbe Interactions, **22**, 115-122.

Houterman, P. M., Cornelissen, B. J. C., Rep, M., (2008). Suppression of plant resistance gene-based immunity by a fungal effector. PLoS Pathogens, doi:10.1371/journal.ppat.1000061.

Houterman, P. M., Ma, L., van Ooijen, G., de Vroomen, M. J., Cornelissen, B. J., Takken, F. L., Rep, M. (2009). The effector protein Avr2 of the xylem-colonizing fungus *Fusarium oxysporum* activates the tomato resistance protein I-2 intracellularly. Plant Journal, **58**, 970-978.

Hughes, H. B., Carzaniga, R., Rawlings, S.L., Green, J. R. and O'Connell, R. J. (1999). Spore surface glycoproteins of *Colletotrichum lindemuthianum* are recognized by a monoclonal antibody which inhibits adhesion to polystyrene. Microbiology, **145,** 1927-1936.

Huser, A., Takahara, H., Schmalenbach, W. and O'Connell, R. (2009). Discovery of pathogenicity genes in the crucifer anthracnose fungus *Colletotrichum higginsianum*, using random insertional mutagenesis. Molecular Plant-Microbe Interactions, **22**, 143-156.

Hutchison, K. A., Green, J. R., Wharton, P S. and O'Connell, R. J. (2002). Identification and localisation of glycoproteins in the extracellular matrices around germ-tubes and appressoria of *Colletotrichum* species. Mycological Research, **106**, 729-736.

Iizasa, E., Mitsutomi, M., Nagano, Y. (2010). Direct binding of a plant LysM receptor-like kinase, LysM RLK1/CERK1, to chitin in vitro. The Journal of Biological Chemistry, **285**, 2996-3004.

Iriti, M. and Faoro, F. (2006). Chitosan as a MAMP, searching for a PRR. Plant Signaling & Behaviour, **4**, 66–68.

Jacobs, A.K., Lipka, V., Burton, R.A., Panstruga, R., Strizhov, N., Schulze-Lefert, P. and Fincher, G.B. (2003). An *Arabidopsis* callose synthase, GSL5, is required for wound and papillary callose formation. Plant Cell, **15,** 2503-2513.

Jeong, J. S., Mitchell, T. K., Dean, R. A. (2007). The *Magnaporthe grisea* snodprot1 homolog, MSP1, is required for virulence. FEMS Microbiology Letters, **273**, 157–165.

Jiang, R. H. Y., Tripathy, S., Govers, F.and Tyler, B. M. (2008). RXLR effector reservoir in two *Phytophthora* species is dominated by a single rapidly evolving superfamily with more than 700 members. Proceedings of the National Academy of Sciences of the United States of America, **105**, 4874-4879.

Jia, Y., McAdams, S. A., Bryan, G. T., Hershey, H. P. and Valent, B. (2000). Direct interaction of resistance gene and avirulence gene products confers rice blast resistance. EMBO Journal, 19, 4004–4014.

Jones, G. L., Bailey, J. A. and Richard J. O'Connell, R. J. (1995). Sensitive staining of fungal extracellular matrices using colloidal gold. Mycological Research, **99**, 567-573.

Jones, J. D. G. and Dangl, J. L. (2006). The plant immune system. Nature, **444**, 323-329

Kaku, H., Nishizawa, Y., Ishii-Minami, N., Akimoto-Tomiyama, C., Dohmae, N., Takio, K., Minami E. and Shibuya, N. (2006). Plant cells recognize chitin fragments for defense signaling through a plasma membrane receptor. Proceedings of the National Academy of Sciences of the United States of America, **103**, 11086-11091.

Kamoun, S. (2006). A catalogue of the effector secretome of plant pathogenic oomycetes. Annual Review of Phytopathology, **44**, 41-60.

Kang S., Lebrun, M. H., Farrall, L. and Valent, B. (2001). Gain of virulence caused by insertion of a Pot3 transposon in a *Magnaporthe grisea* avirulence gene. Molecular Plant-Microbe Interactions, **14**, 671-674

Kanneganti, T.-D., Huitema, E., Cakir, C. and Kamoun, S. (2006). Synergistic interactions of the plant cell death pathways induced by *Phytophthora infestans* Nep1-like protein PiNPP1.1 and INF1 elicitin. Molecular Plant-Microbe Interactions, **19**, 854-863.

Kanneganti, T.-D., Bai, X., Tsai. C.-W., Win, J., Meulia, T., Goodin, M., Kamoun, S., Hogenhout, S. A. (2007). A functional genetic assay for nuclear trafficking in plants. The Plant Journal, **50**, 149-158.

Kay, S., Hahn, S., Marois, E., Hause, G., Bonas, U. (2007). A bacterial effector acts as a plant transcription factor and induces a cell size regulator. Science, **318**, 648-665.

Kelley, B. S., Lee, S.-J., Damasceno, C. M. B., Chakravarthy, S., Kim, B.-D., Martin, G. B. and Jocelyn K. C. Ros, J. K. C. (2010). A secreted effector protein (SNE1) from *Phytophthora infestans* is a broadly acting suppressor of programmed cell death. Plant Journal, **62**, 357-366.

Kemen, E., Kemen, A.C., Rafiqi, M., Hempel, U., Mendgen, K., Hahn, M. and Voegele, R.T. (2005). Identification of a protein from rust fungi transferred from *haustoria* into infected plant cells. Molecular Plant-Microbe Interactions 18, 1130-1139.

Khang, C. H., Berruyer, R., Giraldo, M. C., Kankanala, P., Park, S. Y., Czymmek, K., Kang, S. and Valent, B. (2010). Translocation of *Magnaporthe oryzae* effectors into rice cells and their subsequent cell-to-cell movement. Plant Cell, **22**,1388-1403

Khang, C. H., Park, S. Y., Lee, Y. H., Valent, B. and Kang, S. (2008). Genome organization and evolution of the AVR-Pita avirulence gene family in the *Magnaporthe grisea* species complex. Molecular Plant-Microbe Interactions, **21**, 658-670.

Kim, Y.K., Liu, Z.M., Li, D. and Kolattukudy, P.E. (2000). Two novel genes induced by hard-surface contact of *Colletotrichum gloeosporioides* conidia. Journal of Bacteriology, **182,** 4688-4695.

Kim, M. G., da Cunha, L, McFall, A. J., Belkhadir, Y, DebRoy, S, Dangl JL, Mackey, D. (2005). Two Pseudomonas syringae type III effectors inhibit RIN4-regulated basal defense in Arabidopsis.Cell. **121**, 749-759.

Kimura, A., Takano, Y., Furusawa, I. and Okuno, T. (2001). Peroxisomal metabolic function is required for appressorium-mediated plant infection by *Colletotrichum lagenarium*. Plant Cell. **13**, 1945–1958.

Kleemann, J., Takahara, H., Stueber, K. and O'Connell, R. (2008). Identification of soluble secreted proteins from appressoria of *Colletotrichum higginsianum* by analysis of expressed sequence tags. Microbiology, **154,** 1204-1217.

Klis, F. M., Brul, S., de Groot P. W. J. (2010). Covalently linked wall proteins in ascomycetous fungi. Yeast, **27**, 489-493.

Kobayashi, I. and Hakuno, H. (2003). Actin-related defense mechanism to reject penetration attempt by a non-pathogen is maintained in tobacco BY-2 cells. Planta, **217**, 340-345.

Kohany, O., Gentles, A. J., Hankus, L. and Jurka, J. (2006). Annotation, submission and screening of repetitive elements in repbase: repbasesubmitter and censor. BMC Bioinformatics 2006, **7,** 474doi:10.1186/1471-2105-7-474.

Krappmann, S. (2007). Gene targeting in filamentous fungi: the benefits of impaired repair. Fungal Biology Reviews. **21**, 25-29.

Krijger, J. J., Horbach, R., Behr, M., Schweizer, P., Deising, H.B. and Wirsel, S. G. R. (2008). The yeast signal sequence trap identifies secreted proteins of the hemibiotrophic corn pathogen *Colletotrichum graminicola.* Molecular Plant-Microbe Interactions, **21**, 1325-1336.

Kuo, K. C. and Hoch, H. C. (1995). Visualization of the extracellular matrix surrounding pycnidiospores, germlings and appressoria of *Phyllosticta ampelicida.* Mycologia, **87**, 759-771.

Kwon, C., Bednarek, P. and Schulze-Lefert, P. (2008). Secretory pathways in plant immune responses. Plant Physiology, **147**, 1575-1583.

Latunde-Dada, A.O. (2001). *Colletotrichum*: tales of forcible entry, stealth, transient confinement and breakout. Molecular Plant Pathology, **2,** 187-198.

Latunde-Dada, A. O. and Lucas, J. A. (2007). Localized hemibiotrophy in *Colletotrichum* cytological and molecular taxonomic similarities among *C. destructivum, C. linicola* and *C. truncatum*. Plant Pathology, **56**, 437-447.

Lawrence, G. J., Dodds, P. N., Ellis, J. G. (2010). Transformation of the flax rust fungus, *Melampsora lini*: selection via silencing of an avirulence gene. Plant Journal, **61**, 364-369.

Lee, S. A., Wormsley, S., Kamoun, S., Lee, A. F., Joiner, K. and Wong, B. (2003). An analysis of the Candida albicans genome database for soluble secreted proteins using computer-based prediction algorithms. Yeast, **20**, 595-610.

Lee, S. J., Kelley, B. S., Damasceno, C. M. B., John, B. S., Kim, B.-S., Kim, B.-D. and Rose, J. K. C. (2006). A functional screen to characterize the secretomes of eukaryotic pathogens and their hosts in planta. Molecular Plant-Microbe Interactions, **19**, 1368-1377.

Liu, G., Kennedy, R., Greenshields, D. L., Peng, G., Forseille, L., Selvaraj, G. and Wei, Y. (2007). Detached and attached Arabidopsis leaf assays reveal distinctive defense reponses against hemibiotrophic *Colletotrichum spp*. Molecular Plant-Microbe Interactions, **20**, 1308-1319.

Liu, Z. M. and Kolattukudy, P. E. (1998). Identification of a gene product induced by hard-surface contact of *Colletotrichum gloeosporioides* conidia as a ubiquitin-conjugating enzyme by yeast complementation. Journal of Bacteriology, **180,** 3592-3597.

Luderer, R., Takken, F. L., de Wit, P. J., Joosten, M. H. (2002). *Cladosporium fulvum* overcomes Cf-2-mediated resistance by producing truncated AVR2 elicitor proteins. Molecular Microbiology, **45**, 875-884.

Macho, A. P., Carlos M. Gu, C. M. (2010) The *Pseudomonas syringae* effector protein HopZ1a suppresses effector-triggered immunity. New Phytologist, **187**, 1018–1033.

Mackey, D., Belkhadir, Y., Alonso, J. M., Ecker, J. R., and Dangl, J. L. (2003). **Arabidopsis** RIN4 is a target of the type III virulence effector AvrRpt2 and modulates RPS2-mediated resistance. Cell **112**, 379-389.

Ma, L.-J., van der Does, H. C., Borkovich, K. A., Coleman, J. J., Daboussi, M.-J., Di Pietro, A., Dufresne, M., Freitag, M., Grabherr, M., Bernard Henrissat, B. *et al*. (63 authors) (2010). Comparative genomics reveals mobile pathogenicity chromosomes in *Fusarium*. Nature, **464,** 367-373.

Manning, V. A., Hamilton, S. M., Karplus, P. A. and Ciuffetti, L. M. (2008). The Arg-Gly-Asp-containing, solvent-exposed loop of Ptr ToxA is required for internalization. Molecular Plant-Microbe Interactions, **21**, 315-325.

Marion, J., Bach, L., Bellec, Y., Meyer, C., Gissot, L., Faure, J.-D. (2008). Systematic analysis of protein subcellular localization and interaction using high-throughput transient transformation of *Arabidopsis* seedlings. Plant Journal, 56, 169–179.

Matern, U., Grimmig, B. and Kneusel, R. (1995). Plant cell wall reinforcement in the disease resistance response - molecular composition and regulation. Canadian Journal of Botany, **73,** S511-S517.

Ma, Z., Proffer, T. J., Jacobs, J. L. and Sundin, G.W. (2006). Overexpression of the 14α-demethylase target gene (CYP51) mediates fungicide resistance in *Blumeriella jaapii*. Applied and Environmental Microbiology, **72**, 2581-2585.

Medzhitov, R., Janeway Jr., C. A. (2002). Decoding the patterns of self and nonself by the innate immune system. Science, **296**, 298-300.

Mendgen, K. and Hahn, M. (2002). Plant infection and the establishment of fungal biotrophy. Trends in Plant Science, **7,** 352-356.

Miya, A., Albert, P., Shinya, T., Desaki, Y., Ichimura, K., Shirasu, K., Narusaka, Y., Kawakami, N-. Kaku, H., Shibuya N. (2007). CERK1, a LysM receptor kinase, is essential for chitin elicitor signaling in *Arabidopsis.* Proceedings of the National Academy of Sciences of the United States of America, 104, 19613-19618.

Money, N.P. (1999). Biophysics: fungus punches its way in. Nature, **401,** 332-333.

Moriwaki, J., Tsukiboshi, T. and Sato, T. (2002). Grouping of *Colletotrichum* species in Japan based on rDNA sequences. Journal of General Plant Pathology, **68**, 307-320.

Mosquera, G., Giraldo, M. C., Khang, C. H., Coughlan, S. and Valent, B. (2009). Interaction transcriptome analysis identifies *Magnaporthe oryzae* BAS1-4 as biotrophy-associated secreted proteins in rice blast disease. Plant Cell, **4**, 1273–1290.

Motteram, J., Kuefner, I., Deller, S., Brunner, F., Hammond-Kosack, K. E., Nuernberger, T. and Rudd, J. J. (2009). Molecular characterization and functional analysis of MgNLP, the sole NPP1 domain–containing protein, from the fungal wheat leaf pathogen *Mycosphaerella graminicola*. Molecular Plant-Microbe Interactions, **22**, 790-799.

Narusaka, M., Shirasu, K., Noutoshi, Y., Kubo, Y., Shiraishi, T., Iwabuchi, M., Narusaka, Y. (2009). RRS1 and RPS4 provide a dual resistance-gene system against fungal and bacterial pathogens. Plant Journal, **60**, 218-226.

Narusaka, Y., Narusaka, M., Park, P., Kubo, Y., Hirayama, Seki, M., Shiraishi, T., Ishida, J., Nakashima, M., Enju, A., Sakurai, T., Satou, M., Kobayashi, M. and Shinozaki. K. (2004). RCH1, a locus in *Arabidopsis* that confers resistance to the hemibiotrophic fungal pathogen *Colletotrichum higginsianum.* Molecular Plant-Microbe Interactions, **17,** 749-762.

Nicholson, R. L. and Hammerschmidt, R. (1992). Phenolic compounds and their role in disease resistance. Annual Review of Phytopathology, **30,** 369-389.

Nickel, W. (2005). Unconventional secretory routes: direct protein export across the plasma membrane of mammalian cells. Traffic, **6**, 607-614.

Nishimura, M. T., Stein, M., Hou, B. H., Vogel, J. P., Edwards, H. and Somerville, S. C. (2003). Loss of a callose synthase results in salicylic acid-dependent disease resistance. Science, **301,** 969-972.

Noir, S., Colby, T., Harzen, A., Schmidt, J., Panstruga, R. (2009). A proteomic analysis of powdery mildew (*Blumeria graminis* f.sp. *hordei*) conidiospores. Molecular Plant Pathology, **10**, 223–236.

Nombela, C., Gil, C. and Chaffin, W.L. (2006). Non-conventional protein secretion in yeast. Trends in Microbiology, **14**, 15-21.

Nomura, K., DebRoy, S., Lee, Y. H., Pumplin, N., Jones, J., He, S. Y. (2006). A bacterial virulence protein suppresses host innate immunity to cause plant disease. Science, **313**, 220 – 223.

Nuernberger, T., Brunner, F., Kemmerling, B., Piater, L. (2004). Innate immunity in plants and animals: striking similarities and obvious differences. Immunological Reviews, **198**, 249-266.

O'Connell, R. J., Bailey, J. A. and Richmond, D. V. (1985). Cytology and physiology of infection of *Phaseolus vulgaris* by *Colletotrichum lindemuthianum*. Phvsiologiral Plant Pathology, **27**, 75-98.

O'Connell, R. J. (1991). Cytochemical analysis of infection structures of *Colletotrichum lindemuthianum* using fluorochrome-labelled lectins. Physiological and Molecular Plant Pathology, **39,** 189-200.

O'Connell, R. J., Pain, N. A., Hutchison, K. A., Jones, G. L., Green, J. R. (1996). Ultrastructure and composition of the cell surfaces of infection structures formed by the fungal plant pathogen *Colletotrichum lindemuthianum.* Journal of Microscopy, **181**, 204–212.

O'Connell, R. J., Herbert, C., Sreenivasaprasad, S., Khatib, M., Esquerré-Tugayé, M.-T., Dumas, B. (2004). A novel *Arabidopsis-Colletotrichum* pathosystem for the molecular dissection of plant-fungal interactions. Molecular Plant-Microbe Interactions, **17**, 272-282.

O'Connell, R. J. and Panstruga, R. (2006). Tête à tête inside a plant cell: establishing compatibility between plants and biotrophic fungi and oomycetes. New Phytologist, **171,** 699-718.

Orbach, M. J., Farall, L., Schweigard, J. A., Chumley, F. G., Valent, B. (2000). Atelomeric avirulence gene determines efficacy for the rice blast resistance gene Pi-ta. Plant Cell, **12**, 2019-2032.

Ottmann, C., Luberacki, B., Kuefner, I, Koch, W., Brunner, F., Weyand, M., Mattinen, L., Pirhonen, M., Anderluh, G., Seitz, H. U., Nuernberger, T. and Oecking, C. (2009). A common toxin fold mediates microbial attack and plant defense. Proceedings of the National Academy of Sciences of the United States of America, **106**, 10359-10364.

Pan, S. and Cole, G. T. (1995). Molecular and biochemical characterization of a *Coccidioides immitis*-specific antigen. Infection and Immunity **10**, 3994-4002.

Paper, J. M., Scott-Craig, J. S., Adhikari,.N. D., Cuomo, C. A., Walton, J. D. (2007). Comparative proteomics of extracellular proteins in vitro and in planta from the pathogenic fungus *Fusarium graminearum*. Proteomics, **7**, 3171–3183.

Pazzagli, L., Cappugi, G., Manao, G., Camici, G., Santini, A. and Scala, A. (1999). Purification, characterization, and amino acid sequence of *Cerato-platanin*, a new phytotoxic protein from *Ceratocystis fimbriata* f. sp. *platani*. Journal of Biological Chemistry, **274**, 24959-24964.

Peres, N. A., Adaskaveg, J. E., Correll, J. C. (2005). Lifestyles of *Colletotrichum acutatum*. Plant Disease, **89**, 784-796.

Perfect, S. E., Hughes, H. B., O'Connell, R .J. and Green, J. R. (1999). *Colletotrichum*: A model genus for studies on pathology and fungal-plant interactions. Fungal Genetics and Biology, **27,** 186-198.

Perfect, S. E., O'Connell, R. J., Green, E. F., Doering-Saad, C. and Green, J.R. (1998). Expression cloning of a fungal proline rich glycoprotein specific to the biotrophic interface formed in the *Colletotrichum*-bean interaction. Plant Journal **15,** 273-279.

Perpetua, N. S., Kubo, Y., Yasuda, N., Takano. Y., Furusawa, I. (1996). Cloning and characterization of a melanin biosynthetic THR1 reductase gene essential for appressorial penetration of *Colletotrichum lagenarium*. Molecular Plant-Microbe Interactions, **9**, 323-329.

Peter, M., Courty, P.-E., Kohler, A., Delaruelle, C., Martin, D., Tagu, D., Frey-Klett, P., Duplessis, S., Chalot, M., Podila, G., Martin, F. (2003). Analysis of expressed sequence tags from the ectomycorrhizal basidiomycetes *Laccaria bicolor* and *Pisolithus microcarpus.* New Phytologist, **159**, 117-129.

Petutschnig, E. K., Jones, A. M. E., Serazetdinova, L., Lipka, U. and Volker Lipka, V. (2010). The LysM-RLK CERK1 is a major chitin binding protein in *Arabidopsis thaliana* and subject to chitin-induced phosphorylation. The Journal of Biological Chemistry, doi: 10.1074/jbc.M110.116657.

Podila, G. K., Rogers, L. M. and Kolattukudy, P. E. (1993). Chemical signals from avocado surface wax trigger germination and appressorium formation in *Colletotrichum gloeosporioides*. Plant Physiology, **103,** 267-272.

Qutob, D., Kamoun, S. and Gijzen, M. (2002). Expression of a *Phytophora sojae* necrosis-inducing protein occurs during transition from biotrophy to necrotrophy. Plant Journal **32**, 361-373.

Qutob, D., Kemmerling, B., Brunner, F., Kuefner, I., Engelhardt, S., Gust, A. A., Luberacki, B., Seitz, H. U., Stahl, D., Rauhut, T., Glawischnig, E., Schween, G., Lacombe, B., Watanabe, N., Lam, E., Schlichting, R., Scheel, D., Nau, K., Dodt, G., Hubert, D., Gijzen M. and Nuernberger, T. (2006). Phytotoxicity and innate immune responses induced by Nep1-like proteins. Plant Cell, **18**, 3721-3744.

Rafiqi, M., Gan, P. H., Ravensdale, M., Lawrence, G. J., Ellis, J. G., Jones, D. A., Hardham, A. R., Dodds, P. N. (2010). Internalization of flax rust avirulence proteins into flax and tobacco cells can occur in the absence of the pathogen. Plant Cell, **22**, 2017-2032.

Redman, R.S. and Rodriguez, R.J. (1994). Factors affecting the efficient transformation of *Colletotrichum* species. Experimental Mycology, **18,** 230-246.

Redman, R.S., Rodriguez, R.J. and Ranson, J.C. (1999). Conversion of the pathogenic fungus *Colletotrichum magna* to a nonpathogenic, endophytic mutualist by gene disruption. Molecular Plant-Microbe Interactions, **12,** 969-975.

Rep, M., Meijer, M., Houterman, P. M., van der Does, H. C. and Cornelissen, B. J. C. (2005a). *Fusarium oxysporum* evades I-3-mediated resistance without altering the matching avirulence gene. Molecular Plant-Microbe Interactions, **18**, 15-23.

Rep, M., van der Does H.C. and Cornelissen, B.J.C. (2005b). Drifter, a novel, low copy hAT-like transposon in *Fusarium oxysporum* is activated during starvation. Fungal Genetics and Biology, **42**, 546-553.

Richardt, S., Lang, D., Reski, D., Frank, W. and Stefan A. Rensing, S. A. (2007). PlanTAPDB, a phylogeny-based resource of plant transcription-associated proteins. Plant Physiology, 143, 1452-1466.

Ridout, C. J., Skamnioti, P., Porritt, O., Sacristan, S., Jones J. D. G. and Brown, J. K. M. (2006). Multiple avirulence paralogues in cereal powdery mildew fungi may contribute to parasite fitness and defeat of plant resistance. Plant Cell, **18**, 2402-2414.

Robinson, M. and Sharon, A. (1999). Transformation of the bioherbicide *Colletotrichum gloeosporioides* f. sp. *aeschynomene* by electroporation of germinated conidia. Current Genetics, **36,** 98-104.

Rodrigues, M. L., Nakayasu, E. S., Oliveira, D. L., Nimrichter, L., Nosanchuk, J. D., Almeida, I. C. and Casadevall, A. (2008). Extracellular vesicles produced by *Cryptococcus neoformans* contain protein components associated with virulence. Eukaryotic Cell, **7**, 58-67.

Roemer, P., Hahn, S., Jordan, T., Strauß, T., Bonas, U., Lahaye, T. (2007). Plant pathogen recognition mediated by promoter activation of the pepper Bs3 resistance gene. Science, **318**, 645 – 648.

Rooney, H. C. E. et al. (2005). Cladosporium Avr2 inhibits tomato Rcr3 protease required for Cf-2-dependent disease resistance. Science, **308,** 1783-1786**.**

Roy, S. W., Penny, D. and Neafsey, D. E. (2007). Evolutionary conservation of UTR intron boundaries in *Cryptococcus*. Molecular Biology and Evolution, **24**, 1140-1148.

Sacadura, N. T., Saville, B. J. (2003). Gene expression and EST analyses of *Ustilago maydis* germinating teliospores. Fungal Genetics and Biology. **40**, 47-64.

Sacristán, S., Vigouroux, M., Pedersen, C., Skamnioti, P., Thordal-Christensen H. et al. (2009). Coevolution between a family of parasite virulence effectors and a class of LINE-1 retrotransposons. PLoS ONE 4(10): e7463. doi:10.1371/journal.pone.0007463.

Sambrook, J., Fritsch, E.F. and Maniatis, T. (1989). Molecular cloning: a laboratory manual. Cold Spring Harbour, NY: Cold Spring Harbor Laboratory Press.

Scala, A., Pazzagli, L., Comparini, C., Santini, A., Tegli, S. and Cappugi, G. (2004). Cerato-platanin, an early-produced protein by *Ceratocystis fimbriata* F.SP. *platani*, elicts phytoalexin synthesis in host and non-host plants. Journal of Plant Pathology, **86**, 27-33.

Schulze-Lefert, P. (2004). Knocking on the heaven's wall: pathogenesis of and resistance to biotrophic fungi at the cell wall. Current Opinion in Plant Biology, **7,** 377-383.

Shah, P., Atwood, J. A., Orlando, R., Mubarek, H. E., Podila, G. H. and Davis, M. R. (2009). Comparative proteomic analysis of *Botrytis cinerea* secretome. Journal of Proteome Research, **8**, 1123–1130.

Shaner, N. C., Steinbach, P. A. and Tsien, R. Y. (2005). A guide to choosing fluorescent proteins. Nature Methods, **2**, 905-909.

Shan, X. C. and Goodwin, P. H. (2004). Monitoring host nuclear migration and degradation with green fluorescent protein during compatible and incompatible interactions of nicotiana tabacum with *Colletotrichum* species. Journal of Phytopathology, **152,** 454-460.

Shan, X. C. and Goodwin, P.H. (2005). Reorganization of filamentous actin in *Nicotiana benthamiana* leaf epidermal cells inoculated with *Colletotrichum destructivum* and *Colletotrichum graminicola*. International Journal of Plant Science, **166,** 31-39.

Shimada, C., Lipka, V., O'Connell, R., Okuno, T., Schulze-Lefert, P. and Takano, Y. (2006). Nonhost resistance in *Arabidopsis-Colletotrichum* interactions acts at the cell periphery and requires actin filament function. Molecular Plant-Microbe Interactions **19,** 270-279.

Shimizu, T., Nakano, T., Takamizawa, D., Desaki, Y., Ishii-Minami, N., Nishizawa, Y., Minami, E., Okada, K., Yamane, H., Kaku, H., Shibuy, N. (2010). Two LysM receptor molecules, CEBiP and OsCERK1, cooperatively regulate chitin elicitor signaling in rice. Plant Journal, DOI: 10.1111/j.1365-313X.2010.04324.x.

Schouten, A., van Baarlen, P., van Kan, J. A. (2008). Phytotoxic Nep1-like proteins from the necrotrophic fungus *Botrytis cinerea* associate with membranes and the nucleus of plant cells. The New Phytologist, **177**, 493-505.

Siegrist, J. and Kauss, H. (1990). Chitin deacetylase in cucumber leaves infected by *Colletotrichum lagenarium*. Physiological and Molecular Plant Pathology, **36**, 267-275.

Sohn, K. H., Lei, R., Nemri, A. and Jones, J. D. G. (2007). The downy mildew effector proteins ATR1 and ATR13 promote disease susceptibility in *Arabidopsis thaliana*. Plant Cell, **19**, 4077-4090.

Stein, L. D., Mungall, C., Shu, S., Caudy, M., Mangone, M., Day, A., Nickerson, E., Stajich, J. E., Harris, T. W., Arva, A., Lewis, S. (2002). The generic genome browser: a building block for a model organism system database. Genome Research, **12**, 1599-1610.

Stephenson, S. A., Hatfield, J., Rusu, A. G., Maclean, D. J., Manners, J. M. (2000). CgDN3: an essential pathogenicity gene of *Colletotrichum gloeosporioides* necessary to avert a hypersensitive-like response in the host *Stylosanthes guianensis*. Molecular Plant-Microbe Interactions, **13**, 929-941.

Stergiopoulos, I. and de Wit, P. J. G. M. (2009). Fungal effector proteins. Annual Review of Phytopathology, **47**, 233-263.

Stergiopoulos, I., de Kock, M. J. D., Lindhout, P. and de Wit, P. J. G. M. (2007). Allelic variation in the effector genes of the tomato pathogen *Cladosporium fulvum* reveals different modes of adaptive evolution. MPMI, **20**, 1271-1283.

Suárez, M. B., Sanz, L., Chamorro, M. I., Rey, M., González, F. J., Llobell, A., Monte, E. (2005). Proteomic analysis of secreted proteins from *Trichoderma harzianum*. Identification of a fungal cell wall-induced aspartic protease. Fungal Genetics and Biology, **42**, 924-934.

Sugui, J. A., Leite, B. and Nicholson, R.L. (1998). Partial characterization of the extracellular matrix released onto hydrophobic surfaces by conidia and conidial germlings of *Colletotrichum graminicola*. Physiological and Molecular Plant Pathology, **52,** 411-425.

Sun, H. and Zhang, J.-Z. (2009). *Colletotrichum destructivum* from cowpea infecting *Arabidopsis thaliana* and its identity to *C. higginsianum*. European Journal of Plant Pathology, **125**, 459-469.

Sutton, B. C. (1992) The genus *Glomerella* and its anamorph *Colletotrichum*. In: Bailey JA, Jeger MJ (eds) *Colletotrichum*: biology, pathology and control. CAB International, Wallingford, 1–26.

Szewczyk, E., Nayak, T., Oakley, C. E., Edgerton, H., Xiong, Y., Taheri-Talesh, N., Osmani, S. A., Oakley, B. R. (2006). Fusion PCR and gene targeting in *Aspergillus nidulans*. Nature Protocols, 2006, **1**, 3111-3120.

Takahara, H., Dolf, A., Endl, E., O'Connell, R. (2009). Flow cytometric purification of *Colletotrichum higginsianum* biotrophic hyphae from *Arabidopsis* leaves for stage-specific transcriptome analysis. Plant Journal, **59**, 672–683.

Takken, F., Rep, M. (2010). The arms race between tomato and *Fusarium oxysporum*. Molecular Plant Pathology, **11**, 309-314.

Talhinhas, P., Muthumeenakshi, S., Neves-Martins, J., Helena Oliveira, H. and Sreenivasaprasad, S. (2008). Agrobacterium-mediated transformation and insertional mutagenesis in *Colletotrichum acutatum* for investigating varied pathogenicity lifestyles. Molecular Biotechnology, **39**, 57-67.

Tanaka S., Yamada K., Yabumoto K., Fujii S., Huser A., Tsuji G., Koga H., Dohi K., Mori M., Shiraishi T., O'Connell R., Kubo Y. (2007). Saccharomyces cerevisiae SSD1 orthologues are essential for host infection by the ascomycete plant pathogens *Colletotrichum lagenarium* and *Magnaporthe grisea*. Molecular Microbiology, **64**, 1332-1349.

Thilmony, R., Underwood, W., He, S. Y. (2006). Genome-wide transcriptional analysis of the *Arabidopsis thaliana* interaction with the plant pathogen Pseudomonas syringae pv. tomato DC3000 and the human pathogen *Escherichia coli* O157:H7. Plant Journal, **46**, 34-53.

Thordal-Christensen, H., Zhang, Z., Wei, Y. and Collinge, D.B. (1997). Subcellular localization of H_2O_2 in plants. H_2O_2 accumulation in papillae and hypersensitive response during the barley-powdery mildew interaction. Plant Journal, **11,** 1187-1194.

Tian, M., Huitema, E., da Cunha, L., Torto-Alalibo, T. and Kamoun, S. (2004). A Kazal-like extracellular serine protease inhibitor from *Phytophthora infestans*. targets the tomato pathogenesis-related protease P69B. Journal of Biological Chemistry, **279**, 26370.

Tsuji, G., Fujii, S., Fujihara, N., Hirose, C., Tsuge, S., Shiraishi, T and Kubo, Y. (2003). Agrobacterium tumefaciens-mediated transformation for random insertional mutagenesis in *Colletotrichum lagenarium*. Journal of General Plant Pathology, **69,** 230-239.

Tsuji, G., Fujii, S., Tsuge, S., Shiraishi, T. and Kubo, Y. (2003). The *Colletotrichum lagenarium* Ste12-like gene CST1 is essential for appressorium penetration. Molecular Plant-Microbe Interactions, **16,** 315-325.

Van den Burg, H. A., Westerink, N., Francoijs, K. J., Roth, R., Woestenenk, E., *et al*. (2003). Natural disulfide bond-disrupted mutants of AVR4 of the tomato pathogen *Cladosporium fulvum* are sensitive to proteolysis, circumvent Cf-4-mediated resistance, but retain their chitin binding ability. The Journal of Biological Chemistry, **278**, 27340-27346.

Van den Hooven, H. W., van den Burg, H. A., Vossen, P., Boeren, S., de Wit, P. J. G. M. and Vervoort, J. (2001). Disulfide bond structure of the AVR9 elicitor of the fungal tomato pathogen *Cladosporium fulvum*: evidence for a cystine knot. Biochemistry, **40**, 3458-3466.

Van der Does, H. C. and Rep. M. (2007). Virulence genes and the evolution of host specificity in plant-pathogenic fungi. MPMI, 20, 1175-1182.

Van der Does, H. C., Lievens, B., Claes, L., Houterman, P.M., Cornelissen, B. J., Rep, M. (2008). The presence of a virulence locus discriminates *Fusarium oxysporum* isolates causing tomato wilt from other isolates. Environmental Microbiology, **10**, 1475-1485.

Van der Hoorn, R. A. L. and Kamoun, S. (2008). From guard to decoy: a new model for perception of plant pathogen effectors. Plant Cell, **20,** 2009-2017.

Van Esse, H. P., Bolton, M. D., Stergiopoulos, I., de Wit, P. J. G. M. and Thomma, B. P. H. J. (2007). The chitin-binding Cladosporium fulvum effector protein Avr4 is a virulence factor. Molecular Plant-Microbe Interaction, **20**, 1092–1101.

Van Esse, H. P., Fradin, E. F., de Groot, P. J., de Wit, P. J., Thomma, B. P. (2009). Tomato transcriptional responses to a foliar and a vascular fungal pathogen are distinct. Molecular Plant-Microbe Interactions, **22**, 245-258.

Van Esse, H. P., van't Klooster, J. W., Bolton, M. D., Yadeta, K. A., van Baarlen, P. Boeren, S., Vervoort, J., de Wit, P. J. G. M. and Thomma, B. P. H. J. (2008). The *Cladosporium fulvum* virulence protein Avr2 inhibits host proteases required for basal defense. Plant Cell, **20**, 1948-1963.

Van Kan, J. A. L. (2006). Licensed to kill: the lifestyle of a necrotrophic plant pathogen. Trends in Plant Science, **11,** 247-253.

Venard, C., Kulshrestha, S., Sweigard, S., Nuckles, E. and Vaillancourt, L. (2008). The role of a fadA ortholog in the growth and development of *Colletotrichum graminicola* in vitro and in planta. Fungal Genetics and Biology**, 45**, 973-983.

Veneault-Fourrey, C., Barooah, M., Egan, M., Wakley, G., Talbot, N. J. (2006). Autophagic fungal cell death is necessary for infection by the rice blast fungus. Science, **312**, 580 – 583.

Veneault-Fourrey, C., Laugé, R. and Langin, T. (2005). Nonpathogenic strains of *Colletotrichum lindemuthianum* trigger progressive bean defense responses during appressorium-mediated penetration. Applied and Environmental Microbiology, **71**, 4761-4770.

Vincent, D., Balesdent, M.-H., Gibon, J., Claverol, S., Lapaillerie, D., Lomenech, A.-M., Blaise, F., Rouxel, T., Martin, F., Bonneu, M., Amselem, J., Dominguez, V., Howlett, B. J., Wincker, P., Joets, J., Lebrun, M.-H., Plomion, C. (2009). Hunting down fungal secretomes using liquid-phase IEF prior to high resolution 2-DE. Electrophoresis, **30**, 4118–4136.

Voegele, R.T., Wirsel, S., Moll, U., Lechner, M. and Mendgen, K. (2006). Cloning and characterization of a novel invertase from the obligate biotroph *Uromyces fabae* and analysis of expression patterns of host and pathogen invertases in the course of infection. Molecular Plant-Microbe Interactions, **19,** 625-634.

Voinnet, O., Rivas, S., Mestre, P., Baulcombe, D. (2003). An enhanced transient expression system in plants based on suppression of gene silencing by the p19 protein of tomato bushy stunt virus. Plant Journal, **33**, 949–956.

Wada, M., Kato, H., Malik, K., Sriprasertsak, P., Ichinose, Y., Shiraishi, T., Yamada, T. (1995). A supprescin from a phytopathogenic fungus deactivates transcription of a plant defense gene encoding phenylalanine ammonia-lyase. Journal of Molecular Biology, **249**, 513-529.

Wan, J., Zhang, X.-C., Neece, D., Ramonell, K. M., Clough, S., Kim, S.-Y., Stacey, M. G. and Stacey, G. (2008). A LysM receptor-like kinase plays a critical role in chitin signaling and fungal resistance in *Arabidopsis*. Plant Cell, **20**, 471-481.

Wang, Y., Bao, Z., Zhu, Y.and Hua, J. (2009). Analysis of temperature modulation of plant defense against biotrophic microbes. Molecular Plant-Microbe Interactions, **22**, 498-506.

Wang, Z.-Y., Soanes, D. M., Kershaw, M. J. and Talbot, N. J. (2007). Functional analysis if lipid metabolism in *Magnaporthe grisea* reveals a requirement for peroxisomal fatty acid oxidation during appressorium-mediated plant infection. Molecular Plant-Microbe Interactions, **20**, 475-491.

Weigel, D., **Glazebrook**, J. **eds, (2002).** *Arabidopsis*: A Laboratory Manual**.** Cold Spring Harbor Laboratory Press, Cold Spring Harbor, NY, USA.

Wheat, C. W. (2010). Rapidly developing functional genomics in ecological model systems via 454 transcriptome sequencing. Genetica, **138**, 433-451.

Whisson, S. C., Boevink, P. C., Moleleki, L., Avrova, A. O., Morales, J. G., Gilroy, E. M., Armstrong, M. R., Grouffaud, S., van West, P., Chapman, S., Hein, I., Toth, I. K., Pritchard, L. and Birch, P. R. J. (2007). A translocation signal for delivery of oomycete effector proteins into host plant cells. Nature, **450**, 115-118.

Wilson, L. M., Idnurm, A., Howlett, B. J. (2002). Characterization of a gene (sp1) encoding a secreted protein from *Leptosphaeria maculans*, the blackleg pathogen of *Brassica napus*. Molecular Plant Pathology. **3**, 487-493.

Wiermer, M., Feys, B. J. and Jane E Parker, J. E. (2005). Plant immunity: the EDS1 regulatory node. Current Opinion in Plant Biology, **8**, 383-389.

Wirsel, S., Voegele, R.T., Baenninger, R. and Mendgen, K. (2004). Cloning of β-tubulin and succinate dehydrogenase genes from *Uromyces fabae* and establishing selection conditions for their use in transformation. European Journal of Plant Pathology , **110,** 767-777.

Wirthmueller, L., Zhang, Y., Jones, J. D., Parker, J. E. (2007). Nuclear accumulation of the *Arabidopsis* immune receptor RPS4 is necessary for triggering EDS1-dependent defense. Current Biology, **17**, 2023-2029.

Xue, C., Park, G., Choi, W., Zheng, L., Dean, R. A. and Jin-Rong Xu, J.-R. (2002). Two novel fungal virulence genes specifically expressed in appressoria of the rice blast fungus. Plant Cell, **14**, 2107-2119.

Yoshida, K., Saitoh, H., Fujisawa, S., Kanzaki, H., Matsumura, H., Yoshida, H., Tosa, Y., Chuma, I., Takano, Y., Win, J., Kamoun, S. and Terauchi, R. (2009). Association genetics reveals three novel avirulence genes from the rice blast fungal pathogen *Magnaporthe oryzae*. Plant Cell, **21,** 1573-1591.

Zheng, H., Kunst, L., Hawes, C. and Moore, I. (2004). A GFP-based assay reveals a role for RHD3 in transport between the endoplasmic reticulum and Golgi apparatus. Plant Journal, **37**, 398-414.

Zhou, E., Jia, Y., Singh, P., Correll, J. C., Lee, F. N. (2007). Instability of the *Magnaporthe oryzae* avirulence gene AVR-Pita alters virulence. Fungal Genetics and Biology, **44**, 1024-1034.

Zipfel, C., Kunze, G., Chinchilla, D., Caniard, A., Jones, J. D., Boller, T., Felix, G. (2006). Perception of the bacterial PAMP EF-Tu by the receptor EFR restricts Agrobacterium-mediated transformation. Cell, **125**, 749-760.

Acknowledgements

An dieser Stelle möchte ich mich bei allen bedanken, die zum Gelingen dieser Arbeit maßgeblich beigetragen haben. Besonderer Dank gilt:

Prof. Paul Schulze-Lefert für die Möglichkeit, in seiner Abteilung am Max-Planck-Institut für Pflanzenzüchtungsforschung promovieren zu können, für hilfreiche Ideen und Diskussionen während meiner Arbeit und die ansteckende Begeisterung für Wissenschaft!

Dr. Richard O'Connell for his excellent supervision, for helpful discussions, for his encouraging optimism and a very kind and honest working atmosphere, and for critical reading the manuscript. Thanks a lot Richard, for heaving a great time in your group!

Prof. Dr. Martin Hülskamp für die freundliche Übernahme des Ko-Referates und Prof. Dr. Ulf-Ingo Flügge für die freundliche Übernahme des Prüfungsvorsitzes.

Many thanks to Prof. Dr. Martijn Rep for being the external examiner of my thesis committee!

Dr. Wim Soppe für die freundliche Übernahme des Prüfungsbeisitzes.

Emiel Ver Loren Van Themaat, for great bioinformatics help in performing all these batch assemblies and BLASTs and for his enormous (+ enormously helpful) matrices.

Der MS-Abteilung des Instituts: Dr. Tom Colby, Dr. Jürgen Schmidt, Anne Harzen und Ursula Wieneke für die gute Kooperation und ihre Hilfbereitschaft.

Isa Will und Wolfgang Schmalenbach für die hervorragende technische Unterstützung im Labor und Rolf-Dieter Hirtz und Rainer Franzen für die Bedienung des SEM. Ganz besonders auch Jaqueline Bautor für ihre große Hilfsbereitschaft und ihre Antworten auf alle meine Fragen!

Dr. G. Tsuji and Prof. Dr. Y. Kubo (Kyoto Prefectural University) for sharing fungal expression or knockout vectors and the *C. higginsianum* ΔKU70 mutant.

Mark Kwaaitaal for help with recording the fluorescence emission spectrum.

Doris Birker. Habe Dich hier so manches Mal vermisst. Vielen Dank für Deine Hilfe.

Allen Laborkollegen, insbesondere Hiroyuki, Aurélie und Bleddyn für die tolle Atmosphäre und die ständige Hilfsbereitschaft. Special thanks to the recently joint group members Lotje and Lynda for having a lots of fun and all the recent encouraging emails.

Meinen Eltern für die große Unterstützung in den letzten Jahren und (insbesondere) Wochen!! Ganz besonderer Dank geht an meine Frau Kerstin. Danke für Deine aufbauenden Worte, aus denen ich immer viel Kraft schöpfen konnte, für Deine Geduld und Dein Organisationstalent in den letzten Wochen. Ohne Dich wäre diese Arbeit nicht möglich gewesen!

Malte, der mir mit seinem zauberhaften Wesen geholfen hat, die wesentlichen Dinge nicht aus den Augen zu verlieren.

Erklärung

Ich versichere, dass ich die von mir vorgelegte Dissertation selbständig angefertigt, die benutzten Quellen und Hilfsmittel vollständig angegeben und die Stellen der Arbeit - einschließlich Tabellen, Karten und Abbildungen -, die anderen Werken im Wortlaut oder dem Sinn nach entnommen sind, in jedem Einzelfall als Entlehnung kenntlich gemacht habe; dass diese Dissertation noch keiner anderen Fakultät oder Universität zur Prüfung vorgelegen hat; dass sie - abgesehen von der unten angegebenen Teilpublikation - noch nicht veröffentlicht worden ist sowie, dass ich eine solche Veröffentlichung vor Abschluss des Promotionsverfahrens nicht vornehmen werde. Die Bestimmungen dieser Promotionsordnung sind mir bekannt. Die von mir vorgelegte Dissertation ist von Prof. Dr. Paul Schulze-Lefert betreut worden.

Teilpublikation:

Kleemann, J., Takahara, H., Stueber, K. and O'Connell, R. (2008). Identification of soluble secreted proteins from appressoria of *Colletotrichum higginsianum* by analysis of expressed sequence tags. Microbiology, **154,** 1204-1217.

Köln, den 08. September 2010

Curriculum Vitae

Jochen Kleemann

Angaben zur Person

geboren am:	17.10.1976 in Köln
Familienstand:	verheiratet, 1 Kind
Nationalität:	deutsch

Ausbildung

1997 - 06.2000:	Berufsausbildung zum Biologielaboranten im Forschungszentrum Jülich, Abschlussnote „sehr gut“ und Auszeichnung als Landesbester
06.2000 - 10.2000:	Angestellter Biologielaborant im Forschungszentrum Jülich
10.2000 - 10.2006:	Studium der Biologie an der Universität zu Köln, Vordiplom und Diplom jeweils mit der Gesamtnote „sehr gut“
11.2006 - heute:	Wissenschaftlicher Mitarbeiter am Max-Planck-Institut für Pflanzenzüchtungsforschung (MPIPZ) in Köln
seit 04.2007:	Promotionsarbeit am MPIPZ in Köln, Abteilung für Molekulare Phytopathologie, AG Dr. R. O’Connell unter der Leitung von Prof. Dr. P. Schulze-Lefert. Thema der Arbeit: „Identification and functional characterization of secreted effector proteins of the hemibiotrophic fungus *Colletotrichum higginsianum”*

Köln, 08. September 2010